Production and recovery of Polyhydroxybutyrate (PHB), biodegradable plastic from cyanobacteria under photoautotrophic conditions

A thesis submitted in fulfillments of the requirements for the degree of

DOCTOR OF PHILOSOPHY

by

Yashavanth P R

166106021

Under the supervision of

Dr. Soumen Kumar Maiti

Associate Professor

April 2025

Department of Biosciences and Bioengineering

Indian Institute of Technology Guwahati

Guwahati-781039, Assam, India

INDIAN INSTITUTE OF TECHNOLOGY GUWAHATI

Department of Biosciences and Bioengineering

DECLARATION

I, hereby declare that the research carried out in the thesis entitled, " **Production and recovery of Polyhydroxybutyrate (PHB), biodegradable plastic from cyanobacteria under photoautotrophic conditions**" submitted by me to the *Indian Institute of Technology Guwahati*, for the award of the Doctor of Philosophy, is a bonafide work carried out by me under the supervision of Dr. Soumen Kumar Maiti. The content of this thesis, in full or in parts, has not been submitted to any other University or Institute for the award of any degree or diploma. I also wish to state that nothing in this report amounts to plagiarism to the best of my knowledge and understanding.

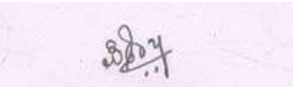

Yashavanth P R
Department of Biosciences and Bioengineering,
Indian Institute of Technology Guwahati,
Guwahati - 781039, Assam, India.

Date: 17-04-2025

INDIAN INSTITUTE OF TECHNOLOGY GUWAHATI

Department of Biosciences and Bioengineering

CERTIFICATE

This is to certify that the thesis entitled **"Production and recovery of Polyhydroxybutyrate (PHB), biodegradable plastic from cyanobacteria under photoautotrophic conditions,"** submitted by **YASHAVANTH P R (166106021)**, a Ph.D. student in the *Department of Biosciences and Bioengineering, Indian Institute of Technology Guwahati*, for the award of the degree of Doctor of Philosophy, is a record of an original research work carried out by him under my supervision and guidance. The thesis has fulfilled all requirements as per the Institute's regulations and, in my opinion, has reached the standard needed for submission. The results embodied in this thesis have not been submitted to any other University or Institute to award any degree or diploma.

Soumen Kr. Maiti

Supervisor: Dr. Soumen Kumar Maiti
Department of Biosciences and Bioengineering,
Indian Institute of Technology Guwahati,
Guwahati-781039, Assam, India.

Date: 17/04/2025

ACKNOWLEDGEMENT

The work presented in this thesis would not have been possible without my close association with many people who were always there when I needed them the most. I take this opportunity to acknowledge them and extend my sincere gratitude for helping me make this thesis a possibility. The journey is timeless when we are blessed with the guidance of peers. My entire Ph.D. days have quite been a journey, and today, finally, I am about to submit my thesis. I embrace the opportunity to express my deep sense of gratitude to my supervisor Dr. Soumen Kumar Maiti, Associate Professor, Department of Biosciences and Bioengineering, IIT Guwahati, Guwahati for his constant guidance, valuable suggestions, and kind encouragement during my association with his research group. I was able to gain a grasp of the subject, thanks to his encouragement, unwavering support, intellectual stimulation, invaluable thoughts, and suggestions from the very start to the end.

My deepest thanks extend towards all the members of my doctoral committee, Dr. Selvaraju Narayanasamy (chairperson), Dr. Prabu Vairakannu, and Dr. Priyadarshi Satpati, for their insightful remarks, recommendations, and helpful critiques that ultimately enabled me to accomplish this goal.

My special acknowledgement to the Department of Biosciences and Bioengineering (BSBE), Indian Institute of Technology Guwahati for giving me a wonderful chance to be a part of this prestigious Institute. The faculty members and staff of BSBE are also acknowledged for their help and support. Also, I am thankful to the Central Instrument Facility (CIF), IIT Guwahati, for letting me perform my experiments using sophisticated instruments. I am grateful for the access to the

FESEM facility (BT/NER/143/SP44675/2023) that was granted by the North East Centre for Biological Sciences and Healthcare Engineering, Research Building, Indian Institute of Technology Guwahati, Assam. Additionally, I would like to thank School of Energy Sciences and Engineering, Indian Institute of Technology Guwahati, Assam for granting me the use of Differential Scanning Calorimetry.

I would also like to thank IIT Guwahati and the Ministry of Education (formerly MHRD) for providing financial assistance in my research.

My acknowledgement will never be complete without the special mention of my lab members: Dr. Venkateswara Rao Naira, Dr. Mahesh R, Dr. Suraj Kumar Panda, Sahil Dhull, Meenakshi Das, Jitendra Singh, Bhoomika Patel, Pragatisheel, Nitish Kumar, Maibam Premeshworii Devi, Chhavi Bansal and Atchaya. I would like to thank my best friend Vikram K. M. and his parents for their support; without them, earning a PhD would be unthinkable. I want to express my gratitude to my teachers for imparting their expertise with me and for giving me the confidence to dive into the world of research. I thank specially to my friends Dr. Angshu Dutta, Dr. Vimalathithan Devaraj, Dr. Saddam Hussain, Dr. Muniraja Tippa, Dr. Uttariya Pal, Dr. Aman Bhardwaj, Dr. Laipubam Gayatri Sharma, Ansuman Sahoo, Madhav Bhat, Saptaswa Biswas, Rushikesh Fopase and Vijaya Bhat for being supportive in critical situations during my research work.

I would especially like to express my gratitude to my parents Ramachandrappa D and Rathnamma B P, my brother Harish and my sister Kruthika for their love, support, and understanding during my academic career. I am very grateful to the Supreme Being Shiva and the universal mother Kamakhya for their blessings in my life.

Abstract

Cyanobacteria are photosynthetic prokaryotes capable of converting atmospheric CO_2 into polyhydroxybutyrate, a bioplastic under stress conditions. Polyhydroxybutyrate (PHB) is a carbon storage compound produced by several species of cyanobacteria but is not commercialized due to high production costs. *Chlorogloea fritschii* TISTR 8527 is capable of accumulating PHB under nitrogen or phosphate limitations with the utilization of diurnal light. *C. fritschii* having capability of CO_2 fixation, can replace the heterotrophic bacteria in PHB production with acetate as an inducer without supplementation of sugars. Nutrients and light availability, temperature, mixing and mass transfer, pH, and CO_2 levels are crucial for cyanobacterial growth. Two stage cultivation of cyanobacteria may result in higher PHB production, but it is not economical due to intermediate biomass harvesting step with media replacement. PHB production in cyanobacteria is not straight forward since growth of the same required nutrient sufficient conditions whereas PHB production requires stress or nutrient deprivation conditions. *C. fritschii* has unique nature of auto-sedimentation which reduces the cost of biomass harvesting by centrifugation and eases the down-stream process. PHB extraction from cyanobacteria increases production cost since PHB is an intracellular product and must be purified in various steps. The presence of pigments in the recovered polymer affects material properties of PHB. Arising from the above, the objectives of the study were formulated to develop process strategy for cost-effective single stage cultivation with utilization of diurnal light and CO_2 with minimal supply of acetate as PHB inducer without media replacement and recovery of the biopolymer with considerable yield.

The current study investigates the single-stage cultivation of *Chlorogloea fritschii* with phototrophic CO_2 assimilation and polyhydroxybutyrate (PHB) production using acetate as an inducer under dark. The study focuses on the improvement of PHB production photobioreactor

under diurnal light mimic to sunlight. Initially the effect of constant and diurnal light on growth of *C. fritschii* and effect of nitrate under diurnal light on PHB production have been explored. Also, the optimum level of acetate inducer has been decided based on experiments. A phosphate and nitrate feeding strategy has been used to improve the PHB production using single-stage cultivation. The multi-objective media optimization was performed to simultaneously enhance the dry cell weight (DCW), PHB (% w/w) and auto-sedimentation concentration factor (SCF) in single stage cultivation under diurnal light to reduce the process cost. The effect of CO_2 supply and multiple addition of acetate inducer on growth, PHB accumulation and SCF was also studied under diurnal simulated sunlight with optimized medium in flat panel photobioreactor (PBR). The intracellular PHB was recovered with various methods utilizing pretreatment of biomass with hypochlorite or methanol along with solvent extraction by halogenated and green solvents.

Effect of constant light on growth of *C. fritschii* was studied using unidirectional LED system with peak light intensity of 1890 µmol/m^2/s resulting in biomass concentration of 1.84 g/L. The diurnal simulated sunlight resulted in maximum biomass concentration of 2.1 g/L and 2.06 g/L with optimized BG-11 medium and 1 % CO_2 in flask equipped with silicone rubber sparging and flat panel photobioreactor (PBR) on 16^{th} d and 10^{th} d, respectively. The nitrate variation experiment resulted in a maximum biomass of 2.8 g/L with 2.6 g/L $NaNO_3$. Polymer content of 14.74 % (w/w) was obtained with 1.5 g/L nitrate due to stress caused by nutrient limitations in BG-11 after acetate supplementation under dark. Single stage PHB accumulation of *C. fritschii* with phototrophic growth using diurnal light intensity resulted in a maximum PHB content of 16.4 % on the 4^{th} day of induction with 0.2 % (w/v) acetate under dark. Fed-batch of phosphate and nitrate under diurnal light resulted in PHB accumulation of 46.9 % with 4.2-fold increment when compared to the control.

Multi-objective optimization aims to optimize the nutrients for maximization of cyanobacterial biomass with higher content of PHB and recovery of biomass by autosedimentation under diurnal light mimic to sunlight. Initially, $NaNO_3$, K_2HPO_4, TRACE (micronutrient solution), Na_2EDTA, and $MgSO_4.7H_2O$ were screened as important media compositions. The multi-objective optimization with desirability approach with response surface methodology (RSM) was used to improve dry cell weight (DCW), PHB content, and auto-sedimentation concentration factor (SCF) of biomass. The optimized media selected from many optimal solutions; a set of Pareto solutions generated by multi-objective optimization was validated in a flat panel PBR. Using a single-stage cultivation strategy under diurnal light, *C. fritschii* has shown capability to produce DCW of 1.23 g/L with PHB content of 31.78 % and SCF of 93.63 with optimal media. This leads to the enhancement of both PHB content (2.72-fold) and SCF (1.64-fold) when compared to the nonoptimal medium. This is the first multi-objective optimization study for media optimization using cyanobacteria reported till now under diurnal light mimic to sunlight for bioplastic production.

C. fritschii was cultivated in flat panel PBR using optimized BG-11 medium under diurnal simulated sunlight with various levels of CO_2 starting from air to 5 %. A higher specific growth rate of 1.538 d^{-1} resulted with 1 % CO_2 with PHB accumulation of 31.78 % in single stage cultivation. The maximum PHB productivity of 33.15 mg/L/d with polymer production of 28 % was observed with 3 % CO_2. Air resulted in higher SCF values of 148 and PHB content of 19.85 %. Lower levels of CO_2 resulted in higher SCF values. Intracellular phosphate plays a significant role in cellular growth and carbon flow towards PHB accumulation. At the initial stage of cultivation, an average intracellular phosphate concentration (P_{intra}) of approximately 105.6 mg/g of cell was observed which was utilized during cultivation process for cellular growth and later for

carbon trafficking of supplemented acetate for PHB synthesis. PHB productivity of 30.3 mg/L/d and 33.15 mg/L/d resulted due to P_{intra} of 0.042 mmol/g and 0.073 mmol/g of cell with 1 and 3 % CO_2 respectively. Fed-batch studies with acetate during induction didn't enhance the PHB productivity after second feeding.

The hypochlorite digestion of NPCM may result in a decrease in the molecular weight of the recovered polymer when hypochlorite is used for single step PHB recovery. The loss in molecular weight of recovered PHB can be reduced while increasing yield and purity by dispersion of hypochlorite and chloroform. The hypochlorite-chloroform dispersion method achieved 95.51 % PHB recovery with 1 % biomass loading with 100 % (v/v) hypochlorite and chloroform along with pigment removal in single step. In addition to this, PHB extraction was performed with various halogenated solvents and green non-halogenated solvents with hypochlorite pretreatment. Selected solvents were unable to recover more than 90 % of polymer yield due to unsuitable operating conditions. Besides this, green solvent dimethyl carbonate (DMC) was employed to PHB recovery with prior pigment removal from biomass using chilled methanol. The DMC was capable of biopolymer recovery of 83.34 ± 0.76 % with a purity of 75 %. PHB recovered from DMC has improved thermal and material characteristics compared to PHB recovered using dispersion.

Single stage cultivation under diurnal light with multi-objective media optimization seeks attention in PHB production from *C. fritschii*. Utilizing CO_2 to produce high density biomass under diurnal light, PHB production with minimal supply of acetate as inducer, the recovery of intracellular polymer using DMC and the reduction in usage of hazardous halogenated solvents with ecofriendly green solvents making the PHB production from *C. fritschii* a sustainable approach.

CONTENTS

ABBREVIATIONS

ANOVA: Analysis of Variance

BCF: Biomass Correlation factor

CCD: Central Composite design

CoA: Coenzyme A

DCW: Dry cell weight

DMC: Dimethyl carbonate

DO: Dissolved oxygen concentration

DSC: Differential scanning calorimetry

EPS: Exopolysaccharides

FID: Flame Ionization Detector

FTIR: Fourier Transform Infrared spectroscopy

GC: Gas chromatography

GPC: Gel-permeation chromatography

HEPES: 4-(2-hydroxyethyl)-1-piperazineethanesulfonic acid

HPLC: High performance liquid chromatography

LED: Light Emitting Diode

MW: Molecular weight

OD: Optical density

PBD: Plackett-Burman design

PBR: Photobioreactor

PE: Polyethylene

polyP: Polyphosphate

PP: Polypropylene

PHB: Polyhydroxybutyrate

PU: Polyurethane

PWM: Pulse Width Modulation

PXRD: Powder X-Ray diffraction

rpm: rotations per minute

RSM: Response Surface Methodology

SCF: Auto-sedimentation Concentration Factor

TGA: Thermogravimetric analysis

UTM: Universal testing machine

VVM: Volume per volume per minute

LIST OF FIGURES

LIST OF TABLES

CHAPTER 1

INTRODUCTION

1.1. Background and rationale of the study

Fossil fuel-based plastics have been found to be severe environmental problems in the present era. Currently more than 390 million tons (Mt) of plastic has been produced throughout the world (Ali et al., 2023). Physical and mechanical properties of plastics are made use in construction, transportation, automotive components, medical equipment, agricultural tools, and electrical and electronic devices. Conventional plastics include polymers such as polyethylene (PE), polypropylene (PP), polyvinyl chloride (PVC), polystyrene (PS), and polyamides (nylons). Due to their difference in density, durability and cost, these polymers have different applications (Leal Filho et al., 2019). These long chain high molecular weight polymers are hydrophobic in nature and decomposition of the same under ambient conditions is difficult due to the resistance by microbial degradation. Excessive usage and improper management with lower rates of recycling resulted in plastic accumulation in the environment. Microplastics resulted by fragmentation of accumulated plastic due to abiotic stresses such as wear and tear and photochemical oxidation. These microplastics uptake by various aquatic species entered through food chain which may affect the physiological functions in human and resulting in various health issues (Issac & Kandasubramanian, 2021). Bio-based plastics can be used as an alternative to conventional plastics. Most bio-based plastics are biodegradable in nature, and they are either synthesized or derived from living systems. First generation bioplastics have been formulated from crop plants and other plant parts, but in the present era, it is not practicable due to the availability of less arable land and enormous food demand for a growing population. Starch-based plastics, which are a blend of starch and PE, came into use a few decades ago. Biodegradable starch is broken down by

soil microbes, while PE remains nondegradable. Later petroleum-based biodegradable plastics such as polyglycolic acid (PGA), polylactic acid (PLA), polyethylene oxide, and polycaprolactone were introduced, but they lack properties of PE (Khanna & Srivastava, 2005). At present 1% of all plastics produced are biodegradable. The degradation of bioplastic depends on the chemical composition, degree of crystallinity, and environmental factors (Tokiwa et al., 2009). Bioplastics of 2.2 Mt were produced in 2022 and the annual production of bioplastics may reach up to 6.3 Mt across the world by 2027 (Ali et al., 2023). Polyhydroxyalkanoates (PHAs) are 100 % degradable biopolymers produced by various microbes under nitrogen or phosphate starvation with excess carbon source. PHAs are similar to PP in nature and are aerobically degraded to water and carbon-di-oxide (CO_2). Under anaerobic conditions, they are degraded to methane by microbes present in the environment (Price et al., 2020). Polyhydroxybutyrate (PHB) is discovered by Lemoigne in 1926. PHB is stored as intracellular energy granules by various prokaryotes under nutrient limitations. Polyhydroxybutyrate is a short chain length PHA (scl-PHA) consisting of hydroxybutyric acid monomers, and has a molecular weight of 10^5-10^6 Da. PHB is isotactic and hence biodegradable (Wölfle et al., 2009). PHB is produced by heterotrophic bacteria such as *Alcaligenes eutrophus*, recombinant *E. coli,* and *Bacillus megaterium* (Ahn et al., 2000; Mohanrasu et al., 2020; Yang et al., 2010). Industrial production of PHB from bacteria may not be economically sustainable as it requires the use of expensive sugar substrates (30 – 40 % of the total production cost), an uninterrupted supply of oxygen, and excessive energy input (Nonato et al., 2001). In spite of properties of biopolymers such as biocompatibility, biodegradability, and non-immunogenicity, their high cost of production restricts their use in day today's life. Petroleum based plastics such PE and PP have a cost of US $1.25 – 2.53 per Kg, whereas the price of per Kg of bacterial PHA varies from $7.6-11.9 based on the quality required for the end use. In a study of

PHB production using sucrose as substrate the estimated cost of PHB found to be US $2.6 per Kg of polymer (Lopez-Arenas et al., 2017). Therefore, low-cost production systems are immediately required as an alternative. Cyanobacteria can also produce PHB with low-cost substrates such as acetate, a PHB inducer. Cyanobacteria are photosynthetic prokaryotes capable of PHB accumulation by CO_2 fixation using sunlight with minimal nutrients under nitrogen or phosphate limitations (Lee et al., 2022). PHB is produced by cyanobacteria such as *Synechocystis elongatus* PCC 6803 (Panda et al., 2006), *Synechococcus* sp. (Nishioka et al., 2001), *Chlorogloea fritschii* TISTR 8527(Monshupanee et al., 2016), *Aulosira fertilissima* CCC444 (Samantaray & Mallick, 2012), *Nostoc muscorum* (Bhati & Mallick, 2016) and *Calothrix scytonemicola* TISTR 8095 (Kaewbai-Ngam et al., 2016) and many others. Production of biopolymers from CO_2 plays significant role in the sustainable method of PHB production by cyanobacteria using CO_2 sequestration from flue gas and air (Garcia-Gonzalez & De Wever, 2017). The potential of cyanobacteria for CO_2 sequestering reduces environmental impacts such as global warming (Kumar et al., 2011). The usage of cyanobacteria is a better option as cyanobacteria can utilize nutrients from waste streams and can be cultivated in large scale using natural sunlight (Rueda et al., 2020). Cyanobacteria can be grown in small areas without competing for arable land required for terrestrial food crops (Das & Maiti, 2022). Cyanobacteria are capable of higher biomass productivity with bioremediation of wastewater with atmospheric CO_2 fixation using natural sunlight. Biomass can be utilized for commercial bioplastic production. However, PHB production from cyanobacteria is still non-viable due to lower growth rates, requirement of closed photobioreactors (PBRs), biomass harvesting and downstream processing of biopolymer with huge requirement of solvents (Yashavanth et al., 2021). Therefore, the present study focusses on cyanobacterial biomass production using sunlight energy along with high polymer content. The

study also focuses on cost effective downstream strategies for biomass harvesting and polymer recovery.

1.2. Problem Statements

Typically, a two-stage cultivation strategy for *C. fritschii*: growth in the presence of sufficient amounts of nitrogen and phosphate in media followed by PHB accumulation in the presence of inducers with nitrogen/phosphate limiting media. But two-stage cultivation is not economic due to the need for extra separation process for cell harvesting after growth in nutrient rich media and then cultivating in nutrient depleted media for PHB synthesis. Therefore, in current study PHB production is carried out using single stage process to avoid intermediate biomass separation step. Auto-sedimentation with a high settling rate is observed in the PHB-producing cyanobacteria *Chlorogloea fritschii* TISTR 8527. However, in the current study with *C. fritschii* TISTR 8527, it has been seen that the auto-sedimentation rate of biomass and percentage of PHB in biomass are conflicting with each other and both are dependent on the nutrient composition in media. Also, biomass concentration and percentage of PHB in biomass conflict with each other since there is a requirement of nutrient rich media for biomass growth and nutrient-depleted media for PHB accumulation. Therefore, the optimization of PHB production processes is a multi-objective optimization problem. Despite this, the application of multi-objective optimization to the PHB fermentation process has not been explored till now. Media optimization for achieving high biomass densities play a significant role in effectively utilizing sunlight or mimicked diurnal sunlight for the growth of cyanobacteria under different CO_2 levels. Apart from these, PHB recovery from bacteria has been widely explored till now. Studies have shown that pigments present in cyanobacteria affect the properties of recovered bioplastic. Hence our study focuses on

recovery of polymer with various extraction methods which include halogenated and green solvents with pigment removal.

1.3. Objectives of the study

The following goals were set for advancing research toward a sustainable future of bioplastics based on the problem statements, current difficulties, and anticipated requirements for commercial biopolymer synthesis from cyanobacteria. The main goal of the current study is to create a process design that is both efficient and affordable for growing cyanobacteria in a customized PBR with good gas mass transfer and mixing for high biomass and polymer production. Except for the initial screening with different nutrient limitations, the temperature was not intentionally adjusted throughout the investigation to reduce the process cost.

I. Development of media to increase biomass density by photoautotrophic assimilation of CO_2 as the sole carbon source using sunlight energy.

II. Development of process techniques to increase Polyhydroxybutyrate (PHB) concentration by using various strategies.

III. Development of a cost-economic biomass harvesting technique to ease the PHB extraction.

IV. Improvement of the PHB extraction strategy to obtain good quality and quantity PHB with the recovery of solvents.

1.4. Uniqueness of the study

The study highlights the media optimization for the single stage cultivation of cyanobacteria with phototrophic growth under diurnal light (artificial simulated) and dark based PHB production with inducers.

- Single stage cyanobacterial diurnal light for phototrophic growth and PHB production under dark with various concentration of acetate.
- Cultivation of cyanobacteria under diurnal light to study the effect of nitrate and dark based PHB production using acetate as inducer.
- Development of PBR setup using flasks and perforated silicone rubber tubing as a sparger for initial screening experiments (rather than using shaking incubator) which supports *C. fritschii* TISTR 8527 to perform better at higher light intensity of 140000 lux (1890 $\mu E/m^2/s$ for cool white LED).
- Simultaneous feeding of phosphate and nitrate for enhancing PHB production in photobioreactor systems.
- This is the first study which aims for multi-objective media optimization of growth (under diurnal simulated sunlight), polymer production (complete dark) and auto-sedimentation of cyanobacteria in small-scale PBR systems. The media optimization involves statistical designs such as Plackett-Burman design (PBD) and Response surface methodology (RSM).
- Role of Intracellular phosphate concentration in cellular growth and PHB accumulation.
- Fed-batch of phosphate and acetate for growth, PHB production and auto-sedimentation respectively.
- Recovery of biopolymer by green solvents with polymer characterization and solvents reusability.

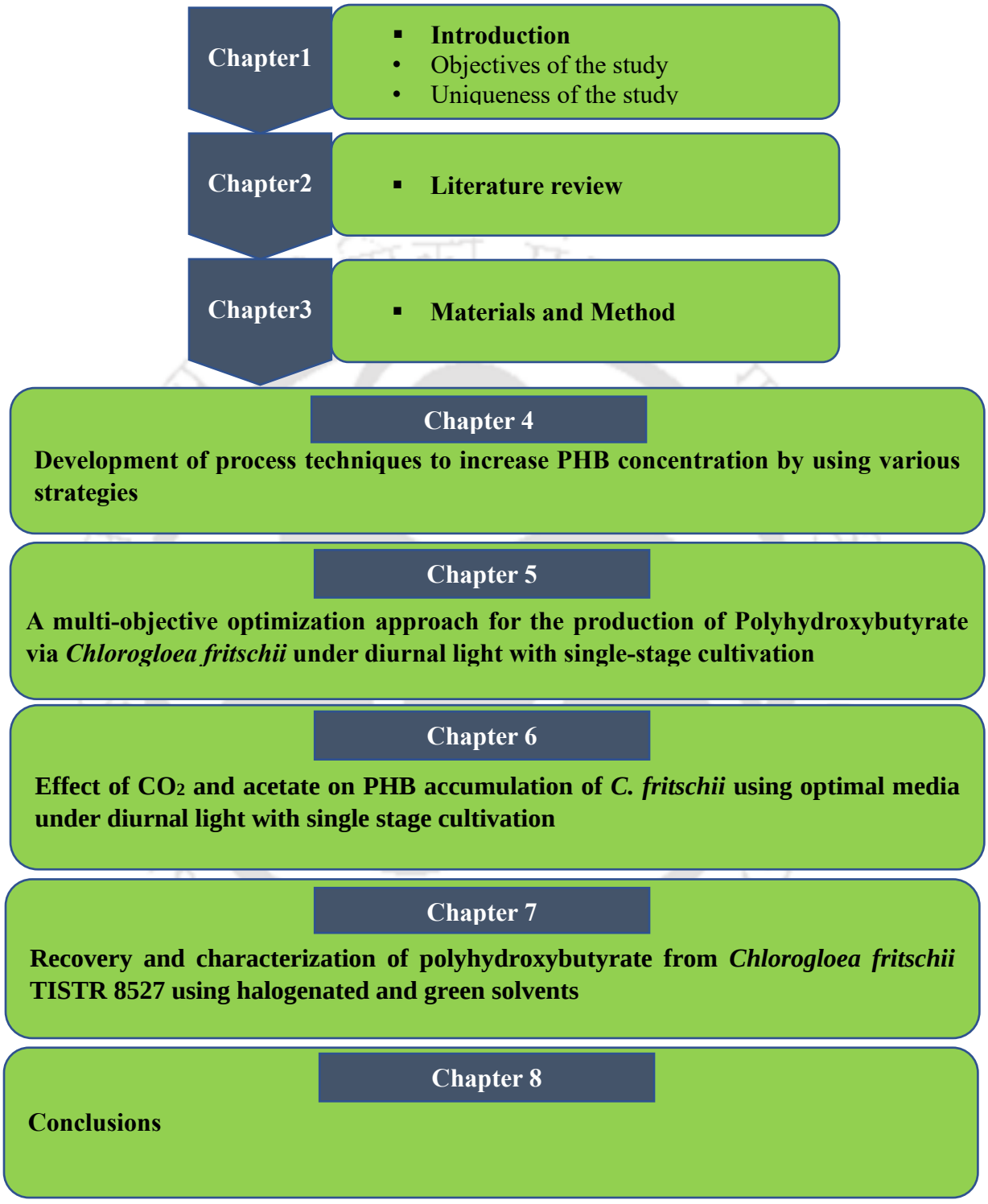

Fig. 1.1: Chapter wise organization of thesis.

1.5. Organization of Thesis

Chapter 1 presents the background and motivation by emphasizing the problem statement (current bottlenecks in cyanobacterial research), objectives of the study, uniqueness of the study, thesis organization (Fig. 1.1).

Chapter 2 reviews the recent scientific literature to contextualize the study against the global issues of conventional plastic, emergence of bioplastic as an alternative, importance of PHB, bacterial PHB production and its demerits, cyanobacteria as a sustainable feedstock, PHB production pathway and factors affecting its production, critical growth factors (e.g., sunlight, CO_2, mixing, etc.), process techniques for bioplastic production and extraction strategies of biopolymer.

Chapter 3 outlines materials and methodologies used for experimentation, experimental setup, and experimental procedures to accomplish the specified research objectives.

Chapter 4 deals with initial screening experiments in flask based PBR and flat panel PBR under constant and diurnal light for phototrophic growth. PHB production with acetate as an inducer under dark i.e. acetate variation. Effect of nitrate on growth and PHB accumulation, effect of phosphate and nitrogen starvation in PHB production with a focus on single-stage cultivation of *C. fritschii* for biopolymer production.

Chapter 5 focuses on multi-objective media optimization of growth under diurnal simulated sunlight, polymer accumulation under complete dark and auto-sedimentation of *C. fritschii* in small-scale PBR systems namely flask PBRs and test-tube PBRs. The media optimization involves statistical designs such as Plackett-Burman design (PBD) and Response surface methodology (RSM). Final validation of the optimized solution was performed in medium scale flat panel PBR.

Chapter 6 was detailed with the effect of different concentrations of CO_2 on growth, PHB accumulation and auto-sedimentation *C. fritschii* using optimal media with single stage cultivation using flat panel PBR. It also focuses on the role of intracellular phosphate on PHB accumulation and maintenance of intracellular phosphate by phosphate fed batch in medium scale flat panel PBR.

Chapter 7 mainly focuses on the recovery of biopolymer from *C. fritschii* TISTR 8527 using hypochlorite-dispersion method, PHB recovery by halogenated and nonhalogenated solvents with hypochlorite pretreatment. Recovery of PHB using green solvent DMC with pigment removal. The recovered polymer was characterized by various techniques such as FTIR, DSC, TGA, UTM, and GPC.

Chapter 8 provides the **overall conclusions** drawn from all the studies conducted towards accomplishing the designated objectives.

CHAPTER 2

Review of Literature

2.1. Global issues of Plastic

Fossil-based plastic has become an integral part of human life owing to its durability. However, this is less degradable due to its inertness to physical and chemical stresses. Petroleum-based plastic has invariably had a wide range of applications in automobiles, home appliances, laboratory instruments, food packaging, and medical devices over the last seven decades. Despite its large application in day-to-day life, these plastics are not eco-friendly and are nonbiodegradable (Khanna & Srivastava, 2005). Plastics production and use have been expanded in recent decades due to a growth in applications that rely on plastics' beneficial characteristics such as light weight, strength, durability, low prices, corrosion resistance, and low production costs. Transparent films made of plastic are strong and impermeable to gas and moisture and are used in food packaging applications. From 1950 to 2015, around 8300 Mt of plastics were produced globally, resulting in roughly 6300 Mt of plastic waste materials, of which approximately 9 % was recycled, 12 % was burnt, and 79 % ended up in landfills (Geyer et al., 2017). Thus, due to rapid expansion of large manufacturers, India creates 9.46 Mt of plastic waste annually, with single-use plastic accounting for 43 % of total waste and uncollected plastic garbage accounting for 40 % (Bansal et al., 2023). Global plastic production reached 368 Mt in 2019 and will be doubled within the next 20 years (Dasgupta et al., 2022). Plastic usage has environmental impacts with concerns raised towards solid waste management. Predictions say that around 53 Mt of plastic waste will be entering the aquatic ecosystem by 2030 which affect the food chain and influence human health (Borrelle et al., 2020; Castro-Castellon et al., 2022; Weber et al., 2022). Apart from these, the processing of plastic results in the emission of greenhouse gases (GHGs) and hence global

warming. Plastic is currently at the topmost agenda of international waste management. The solution to these problems is the large-scale production and usage of bioplastics or biodegradable plastics which are functionally similar to polyethylene (PE) or polypropylene (PP).

Bioplastics are biodegradable in nature which includes polymers such as Polycaprolactone (PCL), Polybutylene succinate (PBS), Polylactic acid (PLA), starch, and cellulose-based bioplastics. The degradation of bioplastic depends on their composition, degree of crystallinity, and environmental factors (Tokiwa et al., 2009). Polyhydroxyalkanoates (PHAs) are bio-based esters that can be synthesized from renewable sources such as plants and heterotrophic bacteria. Polyhydroxybutyrate (PHB) is a bioplastic discovered in bacteria by Lemoigne in the early 1920s (Lemoigne, 1926), belongs to the polyhydroxyalkanoates (PHAs) family. PHB is produced by many prokaryotes and stored intracellularly as an energy source. PHB derived from living cells is a 100 % biodegradable thermoplastic with remarkable resemblance to PP (Markl et al., 2018). It will be produced during times of nutritional limitation and stress. PHB is a homopolymer of 3-hydroxybutyric acid units and it has a linear structure. The presence of amorphous and crystalline regions makes the polymer partially crystalline with 60-70 % of the degree of crystallinity (Nishida & Tokiwa, 1993). The molecular mass of these polymers ranges between 2×10^5 Da and 3×10^6 Da depending on the microorganism and the growth conditions. PHB is a brittle material (Verlinden et al., 2007). Along with other polymers, the stiffness and brittleness of PHB can be reduced. Homo-polymer of 3-hydroxybutyrate i.e. PHB has a helical crystalline structure. This structure seems to be similar in various copolymers of hydroxybutyrate (Padermshoke et al., 2004; Singh, 2015).

PHB is isotactic and hence biodegradable (Wölfle et al., 2009). PHB is hydrophobic and has high solubility in organic solvents such as chloroform, dichloromethane and dichloroethane etc. Thermoplastic nature, biocompatibility, piezoelectricity, and stereospecificity are some of the features of PHB. These qualities allowed PHB to be used in a variety of fields, including health, agriculture, and the environment.

In the biomedical field, PHB is used in the form of surgical sutures, wound dressing, ocular devices, bone plating systems, surgical mesh, cardiovascular patches, and orthopedic pins. PHB is also used for the manufacturing of bone marrow scaffolds, tendon, and cartilage repair devices (Chen & Wu, 2005; Patnaik, 2007). The antimicrobial nature of PHB made its use in aquaculture in preventing the *Vibrio* epidemics (Defoirdt et al., 2007). It is also used in the development of antifouling agents. PHB hydrogels play an important role in the targeted drug delivery and sustained release of drugs (Fang et al., 2023). Methyl groups of PHB help in the adhesion of cells by promoting extracellular matrix (Sangsanoh et al., 2017). This feature made PHB be used in skin healing both in vitro and in vivo (Castellano et al., 2018). Thus, PHB has applications in various fields.

Currently PHB is produced by heterotrophic bacteria such as *Alcaligenes eutrophus*, recombinant *E. coli*, and *Bacillus megaterium* and needs the supply of glucose under sterilized conditions (Ahn et al., 2000; Mohanrasu et al., 2020; Yang et al., 2010). For these fermentation processes, large amounts of organic carbon sources are necessary, accounting for approximately 50 % of the total production costs (Halami, 2008). An alternative way of producing PHB is the use of prokaryotic algae, better known as cyanobacteria which are global primary biomass producers using sunlight as the sole energy source to bind atmospheric CO_2. Blue-green algae or cyanobacteria can produce PHB with minimal nutrients under nitrogen or phosphate limitations (Lee et al., 2022).

Recombinant *E. coli* has been reported to produce PHB with glucose ($ 0.77 USD per Kg) as feedstock with production cost of $ 7.87 per Kg of polymer (Choi & Lee, 1997). Leong et al. has reported PHB production cost of $ 6.72 per Kg of PHB with C. *necator* H16 using glycerol ($ 0.53 per Kg) as a carbon source and annual target of 9000 tons (Leong et al., 2017). Price et al. has reported a PHB selling price of $ 7.7 per Kg from cyanobacteria with PHB content of 10 % (w/w) using CO_2 as a cheap carbon source with annual target of 10000 tons of PHB per year (Price et al., 2022). These prices are three times higher than the production cost of PE/PP ($ 1.25–2.53 per kg) (Chavez et al., 2022; Price et al., 2022). Hence researchers need to use minimal nutrients for PHB production from cyanobacteria using sunlight with considerable PHB yield and usage of minimal steps down-stream processing can reduce total cost of PHB production. Some of the cyanobacteria namely *Aulosira fertilissima* (Samantaray & Mallick, 2012), and *Synechocystis* sp. (Rueda et al., 2022) and *Nostoc muscorum* (Costa et al., 2018) are capable of PHB production without the addition of sugar and good yield.

2.2. Cyanobacteria and PHB synthesis

Cyanobacteria are gram-negative microorganisms that have been evolved for a long time and are the only prokaryote that can accomplish oxygenic photosynthesis with limited nutrients. Its photosynthetic machinery can convert 3-9 % of solar energy into biomass (Lau et al., 2015). PHB is stored inside the cell as granules by cyanobacteria (Jendrossek, 2009), and these granules appear black when stained with Sudan black B (Wei et al., 2011) and brilliant orange when stained with Nile blue A (Shrivastav et al., 2010). Glycogen and PHB are energy and carbon sources for cyanobacterial cells (Khanna & Srivastava, 2005; Koutinas et al., 2007). Many cyanobacteria have a native PHB pathway (Fig. 2.1), whereas others have been genetically modified to produce PHB

via a synthetic pathway (Carpine et al., 2015; Khetkorn et al., 2016). Cyanobacteria can be grown under mixotrophic conditions yielding more biomass in the presence of acetate, citrate, glucose, fructose, propionate, etc. (Yashavanth et al., 2021). As a result of their high photosynthetic efficiency, the ability to grow with less nutrients resulting in high biomass, and availability of modern genetic modification tools, cyanobacteria are a good prospect for commercial PHB production.

It has been seen that a small amount of acetate supplemented (~0.05 % to 1 %) in the medium acts as an inducer for PHB synthesis under nitrate and phosphate-limited conditions (Kaewbai-Ngam et al., 2016). The acetate gets converted to acetyl CoA, a precursor to PHB synthesis and simultaneously breaks the thermodynamic barrier for the conversion of acetyl-CoA to acetoacetyl-CoA by β-ketothiolase (*phaA*), thereby promoting PHB accumulation (Liu et al., 2019; Wu et al., 2001). Aceto-acetyl CoA gets reduced to 3-hydroxybutyryl CoA by aceto-acetyl CoA reductase (*phaB*) with NADPH as a cofactor. PHB synthase (*phaCE*) polymerizes 3-hydroxybutyryl-CoA to PHB (Hondo et al., 2015). *phaA* and *phaB* are organized in one operon encoding for the β-ketothiolase and acetoacetyl-CoA reductase. *phaC* and *phaE* are in another operon encode for the two subunits of the type III PHA synthase (Taroncher-Oldenburg et al., 2000).

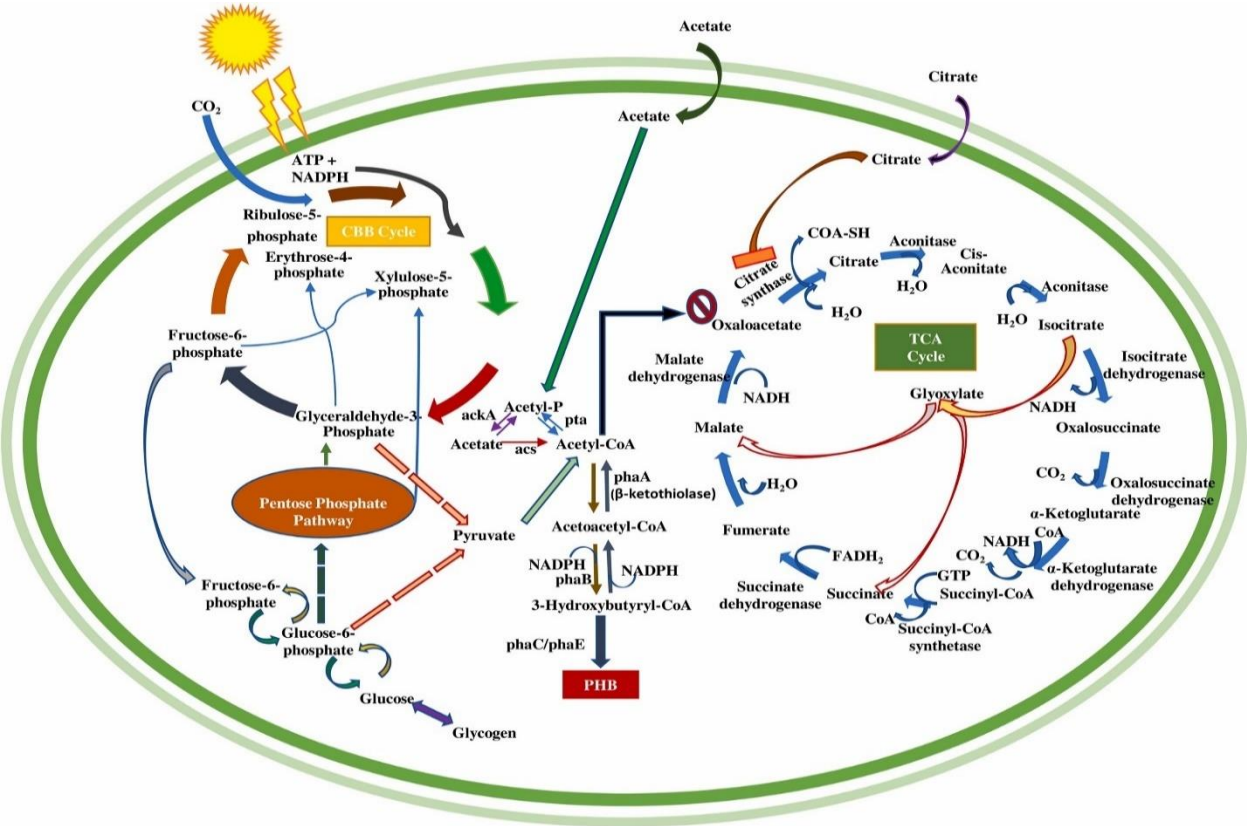

Fig. 2.1: Schematic representation of PHB synthesis pathway. Cyanobacteria with native genes for PHB synthesis uses acetyl CoA as precursor to synthesize PHB in three steps. phaA: β-ketothiolase, phaB: acetoacetyl-CoA reductase, phaC/phaE: PHB synthase, ackA: acetate kinase, pta: Phosphate acetyltransferase, acs: acetyl-CoA synthetase.

2.3. Nutrients and PHB accumulation

Cyanobacteria have been grown in different culture mediums, namely, Pringsheim's Medium (Pringsheim, 2016), BG11 medium (Rippka et al., 1979), Fogg's medium (Fogg & Thake, 1987), etc., while researchers commonly use BG11 and $BG11_0$. The cultivation of cyanobacteria requires macro and micronutrients, mainly nitrogen and phosphate for proper growth. A higher concentration of nutrients may be suitable for the growth of some of the cyanobacteria and vice versa. Limitations of phosphorus and nitrogen source along with

supplementation of inducers such as acetate can trigger PHB accumulation (Kaewbai-Ngam et al., 2016).

2.3.1. Nitrogen starvation and PHB accumulation

During nitrogen starvation, the cells gradually change from a vegetative state to a dormant state. The most obvious feature of this is the change in color from blue-green to brownish yellow. This phenomenon is called “nitrogen chlorosis” (Allen & Smith, 1969). During nitrogen starvation, there is a degradation of phycocyanin and chlorophyll. The growth of the cells decreases due to the decrease in photosynthetic activity. Nitrogen limitation is the most important and best-studied trigger for PHB production in cyanobacteria (Hauf et al., 2013). Non-diazotrophic strains are not able to bind molecular nitrogen and depend on nitrogen in the form of nitrate or ammonium. Nitrogen-depleted cells cannot synthesize the necessary proteins for reproduction and, therefore, start to accumulate storage compounds like PHB. Another important function of PHB synthesis is to compensate for imbalanced metabolic situations, as it acts as an electron sink and delivers new reduction equivalents in the form of NADP+. Cells will adapt to nitrogen deficiency by the activity of two transcription factors NtcA and PII-signalling protein. A gene *sll0783* will be induced more and it has a binding site for NtcA. NtcA will increase the expression of all genes such as β-ketothiolase, acetoacetyl-CoA reductase and PHB synthase. During nitrogen starvation, excess NADPH pool along with all enzymes increases PHB accumulation. Mutation of *sll0783* in *Synechocystis sp.* PCC 6803 alters the localization of PHB synthase and reduces PHB accumulation (Schlebusch & Forchhammer, 2010).

2.3.2. Phosphate starvation and PHB

During phosphate starvation, ATP pools will be reduced in the cell. Phosphate starvation results in a high C/P ratio of the cell. Hence, stored phosphate in polyphosphate (polyP) form will be utilized for phosphate-rich carbon compounds (intermediate of various pathways) required for the survival of blue-green algae. Hence, excess carbon will be stored as PHB granules (Bottomley & Stewart, 1976). Phosphate starvation also activates genes present upstream of PHB synthesis genes, which results in increased expression of PHB synthesis genes (Romano et al., 2015; Schembri et al., 1995). Thus, phosphate starvation or limitation can trigger PHB accumulation in cyanobacteria. When the concentration of phosphate is very low, cell death may occur. Nishioka et al. reported 55 % PHB in *Synechococcus* sp. MA19 under phosphate limitation. The usage of insoluble phosphate such as $Ca_3(PO_4)_2$ helps to increase the PHB to 55 % of cell dry weight by maintenance of intracellular phosphate in the range of 0.043-0.076 mmol of P/g of cell. The above condition supported growth based PHB accumulation in *Synechococcus* sp. MA19 (Nishioka et al., 2001).

2.3.3. Acetate an inducer of PHB accumulation

Cyanobacteria grown in photoautotrophic mode resulted in a PHB of less than 10 % (w/w) (Ansari & Fatma, 2016). *Nostoc muscorum has* grown in BG11 medium without $NaNO_3$ and 2 % CO_2 produces 8.5 % of PHB (Bhati et al., 2010). *Synechocystis* PCC 6803 grown in BG11 medium without $NaNO_3$ produces PHB yield of 4.1 % (Wu et al., 2001). *Spirulina platensis* grown in the mineral salt medium showed an accumulation of PHB of 6 % (Campbell et al., 1982). Therefore, researchers started supplementing media with carbon sources such as glucose, fructose, acetate

and citrate to increase the PHB in algae and cyanobacteria. Glucose and fructose supplementation increase the NADPH pool via the Pentose Phosphate Pathway which acts as a cofactor of aceto-acetyl CoA reductase.

The acetyl CoA is the precursor to PHB accumulation. The acetate supplemented in the medium acts as an inducer for PHB synthesis rather than a carbon source. The added acetate gets converted to acetyl CoA. Apart from this, the acetyl-CoA pool and NADPH (cofactor of acetoacetyl-CoA reductase) come from Embden Meyerhof Parnas (EMP) and Oxidative Pentose Phosphate (OPP) pathways respectively (Koch et al., 2019). Studies showed that PHB accumulation is enhanced when inducers such as citrate or acetate are supplied under nitrate and phosphate-limited conditions (Kaewbai-Ngam et al., 2016). Under such starved conditions, the redox state of the cell (high value of [NADPH]/[$NADP^+$]) and the ratio of [acetyl-CoA]/[CoA] also plays a crucial role in acetyl-CoA flux towards PHB synthesis (Ren et al., 2009). Apart from these, acetate is a low-cost substrate as it can be obtained from the hydrolysis of lignocellulosic biomass and anaerobic digestion and usage of the same reduces the production cost (Lim et al., 2018). Thus, PHB accumulation increase with acetate supplementation in cyanobacteria (Wu et al., 2002).

2.4. PHB accumulation in light and dark

DNA binding regulator *RpaA* is primarily engaged in the regulation of genes linked to CO_2-assimilation in the light and to carbon metabolism in the dark, according to transcriptome analysis. During the night period, *Synechocystis* PCC 6803 Δ*rpaA* mutant exhibited downregulated levels of *phaB*, *phaE*, and *phaC*, which are involved in the PHB synthesis, in comparison to the wildtype strain. In the transcriptome analysis of *Synechococcus elongatus*, elevated levels of mRNA of

phaE, a subunit of PHB synthase (*phaCE*) was observed during dark when compared to light. Hence, PHB accumulation was more in dark condition (Köbler et al., 2018). Limitation of inorganic phosphorus reduces the ATP generation by breakdown of polyP and creating an imbalance in the NADH/ATP ratio. This imbalance has been reported to the activation of PHB synthesis genes. In the case of cyanobacteria acetyl CoA pool comes from CO_2 fixation during light. The glycogen stored will be degraded to increase pyruvate which gets converted to acetyl-CoA. Increased acetyl CoA and NADH enhances the PHB accumulation (Kamravamanesh et al., 2019). **Table 2.1** lists the PHB accumulation in various bacteria and cyanobacteria under various conditions starting from small scale to medium scale.

Table 2.1: PHB accumulation in bacteria and cyanobacteria with various reactor scale under different culture conditions.

Cyanobacteria	***Culture Condition***	***Scale of the rector (L)***	***Inducers***	***% PHB on dry biomass***	***PHB productivity (mg/L/d)***	***References***
Bacillus megaterium	Heterotrophic	3	-	54.56	2109	(Mohanrasu et al., 2020)
Escherichia coli strain CGSC 4401	Heterotrophic	6.6	-	80	61190.48	(Ahn et al., 2000)
Ralstonia eutropha NCIMB 11599	Heterotrophic	0.005	-	-	5230	(Sivashankari et al., 2023)
Ralstonia eutropha	Heterotrophic	5	-	67	74400	(Shang et al., 2003)
Gleocapsa gelatinosa	Photoautotrophic	0.05	-	5.6	-	(Ansari & Fatma, 2016)
Spirulina subsalsa	Photoautotrophic (Nitrogen limitation)	0.1	-	14.7	5.8	(Shrivastav et al., 2010)
Aulosira fertilissima	Photoautotrophy (Phosphorous deficiency)	0.05	-	10.5	1.815	(Samantaray & Mallick, 2012)
Synechococcus sp. MA19	Photoautotrophy (Phosphate starvation, 55 °C)	0.450	-	55	220.8	(Nishioka et al., 2001)

Synechocystis PCC 6803 (recombinant)	Mixotrophic (Nitrogen starvation)	0.05	0.4 % acetate	35	-	(Khetkorn et al., 2016)
Aulosira fertilissima CCC 444	Mixotrophic (5.58 mg/L of K_2HPO_4)	0.05	0.26 % citrate, 0.28 % acetate	85	84.1	(Samantaray & Mallick, 2012)
Chlorogloea fritschii *TISTR 8527*	Heterotrophic (Nitrogen and phosphate starvation)	0.15	0.2 % acetate	30.7	19.6	(Monshupanee et al., 2016)
Synechocystis sp.	Heterotrophic (Salinity stress)	3	0.123 % acetate	26.1	15.7	(Rueda et al., 2022)
Neowollea manoromense	Phototrophic (Nitrogen and phosphate starvation)	0.1	0.4 % acetate	9.1	30.32	(Samadhiya et al., 2023)
Synechocystis sp. PCC 6714	Phototrophic	40	-	16.2	19.2	(Kamravamanesh et al., 2019)
Synechocystis sp. CCALA192	Phototrophic	200	-	6.6	140	(Troschl et al., 2017)

2.5. Regulation of PHB at enzymatic level

During normal growth of cyanobacteria with proper nutrient availability, high citrate synthase activity results in free CoA-SH which inhibits the β-ketothiolase (phaA) activity of the PHB

pathway (Senior & Dawes, 1973). Under nutrient limitation, the abundance of NADH inside the cell inhibits citrate synthase activity, thereby restricting the flow of acetyl-CoA into the TCA cycle. This leads to an increase in the acetyl-CoA, which then gets condensed by β-ketothiolase (Senior & Dawes, 1971). At the same time, increased NADPH enhances aceto-acetyl CoA reductase activity, which is the second step in PHB synthesis. Under nitrogen starvation the enzyme phosphotransacetylase shows higher activity which converts acetyl-CoA to acetyl-phosphate. Acetyl-phosphate activates membrane bound PHB synthase to polymerize 3-hydroxybutyryl CoA to PHB (Miyake et al., 2000). Thus, PHB synthesis is regulated at enzymatic levels.

2.6. Factors affecting cyanobacterial growth and PHB accumulation

The development of the cultivating system, an adequate amount of nutrients, the availability of light intensity, the supply of CO_2, mixing and mass transfer, process pH, and culture temperature are the main parameters that affect cyanobacterial growth and PHB production. Cyanobacteria assimilate CO_2 in nature by photosynthesis using sunlight energy. Approximately 0.04 % (v/v) CO_2 is present in the atmosphere which may limit the growth of algae at high light intensity. Carbon dioxide supplied exist in different forms in culture medium. Buffering by the bicarbonate equilibrium system will influence the transportation of CO_2 and hence the growth kinetics.

$$CO_2\,(g) \rightleftharpoons CO_2\,(aq) + H_2O \rightleftharpoons H_2CO_3 \rightleftharpoons H^+ + HCO_3^- \rightleftharpoons H^+ + CO_3^{2-} \quad \text{……} \quad \textbf{(2.1)}$$

Acidic or neutral pH is suitable for carbon fixation by cyanobacteria due to the preferability of CO_2 (a form of CO_2 at acidic pH) and bicarbonate (a form of CO_2 at neutral pH) over carbonate (a form of CO_2 at alkaline pH) (Eq. 2.1). Supply of elevated levels of CO_2 may be expensive while used in large-scale culture systems may result in an unsustainable process. This is due to formation of carbonic acid which reduces the pH of the culture medium thereby affecting cyanobacterial

growth. Hence there is a need for buffer systems or pH control by acid or base. Bicarbonate and HEPES buffers are some examples of buffers used in the cultivation of cyanobacteria (Imamura et al., 1983; Scherholz & Curtis, 2013).

Several environmental factors such as pH, temperature, light intensity, and nutrients availability and CO_2 concentrations affect CO_2 assimilation by cyanobacteria. CO_2 fixation can be maximized by the usage of controlled conditions for growth in Photo-bioreactors (PBRs) (Kumar et al., 2011). PBR is advantageous for microalgal cultivation as it prevents water loss and contamination issues. Optimal light intensity is the primary requirement for cell growth, which an ideal PBR should provide. Tubular (Meixner et al., 2016), bubble column (Carpine et al., 2015), stirred tank (Eberly & Ely, 2012; Kamravamanesh et al., 2017), bag-based (Ma et al., 2021), and flat-panel PBRs (Krasaesueb et al., 2019; Yashavanth & Maiti, 2024) are widely used for mass culture of cyanobacteria. Cyanobacterial culture is mainly influenced by light and CO_2. Substantial amount of work has been carried out for scaling-up the photobioreactors and developing new photobioreactor considering light availability, mixing, CO_2 and O_2 gas mass transfer and hydrodynamics of the bubbles to reduce the process cost. Proper utilization of supplied CO_2 depends on the availability of light per cell. A high CO_2 supply may result in a decrease in the pH of the culture at low light intensity whereas low CO_2 may decrease productivity at high light intensity due to reactive species generated at high light intensity may result in photo-inhibition of algal cells (Murata et al., 2007). Therefore, the selection of CO_2 level is also decided by light availability. The maximum CO_2 bio-fixation rate of 0.587 g/L/d using *Anabaena* sp. PCC 7120 was reported using $BG11_0$ at a light intensity of 120 $\mu E/m^2/s$ and 5 % (v/v) CO_2 in the airlift photobioreactor. The same species tolerated the CO_2 level up to 7 % (v/v) when checked with different concentrations (Nayak & Das, 2013). Studies with *Thermosynechococcus elongatus* BP-

1 in 2.7 L stirred tank reactor showed that culture grown with atmospheric CO_2 produced PHB of 14.5 % due to carbon limitation when compared to 5, 10, and 20 % CO_2 supplemented cultures. Thus, higher CO_2 supplied may need not result in higher PHB instead it supports higher biomass generation. *Synechococcus* sp. MA19 resulted in PHB accumulation of 21 % and 62 % with 2 % CO_2 under nitrogen and phosphate starvation respectively. The ideal temperature and pH for the thermophilic strain *Synechococcus* sp. MA19 were 50 °C and 8.0, respectively (Miyake et al., 1996; Nishioka et al., 2001). Whereas most of the cyanobacteria require 25 - 32 °C of optimal temperature and optimal pH of 7.5 - 9.5 for PHB production (Ansari & Fatma, 2016; Kaewbai-Ngam et al., 2016; Sharma & Mallick, 2005). In a study with genetically engineered *Synechoccus elongatus* UTEX 2973, PHB of 10.5 % with biomass of 1.2 g/L was obtained using outdoor sunlight with 3 - 6 % CO_2 after 10 d of cultivation (Roh et al., 2021). Usage of optimal CO_2 levels under sunlight (diurnal light, which varies with time) may help in the reduction of production costs. Fig. 2.2 represents the diurnal light pattern of one sunny day in May in Guwahati (Naira et al., 2019).

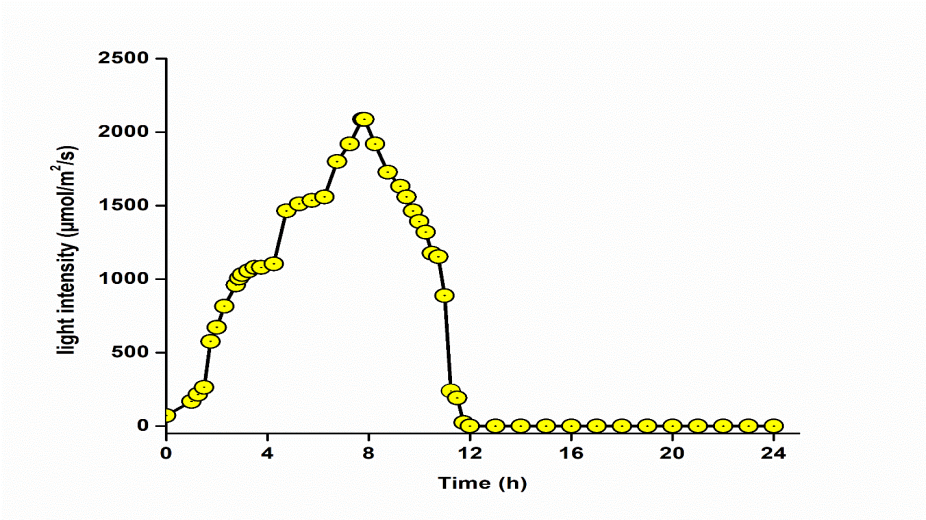

Fig. 2.2: The diurnal simulated sunlight pattern used for the cultivation of *C. fritschii* for media optimization (Yashavanth & Maiti, 2024).

2.7. Role of Intracellular Phosphate in cyanobacterial growth and PHB accumulation

The medium used for culturing the blue-green algae contains an adequate amount of nutrients required for the growth of algae (Rippka et al., 1979). Phosphate is an important factor in the synthesis of nucleic acids and membranes. It plays a significant role in energy metabolism by involving in redox and phosphorylation/dephosphorylation reactions. It plays a unique role in protein modulation for various cellular processes. The supplied inorganic phosphate (P_i) can be transported to cells from the medium and stored as polyP granules via H^+/P_i (Phosphate Transporter 1) or Na^+/P_i (P_i Transporter B) symporters present on the plasma membrane to the vacuoles (Moseley et al., 2006). The formation of polyP implies that excess phosphate is taken by the cells by phosphorylation of ADP to ATP by polyphosphate kinase (Hürlimann et al., 2007). polyP complexes with calcium and other cations and stored in the vacuoles and can be termed acidocalcisomes. Under phosphate deprivation, polyP will be hydrolyzed by endo-polyphosphatases and release P_i from the stored granules which will be utilized by the cell. Under phosphate starvation, PHOSPHATE STARVATION RESPONSE proteins (PHRs) bind to the promoter of Phosphate Transporter 1 and enhance Pi uptake from medium to cell and also from the phosphate granules (Bustos et al., 2010). During phosphate starvation, reduced levels of phosphorylated intermediates of the Pentose phosphate pathway result in a reduction of carbon fixation (Moseley et al., 2006). PHB synthase gene will be upregulated and hence results in PHB accumulation. In a study with *Synechococcus* sp. MA19, 55 % of PHB was accumulated with intracellular phosphate of 0.043 – 0.076 mmol/g of cell maintained with calcium phosphate than control (Nishioka et al., 2001). Hence, in the present study with *C. fritschii* TISTR 8527, there is a need for minimal intracellular phosphate to be maintained for good levels of polymer production. Various methods are available for the extraction of stored polyP granules by ultrasonication,

incubation using alkali or acids, boiling with water, and freeze and thaw methods (Eixler et al., 2005).

2.8. Biomass harvesting

Harvesting of biomass refers to the concentration of cyanobacterial mass cultures into thick cakes for the extraction of desirable products from them. Cyanobacterial harvesting can be done using filtration, coagulation/flocculation, sedimentation, and flotation. Large-scale production demands cost-effective biomass recovery for affordable end products since 20-30 % of total biomass production cost is due to the harvesting of cells (Grima et al., 2003).

The harvesting methods are categorized into two main stages:

1. **Thickening Procedures:** These concentrate the microalgal slurry to about 2-7 % total suspended solids. Sedimentation, flocculation, flotation and autosedimentation were involved in thickening procedures.

2. **Dewatering Procedures:** These further concentrate the slurry to 15-25 % total suspended solids. Centrifugation and filtration are some dewatering harvesting methods (Fasaei et al., 2018).

2.8.1. Filtration

Filtration is a simple method, which involves a membrane to separate the biomass against pressure drop. Both ultrafiltration and microfiltration methods have been used for harvesting microalgae from broth (Bilad et al., 2012; Drexler & Yeh, 2014). Energy requirement in the filtration process is lesser than other dewatering strategies like centrifugation; however, as filtration occurs, the cake formation increases the resistance and decreases the flux resulting in high operational cost. Fragile microalgal cells were harvested efficiently using tangential flow filtration to minimize the

membrane clogging (Ahmad et al., 2012; Elcik & Cakmakci, 2017; Petrusevski et al., 1995). Hollow fiber and the tubular membrane were also used for microalgae recovery (Bhave et al., 2012; Khademi, 2014). This polymeric membrane showed the capability to achieve 150 g/L (dry weight) biomass of *Nannochloropsis* sp. and 99 % of volume reduction with an estimated energy requirement of 0.3-0.7 kWh/m^3 (Bhave et al., 2012). Microalgal (*Scenedesmus* and *Ankistrodesmus*) and cyanobacteria (*Microcystis*) rich water subjected to filtration using freshwater mussel *Elliptio complanata* at different flow rates were also studied (Stuart et al., 2001).

2.8.2. Coagulation/Flocculation

Coagulation or flocculation is a process of harvesting in which cell surface charges are neutralized by the usage of chitosan-like polymers, cationic salts such as $AlCl_3$, $Fe_2(SO_4)_3$, or $Al_2(SO_4)_3$ (Yuheng et al., 2016). It is suitable for harvesting, but the chemicals alter the biochemical composition of the cell and increase the chance of contamination (Vandamme et al., 2013). Genetic modification of cyanobacterial strains evaded the use of chemicals. Reduced S-protein expression in the outer envelope of *Synechococcus elongatus* PCC 7942 and increased α-flag tag in surface porin SomA resulted in 70% of biomass recovery by protein A coated magnetic beads (Fedeson & Ducat, 2017). *Microcystis aeruginosa* 1343 (M1) and 905 (M9) were subjected to settling by magnetic nanoparticles with the usage of polyethylenimine coated iron oxide nanoparticles, recovered 93.3 % and 97.5 % biomass respectively by neutralizing surface charges with extracellular organic matter removal (Wang et al., 2020). Besides using chemical flocculants, cell recovery by bioflocculation can be done. A quinovose containing bioflocculant MNXY1 from *Klebsiella pneumoniae* strain NY1 had flocculated 50 % of *Synechocystis* UTEX 2470 within 10 mins, with 95 % of biomass recovery after an hour (Nie et al., 2011). Bioflocculation of *Synechococcus subsalsus* and *Spirulina maxima* with *Aspergillus niger* pellets (1:5 cyanobacterial:

fungal ratio) had a 94% efficiency with a biomass concentration factor of 62.8 (Oliveira et al., 2019). A study on biofilm grown with air bubbling and shaking resulted in 70% biomass recovery in the log phase of growth, whereas the decline phase showed poor recovery. The bubbled system with the highest initial biomass concentration (IBC) exhibited better recovery indicating the dependency of bioflocculation on IBC, type of mixing system, and growth period (Iasimone et al., 2020).

2.8.3. Autosedimentation

Instantaneous settling of cyanobacterial cells due to cell clumping and cluster formation is autosedimentation. Some of the lipid-rich microalgae *Desmodesmus* sp. F2 and *Chlorella minutissima* showed this phenomenon and aided easy recovery following cultivation (Bhatnagar et al., 2010; Ho et al., 2013). A cyanobacterium *Chlorogloea fritschii* TISTR 8527 showed this property with 91% biomass recovery in a minute (Monshupanee et al., 2016). Engineering cyanobacterial cells for changing cell morphology can affect the settling rate. FtsZ is a cytoskeletal tubulin-like protein that helps in cell elongation, cell division and also for sedimentation. In *Synechococcus elongatus* PCC 7942 overexpression of *minC* and *cdv3* caused the dislocation of FtsZ and elongation of PCC 7942 up to few millimeters resulting in natural settling of cells (Jordan et al., 2017). In a filamentous cyanobacterium *Fremyella diplosiphon*, overexpression of *bolA*, a transcription factor of actin-like protein MreB causes elongation up to five folds without altering cell function and enhance the sedimentation (Singh & Montgomery, 2015). Thus, biomass separation by sedimentation allows repeated use of media and makes the downstream process easier.

2.8.4. Floatation

Heterocystous cyanobacterium, *Anabaena* sp. PCC 7120 has a high flocculation rate due to its filamentous form and mucilage secretion. Flocs formation, along with biohydrogen production of 0.72–1.10 μmol H_2 per mg dry cell weight, resulted in 91.71 % biomass recovery by auto-flotation of cells (Chen et al., 2014). Cyanobacterial cells subjected to air flotation using a froth forming biodegradable methylated ovalbumin (MeOA), with 0.3 mass flow rate of MeOA gave 85% recovery (Maruyama et al., 2009). Magnesium is an essential nutrient required for proper cyanobacterial growth. The use of magnesium chloride as a coagulant for harvesting *M. aeruginosa* promoted recovery of 84% biomass at high pH (>10) (Taki et al., 2008).

Microbial biomass harvesting is a challenge as the harvesting method is dependent on multiple factors such as cell morphology, surface charge and density, culture pH, PBR design and also the desired product. Fragile microbial cells can be harvested with intact structure by filtration and centrifugation, but clogging of the filters and high-energy demand for large culture volume increases the operational cost. The addition of a low dose of flocculants/coagulants can efficiently recover microalgal cells, but the complexity and species-specific nature of these agents give rise to problems for their utilization. Sedimentation and flotation are density-based separation methods where the former fails under low culture density, and the latter requires surfactant addition with constant bubbling at high density. The pros and cons of recovery methods suggest that any single approach cannot ensure efficient harvesting in all cases due to the variation in biomass type and culture conditions. The addition of flocculants/coagulants prior to gravity sedimentation and centrifugation can increase the settling of small-sized cells and also decrease the energy requirement compared to individual recovery methods (Grima et al., 2003). Combined harvesting methods are therefore necessary for microbial biomass recovery with low energy demand and cost

reduction. Auto-sedimentation is the most convenient method that will allow easy cell separation and media re-utilization as the addition of chemical agents is not required during the process. However, this phenomenon is observed in only a few cyanobacterial/microalgal strains. Therefore, industrial-scale cell recovery requires the use of suitable strain or a multi-factorial process optimization supporting auto-sedimentation for cost-effective recovery.

Table 2.2 compares various harvesting methods of cyanobacteria based on cost, energy and efficiency. The selection of appropriate harvesting techniques depends on the specific characteristics of the microalgal or cyanobacterial species and the end-product. Auto-sedimentation is species specific and involves negligible cost involved in operation with high settling rates. *C. fritschii* has unique nature of autosedimentation which makes the process more feasible (Monshupanee et al., 2016). Hence auto-sedimentation has been used as a cost-economic harvesting strategy.

Table 2.2: Comparison of harvesting methods of microalgae or cyanobacteria based on cost, energy, and efficiency.

Method	Harvesting Stage	Efficiency (% biomass recovery)	Energy Consumption (kWh/m³)	Cost ($/m³)	Advantages	Disadvantages	References
Sedimentation	Thickening	Low (<10%)	**Negligible** (0.1-0.5)	**Low** (<0.1)	Low-cost, easy to operate	Requires large space, slow process, inefficient for small cells	(Pahl et al., 2012)
Flocculation	Thickening	Medium to High (70-90%)	**Low** (0.1-1.5)	**Low-Medium** (0.1-1)	Effective for small cells, can be combined with sedimentation	Chemical cost, potential contamination, pH adjustments required	(tLAM et al., 2014)
Flotation	Thickening	Medium (60-80%)	**Medium** (0.5-5)	**Medium** (0.5-2)	Effective for small cells and large scale	Requires aeration, moderate energy cost	(Barros et al., 2015)
Centrifugation	Dewatering	Very High (80-95%)	**High** (5-20)	**High** (10-50)	Rapid and effective for all microalgal types	High energy cost, potential cell damage	(Barros et al., 2015; Pahl et al., 2012)
F**iltration**	Dewatering	High (80-90%)	**Medium-High** (2-10)	**High** (5-15)	High efficiency, works for small cells	Expensive membranes, frequent cleaning required	(Barros et al., 2015)
Auto-sedimentation	Thickening	High (90-95) %	**Negligible**	**Low** (<0.1)	Low-cost, easy to operate	Species specific	(Yashavanth et al., 2021)

2.9. Recovery of PHB

PHB is stored as intracellular granules by most of the cyanobacteria. While for extracting PHB, cell wall and cell membrane have to be disrupted by numerous methods. The cyanobacterial cell wall contains a thick peptidoglycan layer (10 nm) than other Gram-negative bacteria (6 nm) and is more rigid (Woitzik et al., 1988). PHB can be recovered and purified by various methods such as solvent extraction, surfactants, non-PHB cellular material (NPCM) removal using hypochlorite and ionic liquids, dispersion of hypochlorite and chloroform, and enzymatic digestion (Yashavanth et al., 2021). Recovering PHB from cytoplasm increases production cost by up to 50 % cost of the polymer since PHB has to be purified in multiple steps (Samorì et al., 2015b). Using high concentration of sodium hypochlorite solution (10-20 %, v/v), PHB can be extracted with high purity from bacteria as well as from cyanobacteria but required repeated washing of pellets. The molecular weight of the recovered polymer may decrease as a result of NPCM digestion with hypochlorite. Hypochlorite and chloroform dispersion can decrease the loss in molecular weight of recovered PHB while raising the recovery yield and purity (Hahn et al., 1995).

Solvent recovery is the most used method by industries due to its better recovery efficiency resulting in polymer of high molecular weight along with the removal of endotoxins (Lee et al., 1999). Cyanobacteria contain many pigments that affect material properties of PHB after extraction. Therefore, pigment removal from cyanobacteria is essential before PHB recovery with a minimum number of solvents and steps involved (Troschl et al., 2017). Methanol can be used for pigment removal at 4 °C before PHB extraction (Gopi et al., 2014; Zavřel et al., 2015). The combination of hypochlorite and chloroform may result in higher recovery with pigment removal but both of them are toxic to humans and the environment. Therefore, the selection of solvents based on safety and reusability has significance in the evaluation of the extraction process (Mongili et al., 2021). Various halogenated solvents such as chloroform and dichloroethane and non-

halogenated solvents namely propylene carbonate, dioxolane, DMC and acetic acid have capabilities of to dissolve PHB (Terada & Marchessault, 1999). The selection of a suitable biomass-to-solvent ratio, extraction temperature and mixing time are critical factors as they affect the recovery yield. Usage of solvents such as chloroform and dichloromethane are not feasible at an industrial scale because of high cost and toxicity. 1,2-propylene carbonate, an eco-friendly solvent can extract 95 % PHB at 130 °C from *R. eutropha* with 84 % purity (Fiorese et al., 2009). Other eco-friendly solvents like acetic acid, butyl acetate, ethyl acetate was also studied for PHB recovery. The extraction of PHB from *Burkholderia cepacia* B27 with acetic acid showed higher solubility and purity of PHB while the recovery was only 36 %. Solvent precipitation with chilled methanol is better than the solvent casting method as it removes impurities (Ramos et al., 2020). Dimethyl carbonate (DMC) is a solvent of industrial importance and is used as a reagent in various processes. DMC is considered a green solvent since it is biodegradable and less toxic to humans and the environment (Delledonne et al., 2001) and could be used as an alternative to halogenated solvents (Mongili et al., 2021). Previously, DMC was used for the extraction of homopolymer PHB and copolymer poly-hydroxybutyrate-hydroxyvalerate (PHBHV) from single strains and mixed consortia (Elhami et al., 2022; Samorì et al., 2015a; Samorì et al., 2015b). Ionic liquid (IL) is also shown as a green solvent for the recovery of PHB accumulated in cyanobacteria. Cyanobacterial non-PHB cellular biomass can be dissolved in ionic liquid 1-ethyl-3-methylimidazolium methylphosphonate ($[C_2mim][MeO(H)PO_2]$) while PHB remain insoluble (Kobayashi et al., 2015). Using this IL, 98 % of PHB could be recovered from cyanobacteria, recycled, and used repeatedly. Solvent-free extraction methods such as digestion using alcalase enzyme and digestion by SDS and EDTA surfactants were also used for recovery of PHB (Martino et al., 2014). The purity of PHB recovered using these methods was more than 90 % without crystal formation. The usage of eco-friendly and recyclable solvents seeks more attraction in PHB

recovery from microbial biomass (Koller et al., 2013). Hence an economic recovery of PHB from harvested biomass with high purity, integrity of extracted polymer and selection of eco-friendly solvent with processes involved is still a challenge.

2.10. Factors influencing commercialization of PHB

Beyond media engineering and extraction techniques, there are number of challenges to the commercialization of polyhydroxybutyrate (PHB) from algae. The following are a few of the main factors:

1. High production costs: Compared to traditional plastics, the cost of making PHB from algae is much greater. This is because large scale cultivation of algae requires harvesting, and processing methods before product recovery (McAdam et al., 2020).

2. Low yield: PHB from algae has a comparatively low yield, which reduces its economic viability. To compete with conventional plastics, PHB production efficiency must be increased using various processes and usage of recombinant strains (McAdam et al., 2020).

3. Complex production technology: The technology needed to produce PHB from algae is challenging and has not yet reached its maximum potential. This includes the requirement for specific equipment and processes for cultivation. extraction and purification (McAdam et al., 2020).

4. Downstream processing: Extracting and purifying PHB is a difficult and expensive downstream process. This affects the cost of production overall and restricts commercialization (McAdam et al., 2020).

5. Market competition: Conventional plastics and other bioplastics pose a serious threat to PHB derived from algae. Since the bioplastics business is still in the beginning, PHB needs to compete with more established bioplastics from other sources, such as PLA (Abdo & Ali, 2019).

6. Regulatory and standardization issues: The commercialization of PHB derived from algae requires addressing regulatory and standardization issues. This involves ensuring that the bioplastic satisfies the specifications required for various applications (Abdo & Ali, 2019).

7. Environmental impact: Although PHB is biodegradable, the energy and resource consumption involved in its manufacturing must be carefully assessed and minimized (Abdo & Ali, 2019).

To overcome these obstacles, more investigation and innovative thinking are needed to streamline the manufacturing procedures, reduce costs and raise the overall environmental sustainability and efficiency of PHB derived from algae or cyanobacteria.

CHAPTER 3

Materials and Methods

3.1. Experimental cyanobacteria

The pure culture of *Chlorogloea fritschii* TISTR 8527 was procured from the Thailand Institute of Scientific and Technological Research (TISTR), Thailand. It is known to produce PHB of 19.5 %, 36 % and 28.5 % under starvation of nitrogen, phosphate, and both with supplementation of 0.4 % (w/v) of acetate under two stage cultivation. *C. fritschii* has a unique feature of auto-sedimentation due to clump cell nature. The clump cell clusters of *C. fritschii* can spontaneously settle to the bottom of the culture medium allowing separation of spent medium. Thus, it eases the harvesting of biomass (Kaewbai-Ngam et al., 2016). The microscopic image of the *C. fritschii* under 40 X resolution is as shown in Fig. 3.1.

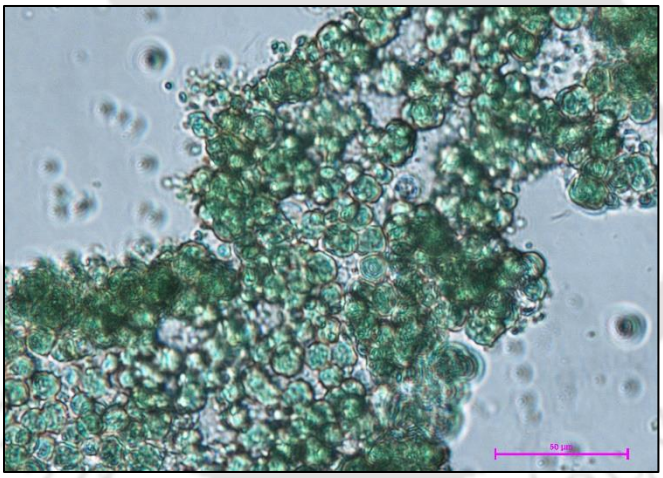

Fig. 3.1: Microscopic image of *Chlorogloea fritschii* TISTR 8527 under 40 X resolution.

3.2. Culture conditions

The pure culture of *C. fritschii* was cultured in sterile modified BG-11 medium in flask under still conditions with an illumination of 100 µmol/m^2/s with 12 h: 12 h light and dark period. The inoculum was prepared in a 1 L flask containing 500 mL modified BG-11 medium under nonsterile

conditions (Fig. 3.2). The composition of BG-11 medium was: 1.5 g/L $NaNO_3$, 40 mg/L K_2HPO_4, 75 mg/L $MgSO_4.7H_2O$, 36 mg/L $CaCl_2.2H_2O$, 6 mg/L Citric acid, 6 mg/L Ferric ammonium citrate, 1 mg/L Na_2EDTA, 20 mg/L Na_2CO_3 and 1 X TRACE (Rippka et al., 1979). The composition of TRACE is as follows: 2.86 g/L H_3BO_3, 1.81 g/L $MnCl_2.4H_2O$, 0.222 g/L $ZnSO_4.7H_2O$, 0.39 g/L $Na_2MoO_4.2H_2O$, 0.079 g/L $CuSO_4.5H_2O$ and 0.049 g/L $Co(NO_3)_2.6H_2O$. While preparing modified BG11 medium, the addition of 1 mL of TRACE per L of media represents usage of 1 X TRACE. Citric acid was replaced with 20 mM (4-(2-hydroxyethyl)-1-piperazineethanesulfonic acid)-NaOH (HEPES–NaOH) and ferric ammonium citrate was avoided by usage of equimolar concentration of ferric chloride hexahydrate with final pH of 7.5 in modified BG-11 medium (Kaewbai-Ngam et al., 2016). The mixture of air containing 1 % CO_2 (v/v) was sparged through a sparger made of silicone rubber tubing at a rate of 1 VVM (volume per volume per min). For inoculum preparation, the unialgal culture was illuminated with cool white LED light (50 W, 6500 K) at 100 µmol/m^2/s and grown for 16 d with 12 h:12 h light and dark periods. Inoculum of 5 % (v/v) was used in all the experiments in production medium to get initial biomass concentration of 0.05 g/L.

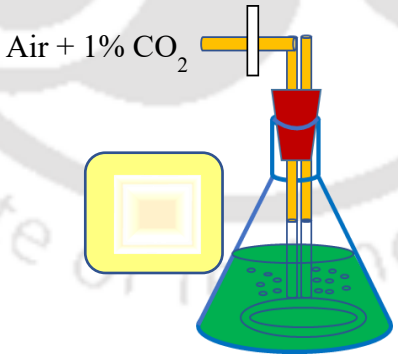

Fig. 3.2: Perforated silicone rubber tubing sparger equipped with transparent flask for inoculum preparation with 50 W LED illumination.

3.3. Quantification of cell dry weight and specific growth rate

The optical density (OD) of the culture was measured at 685 nm using a visible spectrophotometer (Model 2305, Electronics India). The sampling was done by mixing using a 10 mL pipette to avoid errors caused due to high settling rate of *C. fritschii*. The culture was centrifuged at 10000 rpm for 10 min and was dried overnight at 60 °C to get dry cell weight (DCW) (Hosseinizand et al., 2018). The specific growth rate (μ) was estimated using the following equation:

$$Specific\ growth\ rate,\ \mu = \frac{\ln\left(\frac{X_2}{X_1}\right)}{(t_2 - t_1)} \quad \text{..... (3.1)}$$

X_2 and X_1 are biomass density at time t_2 and t_1 respectively.

3.4. Chlorophyll estimation

Cyanobacterial culture of 1 mL was collected and centrifuged at 15000 g for 7 min at room temperature. To the pellet, 1 mL of methanol (precooled at 4 °C) was added, vortexed for 4 sec, and kept for incubation at 4 °C for 20 min. After the incubation, the suspension was centrifuged at 15000 g for 7 min at 4 °C. The supernatant was used to measure the absorbance at 665 nm (A_{665}) and 720 nm (A_{720}) (Zavřel et al., 2015). Chlorophyll-A concentration was calculated using the Eq. 3.2.

$$Chlorophyll\ \left(\frac{\mu g}{mL}\right) = 12.9447\ (A_{665} - A_{720}) \quad \text{..... (3.2)}$$

3.5. Nitrate estimation

The supernatant collected from the cell culture after centrifugation was used for the analysis of nitrate. Nitrate present in the sample was measured by nitrification of salicylic acid (Cataldo et al., 1975). Nitrate in the presence of conc. H_2SO_4 reacts with salicylic acid to form nitro-salicylic acid. At pH ≥ 12, the product nitro-salicylic acid was measured spectrophotometrically at 410 nm.

Reagent preparation for nitrate estimation

Salicylic acid reagent: Weigh 5 g of Salicylic acid in a volumetric flask and dissolve in 100 ml concentrated sulfuric acid. Make the volume to 100 ml using the same conc. H_2SO_4. Store at 4 ºC after every use and bring to normal temperature before use.

2 M NaOH: Weigh 80 g NaOH in 1000 ml volumetric flask and dissolve in 900 ml distilled water. After complete dissolution make the contents up to 1000 ml using distilled water and store at 4 ºC.

Nitrate standard, sample preparation and analysis

The nitrate standards were prepared in deionized water. Standards selected were 0.5, 1.0, 1.5 and 2.0 g/L. To 100 µL of sample, add 0.4 mL of salicylic acid reagent and incubate at room temperature for 20 min. Add 9.5 mL of 2 M NaOH and cool to RT. Measure OD at 410 nm and determine the nitrate present in the medium using standard curve.

3.6. Phosphate estimation

Phosphate present in the cell supernatant was estimated using the ascorbic acid method. In this method, ammonium molybdate and potassium antimonyl tartrate react in acidic medium with phosphate to form a heteropoly acid - phosphomolybdic acid that is reduced to molybdenum blue by ascorbic acid (John, 1970). The intensity of blue color was measured spectrophotometrically at 880 nm.

Reagent preparation for phosphate estimation

5 N H_2SO_4: Dilute 70 mL concentrated H_2SO_4 to 500 mL with distilled water.

Potassium antimony tartrate solution: Dissolve 1.3715 g $K(SbO)C_4H_4O_6.1/2\ H_2O$ in 400 mL distilled water in a 500 mL volumetric flask and dilute to volume. Store in a glass stoppered bottle for up to six months at room temperature.

Ammonium molybdate solution: Dissolve 20 g $(NH_4)_6Mo_7O_{24}.4H_2O$ in 500 mL distilled water. Store in a glass stoppered bottle for up to six months at room temperature.

Ascorbic acid (0.1 M): Ascorbic acid was prepared freshly by dissolving 1.76 g ascorbic acid in 100 mL distilled water. The ascorbic acid solution was stable for 1 week at 4 °C.

Combined reagent: The combined reagent was prepared by mixing 5 N H_2SO_4, potassium antimony tartrate solution, ammonium molybdate solution and 0.1 M ascorbic acid in the ratio 10:1:3:6. The combined reagent was stable for 4 h.

Phosphate standard, sample preparation and analysis

K_2HPO_4 standards were prepared with concentrations 0.95 mg/L and 3.8 mg/L. De-ionized water was used as blank. The K_2HPO_4 samples to be analyzed were diluted with distilled water such that diluted K_2HPO_4 concentrations fall in the range of 0 to 3.8 mg/L K_2HPO_4. Combined reagent of 160 µL was mixed with 1 mL sample and incubated for 10 min at room temperature. Set the spectrophotometer to zero with a blank at 880 nm and measure the absorbance of K_2HPO_4 standard and samples. Graph was plotted by keeping standard K_2HPO_4 concentration along y-axes and measured OD_{880} along x-axes. The slope was calculated from graph and multiplied with dilution factor and OD_{880} of the K_2HPO_4 sample to obtain K_2HPO_4 concentration.

3.7. Quantification of PHB

The PHB (w/w %) present in the dried biomass was quantified using Gas chromatography (GC) equipped with CP-Sil 8 CB column (30 m x 0.25 mm i.d. 0.25 µm film thickness) and a Flame

ionization detector (FID). Sample preparation was done using the propanolysis method using 10 mg of dried biomass. To screw-capped glass vial containing cyanobacterial dried biomass, 2 mL of dichloroethane (DCE), and 2 mL of acidified propanol (4 volumes of propanol and 1 volume of HCl) were added and incubated for 2 h at 100 °C with mixing at regular intervals. Once the vials reached room temperature, 4 mL water was added and vortex for 30 sec. The heavier bottom phase was collected and 1 µL of the sample was injected into GC with a split ratio of 1:100 (Riis & Mai, 1988). Helium was used as carrier gas with a flow rate of 0.7 mL/min. The injector and detector were maintained at 250 °C and 275 °C respectively. The column oven was kept at 80 °C for 2 min followed by ramping at a rate of 10 °C/min to 245 °C with hold for a minute (Juengert et al., 2018). The standard curve was prepared using PHB from Sigma-Aldrich. The percentage PHB present in the dried biomass was calculated using Eq. 3.3.

$$PHB\ (\%) = \frac{mg\ of\ PHB}{mg\ of\ DCW} \times 100 \quad \text{..... (3.3)}$$

The percentage recovery of PHB after a recovery process is calculated using Eq. 3.4.

$$PHB\ recovery\ (\%) = \frac{PHB\ recovered\ in\ g/L}{Total\ PHB\ in\ g/L} \times 100 \quad \text{..... (3.4)}$$

3.8. Auto-sedimentation studies

Auto-sedimentation is the quick settling of cells due to the clump nature of cells. The known volume of culture (V_i) was collected. The OD (OD_i) of the culture was measured and allowed to settle under gravity for 3 h. With time there will be a separation of phases resulting in the concentrated bottom layer whose OD is unknown and referred to as OD_{set}. The OD of the top layer (OD_{top}) was measured and the volumes of the top layer (V_{top}) and settled layer (V_{set}) were noted (Mahesh et al., 2023; Yashavanth & Maiti, 2024). The ratio of OD_{set} to OD_{top} is referred to as the

auto-sedimentation concentration factor (SCF) which can be calculated as follows using Eq. 3.5 and 3.6.

$$OD_{\text{set}} = \frac{((OD_{\text{i}} \text{ x } V_{\text{i}}) - (OD_{\text{top}} \text{ x } V_{\text{top}}))}{V_{\text{set}}} \quad \text{..... (3.5)}$$

$$\text{SCF} = \frac{OD_{\text{set}}}{OD_{\text{top}}} \quad \text{..... (3.6)}$$

3.9. Characterization of PHB

3.9.1. Fourier Transformed Infrared Spectroscopy

A potassium bromide pellet was prepared for 2 mg of standard PHB (sigma) and recovered PHB. Infrared spectra (IR) were recorded using a Perkin Elmer Fourier Transformed Infrared (FTIR) spectrometer with a spectral range of 3600 – 800 cm^{-1} at 25 °C (Ansari & Fatma, 2016).

3.9.2. Thermogravimetric Analysis

The thermal stability of the extracted polymer of 10 mg was studied by thermogravimetric analysis (TGA) from 25 - 700 °C under the argon atmosphere (20 mL /min) at a heating rate of 10 °C /min using NETZSCH STA 449 F3 Jupiter. The decomposition temperature such as T_5 (5 % weight loss) and T (10 % weight loss) were determined using TGA curve and maximum decomposition temperature (T_{max}) was determined by DTG analysis (Ansari & Fatma, 2016).

3.9.3. Differential Scanning Calorimetry

Differential Scanning Calorimetry (DSC) analysis was done using the NETZSCH instrument with 5 mg of sample in an aluminium pan under a nitrogen environment. The sample was heated to a

temperature of -30 to 200 °C, held isothermally at 200 °C for 3 min, and cooled to -30 °C at a rate of 10 °C /min. Similarly, a second cycle was performed (Ansari & Fatma, 2016).

The degree of crystallinity X_c was calculated from the Eq. 3.7.

$$X_c = (\Delta H_f \times 100)/\Delta H_{f_0} \quad \text{..... (3.7)}$$

ΔH_f is melting enthalpy of the recovered PHB (J/g), ΔH_{f_0} is the theoretical melting enthalpy of the 100 % crystalline PHB which is assumed to be 146.6 J/g.

3.9.4. Powder X-Ray Diffraction

X-ray diffractograms (XRD) of the standard and sample were obtained using Smartlab 9KW Powder X-Ray Diffraction System, Rigaku Technologies, JAPAN for 2θ in the range of 10 – 80 °C using Cu-Kα radiation (λ = 1.54 A°). The peaks were analyzed for the crystalline nature of the recovered biopolymer (Devi et al., 2015).

3.9.5. Gel Permeation Chromatography

The molecular weight of recovered PHB was determined using gel permeation chromatography (GPC) (PL-GPC 220 High-Temperature Chromatograph, Agilent Technologies) at 40 °C with a refractive index detector. Tetrahydrofuran, HPLC grade (stabilized) was used as the mobile phase with a flow rate of 1 mL/min. PHB was dissolved in chloroform at a concentration of 1 mg/mL and a 200 µL sample was injected using an autosampler to PLgel Mixed B column (10 µm, 300 x 7.5 mm) with a runtime of 25 min. Mass standards of Polystyrene in the range of 1.6 x 10^2 – 6.5 x 10^6 g/mol were used to calibrate the system before sample injection (Lackner et al., 2019).

3.9.6. Mechanical properties

The solvent casting method was used to prepare PHB films to study the tensile strength and elongation at break using a 5kN Universal Testing Machine (Zwick Roell, Z005TN). The

recovered polymer was dissolved in chloroform while stirring at 60°C for 20 min. The solution was poured into the glass petri dish. The films resulted from the evaporation of solvent. The films were cut into rectangular shapes (5 cm × 2 cm) and subjected to load at a rate of 1 mm/min (Ansari & Fatma, 2016). The tensile strength (MPa) and elongation at break (%) was calculated by stress-strain curve.

3.10. Software used

Design–Expert® 7.0 (Stat Ease) was used to obtain the analysis of variance (ANOVA) and regression analysis from experimental data.

3.11. Monitoring of culture pH, dissolved oxygen, temperature, and light intensity

pH electrode (HAMILTON) and DO probe (HAMILTON) were inserted on the side of medium scale flat panel PBR (Labfors, INFORS HT, 25.5 × 2 × 50 cm) and thermal sensor (Pt100) were inserted on the top of medium scale flat panel photobioreactor (PBR) for online monitoring of culture pH, DO concentration and culture temperature respectively. The data was stored using eve software (INFORS HT).

3.12. Extraction of intracellular phosphate from cyanobacteria

Cyanobacterial culture of 2 mL was centrifuged at 10000 rpm for 10 min at room temperature. The pellet was washed once with deionized water. Then stored intracellular phosphate was extracted using 1 mL of deionized water by boiling at 100 °C in water bath for 20 min (Eixler et al., 2005). The samples were centrifuged again to separate the polyphosphate extract. The stored phosphate content was determined using the ascorbic acid method (section 3.6).

CHAPTER 4

Development of process techniques to increase PHB concentration by using various strategies

4.1. Background and motivation of the study

The cultivation systems, nutrients, availability of light intensity, supply of CO_2, mixing and mass transfer, process pH, and culture temperature are the main parameters that affect cyanobacterial growth and PHB production. PHB production by *Chlorogloea fritschii*, a cyanobacteria has been achieved by a two-stage cultivation strategy: phototrophic growth in the presence of sufficient quantities of nitrogen and phosphate in the media, followed by PHB accumulation under dark in the presence of inducers with nutrient limiting medium (Monshupanee et al., 2016). Two-stage PHB production requires further separation step for cell harvesting after growth and subsequent cultivation in nutrient-depleted media for PHB synthesis. This makes the two-stage cultivation of cyanobacteria uneconomical. To reduce the process cost, a strategy for single-stage cultivation of *C. fritschii* needs to be developed. In single-stage cultivation, the cyanobacteria can be grown to higher biomass density under photoautotrophic conditions till the stationary phase. Later acetate can be supplemented to the same experimental culture without medium replacement for PHB induction under dark.

In the current study, initial screening experiments were performed to study the effects of constant and diurnal light on growth of *C. fritschii*, the effect of nitrogen on biomass growth and PHB accumulation using a modified BG-11 medium. Also, the effect of acetate on PHB accumulation was studied under nutrient deprived conditions. Further experiments are carried out in medium-scale flat panel PBR with single-stage PHB production with the utilization of diurnal light mimic to sunlight. This can decrease the risk of change of culture parameters in real circumstances when the PHB production process is carried out under outdoor sunlight.

4.2. Effect of light intensity on growth of *C. fritschii*

4.2.1. Effect of constant light intensity on growth of *C. fritschii*

Each experiment was carried out in 400 mL modified BG-11 medium (Monshupanee et al., 2016) in 500 mL Borosil flasks with straight and T connectors attached, as depicted in the Fig. 4.1A. The silicone rubber tubing (8 mm OD and 5 mm ID) was used as a sparger and connected to 6 mm PU pipes passed through rubber corks. The mixture of air (1 VVM) and 1 % CO_2 was sparged during daytime and only air was sparged during dark using rotameters via a sterile PTFE filter (50 mm diameter, 0.2 µm, Axiva). A small hole has been made in the rubber cork, which acts as a vent. To attain the desired light intensities of 15, 100, 600, 1285, and 1890 µmol/m^2/s (0 - 2000 µmol/m^2/s), a 50 W cool white light with a 6500 K color temperature and coupled in series was needed for the experiment. This light may be obtained using a constant light source regulator or a Pulse-Width Modulator (PWM) connected to OPTO-22 (OPTO-22, USA). The light and dark period of 12h :12 h was used during phototrophic growth period. Aluminum heat sinks attached to CPU fans absorbed the heat produced by the LED lights. A lux meter (Sigma Instruments, India) was used to measure light (lux), that was then converted to µmol/m^2/s using the factor of "74 lux = 1 µmol/m^2/s PPFD" (Photosynthetic Photon Flux Density) (Apogee Instruments, Inc. USA). Experiments were performed in duplicates with duplicate sampling. The experiments started with an initial cell density of 0.05 g/L (Monshupanee et al., 2016). The sampling was done at regular intervals to measure DCW (section 3.3).

4.2.2. Effect of diurnal light intensity on growth of *C. fritschii*

The experiment was carried out in 400 mL modified BG-11 medium with an initial cell density of 0.05 g/L (Monshupanee et al., 2016) in two 500 mL Borosil flasks with straight and T connectors

attached, as shown in the Fig. 4.1A. A mixture of air and 1 % CO_2 was sparged for the growth of cyanobacteria through silicone sparger. The diurnal light (cycle of light intensities from dawn to dusk) was simulated with reference to a day in May in Guwahati, India (26°11′03″ N and 91°44′44″ E) using a customized unidirectional LED panel for growth of cyanobacteria (Mahesh et al., 2023; Naira et al., 2019). The diurnal light was mimicked to sunlight using OPTO-22 control system and PWM. The sampling was done at regular intervals to measure DCW (section 2.2). Duplicate experiments with duplicate sampling were done (n = 4 × 4) and the average of results were reported.

4.3. Effect of nitrate on growth of *C. fritschii* under diurnal light and PHB accumulation in dark

Nitrate variation experiment was performed in the above set up (Fig. 4.1A). In modified BG11, nitrate was varied from 0.1, 1, 1.5, 2.6 and 4 g/L nitrate keeping other nutrients same as the original composition. The pH of the medium was adjusted to 7.5 before inoculation. The mixture of air and 1 % CO_2 was sparged with utilization of mimicked sunlight pattern using OPTO-22. The sampling was done at regular intervals of 5 d to measure DCW and nitrate utilization rate. After 30 d, PHB induction was performed with supplementation of 0.2 % acetate under dark (Monshupanee et al., 2016). The sampling was done at an interval of 2 d to measure cellular PHB content. Duplicate experiments with duplicate sampling were done and average results were reported.

4.4. Single stage cultivation of *C. fritschii* with the effect of acetate on PHB production

For the experiments, *C. fritschii* was grown in a 1 L flask containing 500 mL modified BG11 medium with an initial cell density of 0.05 g/L. The culture was mixed by sparging of air through silicone rubber tubbing at 1 VVM. Initially, *C. fritschii* was grown to high cell density till 16 d

under phototrophic conditions with diurnal light intensity. During the light period, 1 % CO_2 (v/v) was sparged to support the growth whereas only air was sparged at night for the respiration of *C. fritschii*. The sampling was done at regular intervals to measure DCW. The nitrate and phosphate consumption rate were also estimated. For single-stage PHB production, 100 mL of pre-grown culture under phototrophic mode was transferred to 250 mL flasks equipped with silicone rubber sparger with an aeration of 1 VVM and acetate was added to obtain initial concentrations of 0, 0.2, 0.4, and 0.8 % (w/v) respectively without medium replacement under dark. The concentrations of acetate were selected based on previous reports (Monshupanee et al., 2016). The sampling was done at intervals of 2 days for the measurement of DCW (section 3.3) and PHB content (section 3.7). Duplicate experiments with duplicate sampling were done and average results were reported with standard deviation.

4.5. Single-stage cultivation of *C. fritschii* in flat-panel photobioreactor under diurnal light

To make the process economical, single-stage cultivation of *C. fritschii* under diurnal light mimicked to sunlight using computer-dimmable technology was opted instead of constant light. In single-stage cultivation, the *C. fritschii* was grown to higher biomass density using a modified BG-11 medium under diurnal light using CO_2 till the culture reached the stationary phase in flat-panel photobioreactor (PBR) (Labfors, INFORS HT, 25.5 × 2 × 50 cm) (Fig. 4.1B). Later acetate was added to the same experimental culture without medium replacement for PHB induction under dark. The diurnal light was simulated using PWM via unidirectional LED system similar to section 4.2.2. The experiment was performed with an initial cell density of 0.05 g/L. The culture was mixed through aeration of 0.5 L per min with 1 % CO_2 (v/v) during the light period and only air was sparged during the night period. The culture temperature (°C), pH, dissolved oxygen (DO, %), and light intensity (µmol/m^2/s) were recorded throughout the study. Note that in single-stage cultivation in flat-panel PBR, the temperature was not controlled either during growth or induction.

The sampling was done at regular intervals to measure DCW and chlorophyll from the pellet and nitrate and phosphate in the supernatant (section 3.3-3.6). After 10 d of cultivation, 0.2 % (w/v) acetate was supplemented to induce the PHB accumulation in the dark. The sampling was done to measure the PHB from the dried biomass as mentioned in section 3.7.

4.6. Phosphate and nitrate feeding based cultivation of *C. fritschii* in flat panel PBR

Single-stage cultivation of *C. fritschii* in flat panel PBR using diurnal light (section 4.5) is considered as the control for the present study. Modified BG-11 was selected for the phototrophic growth of *C. fritschii* under diurnal light using 1 % CO_2. The experimental conditions were similar to those of the control. The sampling was done at regular intervals to measure biomass concentration, specific growth rate and chlorophyll content. Nitrate and phosphate present in the culture were estimated as before. The phosphate feeding was done when the limited phosphate didn't enhance the biomass. After 5 d of cultivation, 40 mg/L phosphate was fed to the culture. The second feeding of 40 mg/L phosphate and 0.75 g/L sodium nitrate was done on the 8^{th} day of cultivation. Nitrate was fed when the extracellular nitrate was found to be completely utilized by *C. fritschii*. Afterwards 0.2 % acetate was supplemented for the PHB induction under dark on the 9^{th} day of the cultivation. The culture temperature (°C), pH, DO (%), and light intensity (µmol/m^2/s) were recorded throughout the study. Polymer content was quantified using GC after the transesterification of dried biomass.

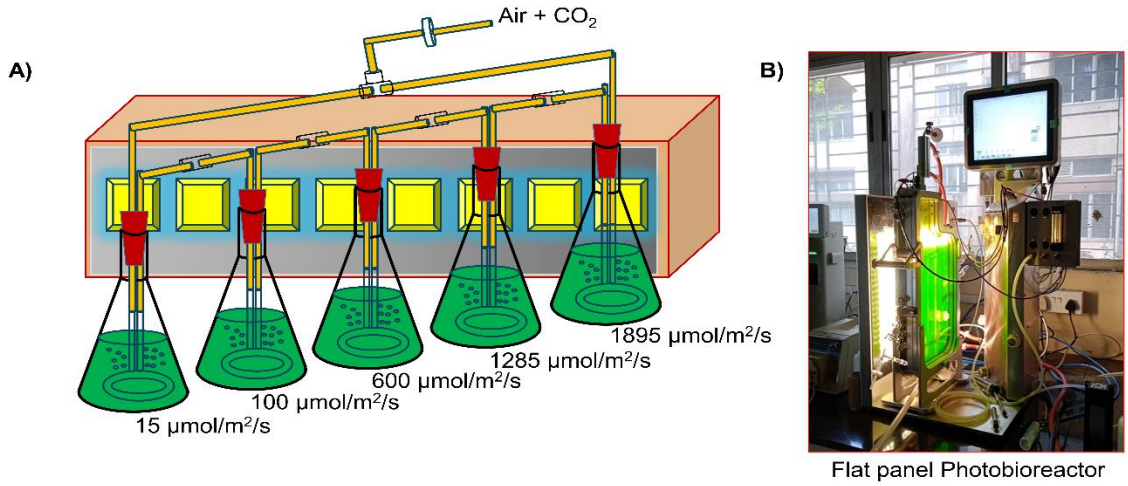

Fig. 4.1: Experimental set up for the study of the effect of constant or diurnal light intensity on the growth of *C. fritschii*. **A)** shake flask with silicone sparger with customized unidirectional LED system and **B)** flat panel PBR with inbuilt LED panel.

4.7. Results and discussion

4.7.1. Effect of light intensity and diurnal light on growth of *C. fritschii*

C. fritschii was cultivated with an initial cell density of 0.05 g/L with 1 % CO_2 under constant light intensities of 15, 100, 600 and 1285 and 1890 µmol/m^2/s with 12 h: 12 h light and dark period. Light intensities of 15 and 100 µmol/m^2/s resulted in dry cell weight (DCW) of 0.22 g/L and 0.52 g/L respectively after 16 d of cultivation (Fig. 4.2A). DCW of 0.81 g/L and 1.6 g/L was obtained with 600 µmol/m^2/s and 1285 µmol/m^2/s respectively after 16 d of cultivation. Highest light intensity of 1890 µmol/m^2/s resulted in maximum dry biomass of 1.84 g/L on 16 d of the experiment (Fig. 4.2A). It was observed that the increase in light intensity enhanced the biomass accumulation. From these experiments, *C. fritschii* can be cultivated under simulated sunlight since it can withstand high light intensity of 1890 µmol/m^2/s which is the peak light intensity of diurnal

pattern (Fig. 4.2B). *C. fritschii* was cultivated in modified BG-11 medium under diurnal simulated sunlight in a similar setup (Fig. 1A) with an initial cell density of 0.05 g/L. The biomass concentration of 0.33 g/L was obtained in the early log phase i.e. on the 4th day of the experiment. After 16 d of cultivation with 1 % CO_2, maximum DCW of 2.1 g/L was obtained (Fig. 4.2B). From the present study, *C. fritschii* can be cultivated under diurnal light mimicked to sunlight as well as in natural sunlight without change in culture parameters.

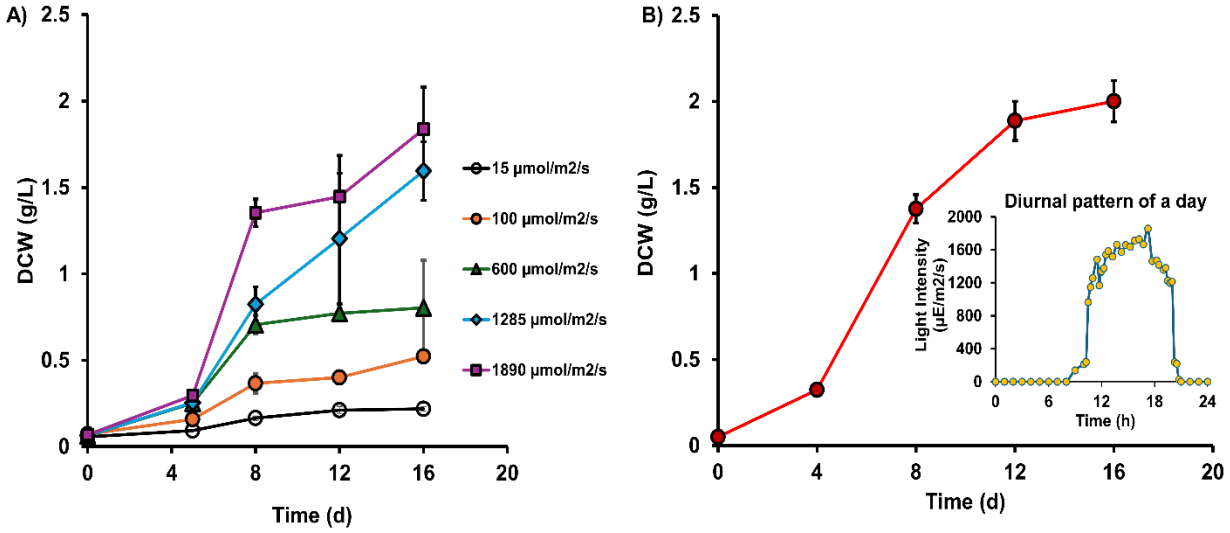

Fig. 4.2: Dry cell weight profile of *C. fritschii* grown in shake flask equipped with silicone rubber sparger. **A)** different constant light intensities of 15, 100, 600 and 1285 and 1890 µmol/m^2/s with 12 h: 12 h light and dark period and **B)** diurnal light.

4.7.2. Effect of nitrate on growth of *C. fritschii* under diurnal light and PHB accumulation in dark

The experiments were carried out to study the effect of sodium nitrate by one variable at a time using diurnal light. On the 20th d of cultivation, 1.5 g/L and 2.6 g/L of sodium nitrate produced the highest biomass concentration of 2.1 g/L and 2.8 g/L respectively, while 0.1 g/L of sodium nitrate produced DCW of 0.85 g/L. On the 25th d, 4 g/L sodium nitrate resulted in DCW of 2.1 g/L. Note that substrate inhibition was observed at 4 g/L of nitrate. Culture with 1 g/L, 1.5 g/L and 2.6 g/L nitrate reached the stationary phase on the 20th d of the experiment (Fig. 4.3A). Culture with 0.1 g/L and 4 g/L nitrate reached the stationary phase on 10th and 25th d respectively. The nitrate present was completely utilized under diurnal light in flasks with 0.1 and 1 g/L on 10th d of cultivation. Nitrate concentration of 2.6 g/L was completely consumed on 15th d and resulted in maximum biomass yield ($Y_{X/N}$) of 1.08. A maximum of 3 g/L nitrate was utilized under diurnal light till the 30th d of cultivation even though 4 g/L nitrate was supplied (Fig. 4.3A). PHB induction was initiated on the 30th d by supplementing 0.2 % (w/v) acetate. PHB content was measured, and it was found that 2.6 g/L nitrate resulted in PHB content of 13.4 % on 4th d of induction (total 34th d culture) under dark. In the case of 1.5 g/L sodium nitrate, a maximum PHB of 14.8 % was obtained after 4 d of induction and later polymer accumulation decreased to 3.6 % (Fig. 4.3B).

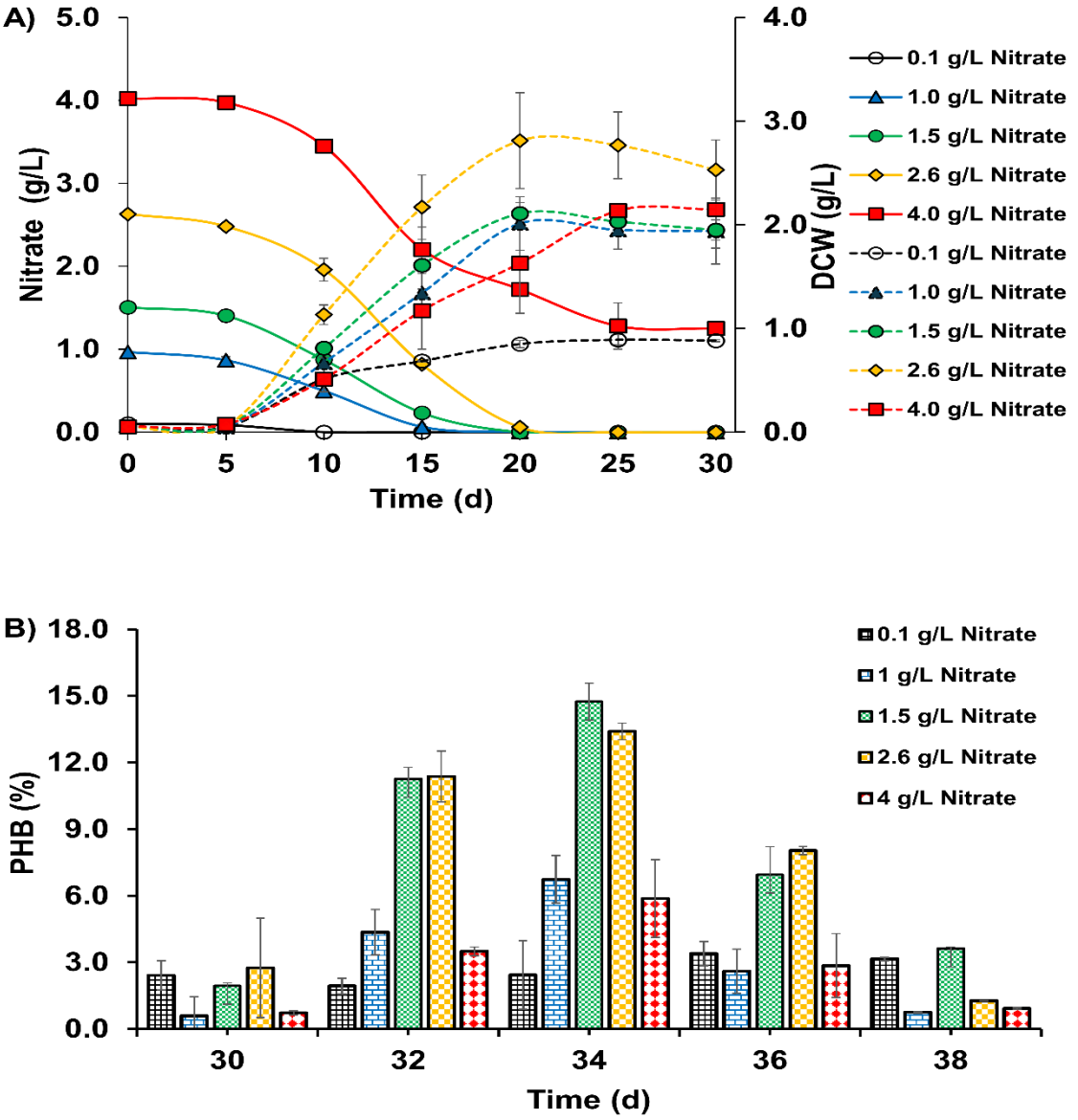

Fig. 4.3: Effect of nitrate on growth and PHB accumulation of *C. fritschii*. **A)** Growth behaviour of *C. fritschii* under diurnal light with different nitrate concentration. Dotted lines represent the DCW, and continuous lines represent nitrate concentration, **B)** PHB accumulation under dark with 0.2 % w/v acetate supplementation.

4.7.3. PHB induction with different levels of acetate in dark condition

Even though two stage cultivation resulted in higher PHB content, it was not economical due to replacement of the growth medium after autotrophic growth with induction medium (Drosg et al., 2015; Monshupanee et al., 2016). Hence single-stage cultivation was opted by avoiding intermediate biomass harvesting step. The experiment started with an initial biomass concentration of 0.05 g/L under diurnal light with 12 h:12 h light and dark period. An initial nitrate concentration of 1.53 g/L was consumed completely at the end of 16 d of cultivation. Phosphate of 40 mg/L was consumed completely after 16 d resulting in biomass concentration of 1.95 g/L ± 0.17 g/L (Fig. 4.4A). During induction with various acetate concentrations of 0, 0.2, 0.4 and 0.8 % (w/v) without medium replacement, 0.8 % acetate resulted in maximum DCW of 4.08 g/L after 4 d of induction with PHB content of 9.22 %. Supplementation of 0.8 % acetate resulted in heterotrophic growth rather than PHB induction. The culture without acetate resulted in PHB content of 5.64 % with 1.69 g/L DCW after 6 d of induction. PHB of 16.4 % was obtained with 0.2 % acetate on 4 d of induction with biomass concentration of 2.5 g/L. The culture with 0.4 % acetate resulted DCW and PHB content of 3.06 g/L and 14.11 % respectively on 2nd d of induction (Fig. 4.4B and 4.4C). Hence for further studies 0.2 % acetate was selected. Previously *C. fritschii* was known to accumulate 10 % of biopolymer with 0.02 M acetate under mixotrophic cultivation with 5 % CO_2 (Carr, 1966). It can be observed that while studying the effect of nitrate, 14.8 % PHB was observed with 1.5 g/L nitrate with PHB induction initiated on 30th d with 0.2 % acetate. Whereas during the study of effect of acetate with same concentrations of nitrate and acetate, 16.4 % polymer was accumulated when PHB induction was done after 16th d. Note that percentage PHB accumulation not only depends on the concentrations of inducer but also on time of induction.

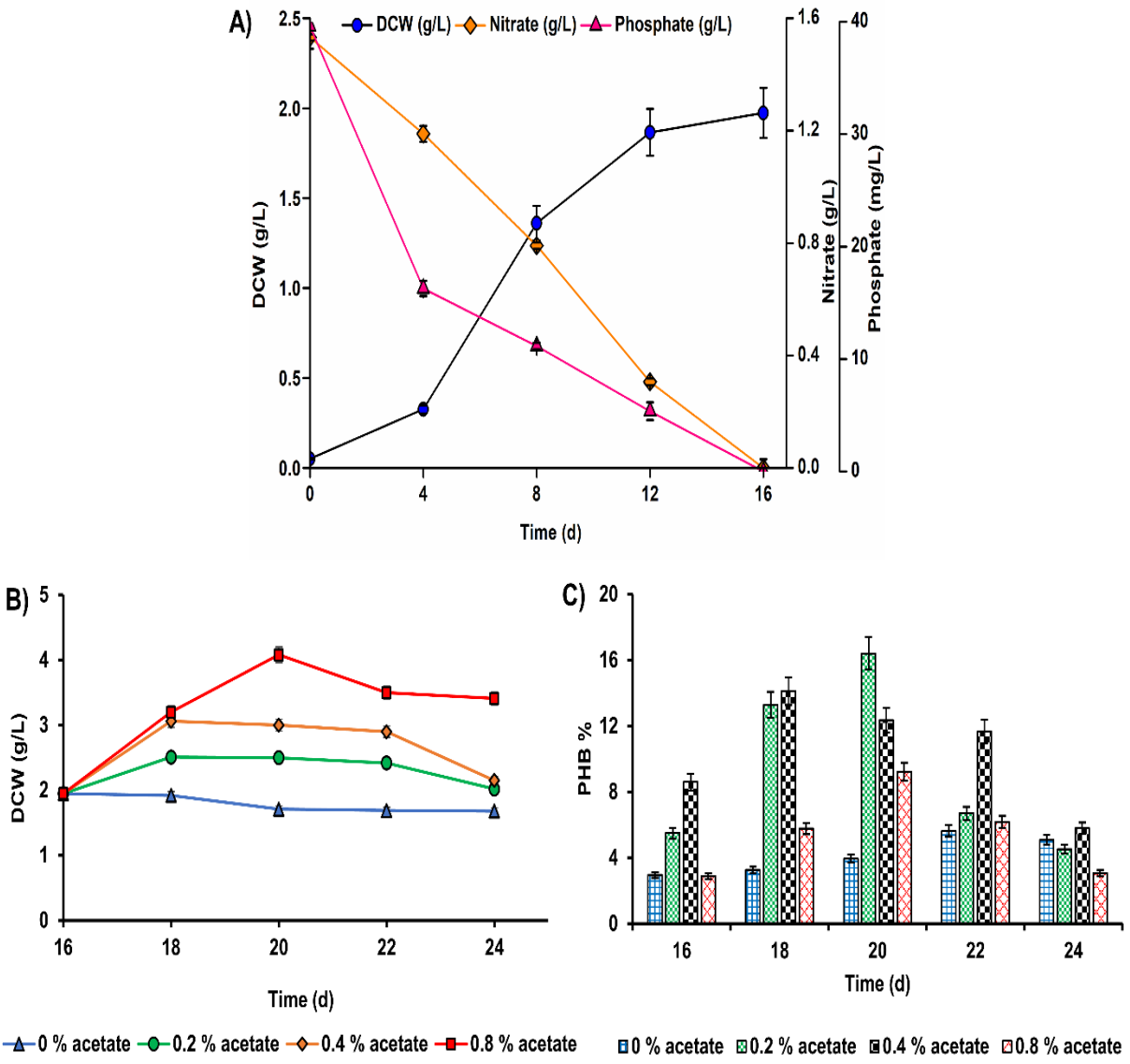

Fig. 4.4: Single stage cultivation of *C. fritschii* under diurnal light with 1 % CO_2 in flask set up equipped with silicone sparger. **A)** DCW, nitrate and phosphate consumption rate, **B)** biomass concentration measured during PHB induction under dark with various acetate concentrations and **C)** PHB accumulation under dark with various acetate concentrations.

4.7.4. Single-stage cultivation of *C. fritschii* in flat-panel PBR under diurnal light

C. fritschii was cultivated in flat panel PBR with modified BG-11 medium (pH 7.5) with an initial cell density of 0.05 g/L with 1 % CO_2 and aeration of 0.5 L/min. After 10 d of cultivation, the culture reached the stationary phase with 1.44 g/L of dry biomass. The nitrate present in the medium was completely utilized after 8 d of cultivation. The phosphate was completely consumed within 24 h of the experiment. There was an increase in the chlorophyll content of the cyanobacteria with growth. The maximum chlorophyll concentration of 29 ± 0.37 µg/mL was obtained on 7^{th} d with DCW of 1.42 ± 0.012 g/L (Fig. 4.5A). The supplied CO_2 decreased pH during the light period, and only air was sparged for cellular respiration during the dark hours. The metabolic activity of the cells was causing the culture's temperature to rise during the day. The photosynthetic uptake of CO_2 provided during the daytime was responsible for the rise in DO percentage. After 10 d of the cultivation, 0.2 % (w/v) acetate was supplemented to the experimental culture without medium replacement. There was a drop in DO % during the dark due to cellular respiration and metabolism after acetate supplementation (Fig. 4.5B). The maximum specific growth rate of 1.52 ± 0.037 d^{-1} was observed after 2^{nd} d of cultivation (Fig. 4.5C). The polymer content of 11.2 % (w/w) was obtained after 4 d (14^{th} day) of induction with biomass concentration of 2.06 ± 0.05 g/L and thereafter decrement in PHB content was observed (Fig. 4.5D).

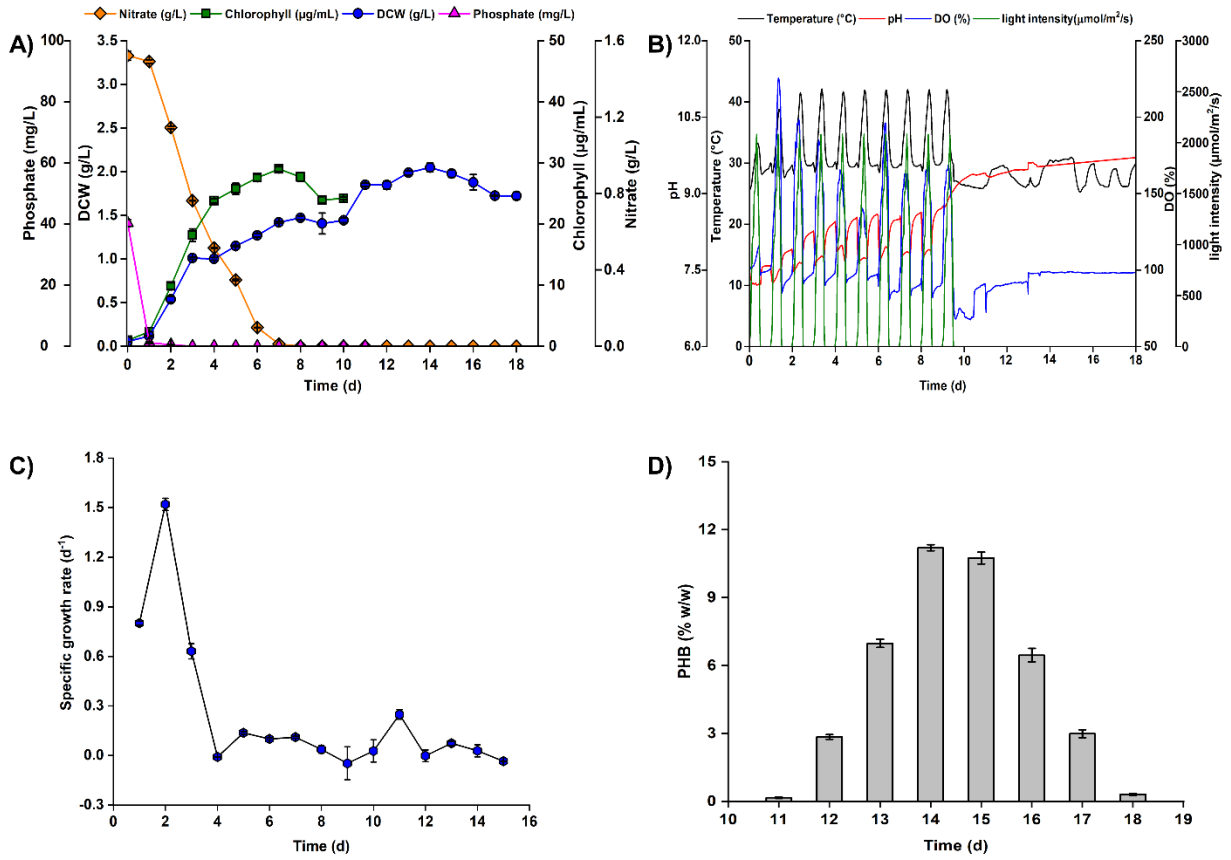

Fig. 4.5: Production of PHB from *C. fritschii* via single-stage cultivation under diurnal light in flat panel PBR using modified BG-11 media with 1 % CO_2 for growth and 0.2 % acetate for PHB induction. **A)** DCW, chlorophyll concentration, nitrate and phosphate consumption, **B)** culture parameters such as temperature (°C), pH and DO (%) along with diurnal light intensity (µmol/m^2/s). The phototrophic growth period was up to 10 d from the start of the experiment and the dark period for PHB induction was from 10 d to 18 d, **C)** specific growth rate (d^{-1}) during phototrophic growth mode and PHB induction, and **D)** PHB accumulation profile under dark.

4.7.5. PHB production via *C. fritschii* using phosphate and nitrate feeding in flat panel PBR under diurnal light

Phosphate present in the medium was completely utilized within 24 h of the growth period in the batch reactor. As 40 mg/L phosphate becomes limiting, a phosphate feeding strategy was implemented to improve biomass as well as PHB production. After 5 d of cultivation, the first feeding of 40 mg/L K_2HPO_4 resulted in an increase in dry cell weight from 1.14 g/L to 2.97 ± 0.04 g/L after single day of feeding (on 6^{th} d) (Fig. 4.6A). This rapid growth of cyanobacteria is due to luxury phosphate uptake after first feeding on the 5^{th} d of the experiment. There was a 1.6-fold increment in the DCW after the first feeding of phosphate. The maximum specific growth rate of 1.44 ± 0.015 d^{-1} was observed after 2^{nd} d (48 h) of cultivation (Fig. 4.6C). The first feeding of K_2HPO_4 after 5^{th} d resulted in a rise in growth rate from 0.044 d^{-1} to 0.947 d^{-1} on 6^{th} d. A maximum chlorophyll concentration of 32.75 µg/mL was obtained on 6^{th} d (Fig. 4.6A). Nitrate was consumed at a slow rate and completed after 8 d of the experiment. When cell growth rate becomes very slow, with the progress of the batch, there was a slight decrement in biomass to 2.6 g/L after 8 d of cultivation with the cells reaching the stationary phase. Both phosphate (40 mg/L) and nitrate (0.75g/L) have been added on the 8^{th} d as both become limiting. Note that feeding of phosphate at the second time along with nitrate on the 8^{th} d didn't enhance the biomass growth rate. Whereas the phosphate was completely consumed, and nitrate fed was utilized at a slower rate (Fig. 4.6A). Either limitation of light or other nutrients might have resulted in insignificant change in biomass concentration. The light intensity, pH, DO (%) and temperature were recorded throughout the study (Fig. 4.6B). The supplementation of 0.2 % acetate under dark on 9^{th} day of the cultivation resulted in PHB induction. After 4 d of induction (i.e. 13^{th} day), PHB content of 46.9 ± 1.07 % (w/w of DCW) was obtained. The later decline in the PHB content was due to the consumption of PHB by *C. fritschii* itself (Fig. 4.6D). An increase in PHB content by 4.2-fold when compared to

control (i.e. without phosphate feeding) was obtained with DCW of 2.43 ± 0.08 g/L. Previously with two stage cultivation of same strain was known to produce 36 % of PHB with phosphate starvation and 0.4 % acetate (Monshupanee et al., 2016). However, current strategy of single-stage cultivation of *C. fritschii* under diurnal light with feeding of phosphate and nitrate not only enhanced the biomass but also resulted in a maximum polymer content of 46.9 % with PHB production of 1.14 g/L with minimal acetate supplementation of 0.2 % (w/v). This could be due to the limitation of other nutrients favoring PHB induction upon acetate addition. Note that this is the maximum PHB production reported till now in *C. fritschii* TISTR 8527.

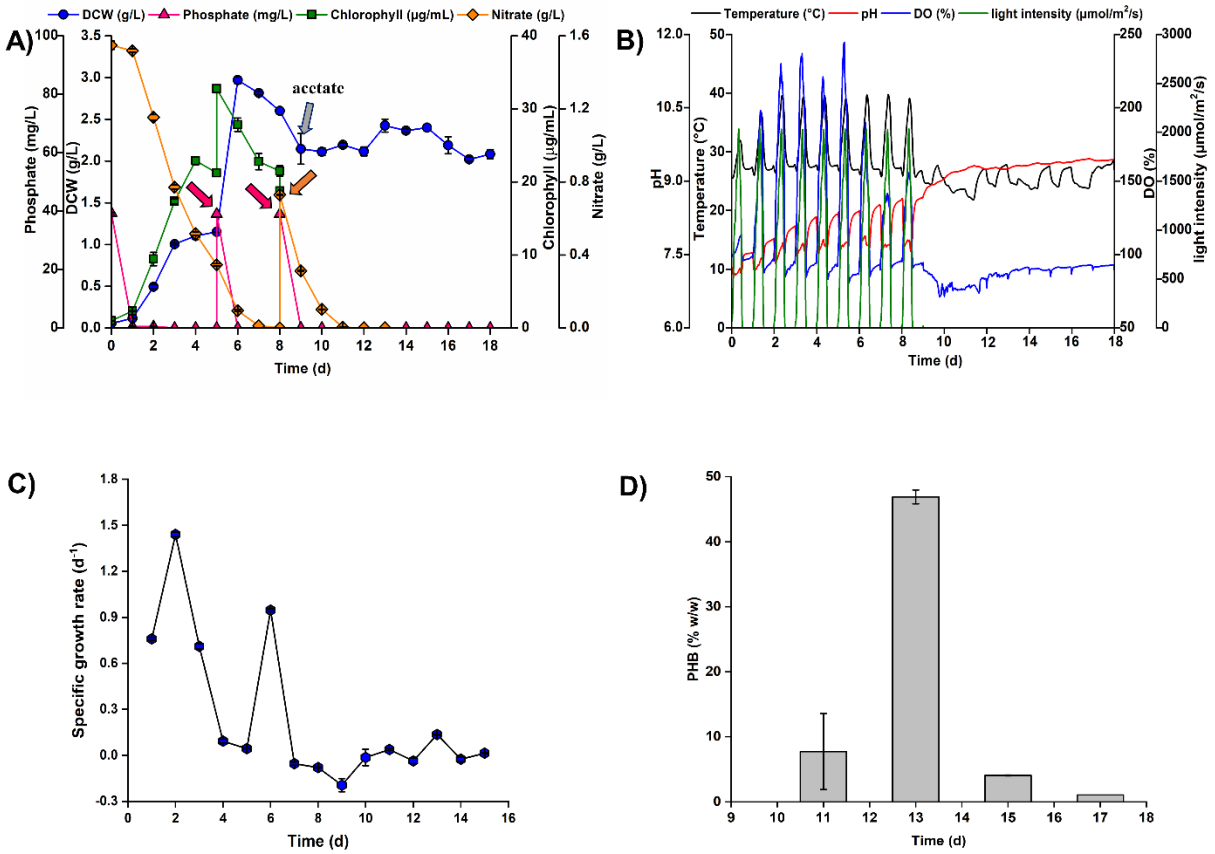

Fig. 4.6: Production of PHB from *C. fritschii* via single-stage cultivation under diurnal light in flat panel PBR using modified BG-11 media with intermittent phosphate feeding and nitrate feeding. **A)** DCW, chlorophyll concentration, nitrate and phosphate consumption, **B)** culture parameters such as temperature (°C), pH and DO (%) along with diurnal light intensity (µmol/m^2/s), The phototrophic growth period was up to 9 d from the start of the experiment and the dark period for PHB induction was from 9 d to 18 d, **C)** specific growth rate (d^{-1}) during phototrophic growth mode and PHB induction, and **D)** PHB accumulation profile under dark with 0.2 % acetate.

4.8. Conclusions

An increase in light intensity enhanced the growth of *C. fritschii* and with high light intensity of 1890 µmol/m^2/s resulting in biomass concentration of 1.84 g/L on 16 d in modified BG-11 medium. *C. fritschii* can be cultivated under simulated diurnal light mimic to sunlight resulting in DCW of 2.1 g/L in flask setup equipped with silicone tubing sparger. Nitrate concentration of 1.5 g/L and acetate level of 0.2 % (w/v) as inducer were shown as optimal levels for PHB production under diurnal light. Cultivation of *C. fritschii* in medium scale flat panel PBR under diurnal light resulted in DCW of 2.06 g/L with 11.2 % polymer content in single stage cultivation. A phosphate and nitrate feeding-batch strategy in flat panel PBR enhanced the PHB content to 46.9 % with a 4.2-fold increment when compared to control. This may be due to rapid utilization of phosphate and nitrate fed during growth resulting in stress or limitations of other nutrients (macro and micronutrients) which resulted in high PHB accumulation during dark upon induction with acetate.

CHAPTER 5

A multi-objective optimization approach for the production of Polyhydroxybutyrate via *Chlorogloea fritschii* under diurnal light with single-stage cultivation

5.1. Background and Uniqueness of the study

Typically, a two-stage cultivation strategy: growth in the presence of sufficient amounts of nitrogen and phosphate in media followed by PHB accumulation in the presence of inducers with nitrogen/phosphate limiting media has been used for PHB production (Monshupanee & Incharoensakdi, 2014). But two-stage cultivation is not economic due to the need of extra separation process for cell harvesting after growth in nutrient rich media and then cultivating in nutrient depleted media for PHB synthesis. Therefore, in current study PHB production was carried out using a single stage process to avoid intermediate biomass separation step.

Optimization of PHB production is not straightforward because there are several metabolically interlinked pathways involved in PHB synthesis, regulated by media components and environmental factors. A study of optimization of PHB production has been done earlier with several heterotrophic strains and very few phototrophic organisms (Mourão et al., 2020; Rueda & García, 2021). In all the studies, single objective optimization, mainly PHB production, has been considered. However, only PHB concentration or percentage of PHB in the cell may not be fully indicative of economic viability since it does not consider the downstream cost for cell harvesting, as the PHB is an intracellular product. Among several biomass harvesting methods such as filtration, sedimentation, centrifugation, flocculation, and flotation; sedimentation is cost-effective (Grima et al., 2003). Auto-sedimentation with a high settling rate is observed in the PHB-producing cyanobacteria *Chlorogloea fritschii* TISTR 8527 (Monshupanee et al., 2016). However, in the current study with *C. fritschii* TISTR 8527, it has been seen that the auto-sedimentation rate

of biomass and percentage of PHB in biomass are conflicting with each other and both are dependent on the nutrient composition in media. Also, biomass concentration and percentage of PHB in biomass conflict with each other since there is a requirement of nutrient rich media for biomass growth and nutrient-depleted media for PHB accumulation. Therefore, the optimization of PHB fermentation processes is a multi-objective optimization problem, the solution of which would involve the optimization of conflicting objectives such as PHB percentage, auto-sedimentation rate, and biomass concentration. Despite this, the application of multi-objective optimization to the PHB fermentation process has not been explored till now. A key step in multi-objective optimization is the generation of a set of non-dominated solutions called Pareto optimal solutions, denoting trade-offs between all the competing objectives (Deb & Gupta, 2005; Paschalidis et al., 2022). A solution is called a Pareto optimal solution when there is no solution present where all the objectives have better values. When comparing these solutions, a decrease of one objective is inevitable to increase another objective. One Pareto solution can be selected out of the set of alternatives for operation based on other practical considerations in real scenarios.

To address this issue, in the current work, the media optimization of PHB production from cyanobacteria is considered as a multiple objective optimization problem requiring simultaneous maximization of PHB percentage in biomass, biomass concentration, and auto-sedimentation rate. Furthermore, rather than using constant light, all optimization experiments conducted indoors under diurnal light mimicking sunlight. This can decrease the risk of change of optimal parameters in real scenarios when the PHB production process will be carried out under outdoor sunlight. The model used for multi-objective optimization has been developed based on Response Surface Methodology (RSM).

5.2. Diurnal lighting system mimic to sunlight for biomass growth

Since cyanobacteria cultivation under sunlight is the only feasible method for PHB production, optimization under diurnal light similar to outdoor sunlight is necessary. An unidirectional LED lighting with computer-dimmable technology was designed to mimic diurnal patterns similar to sunlight (Naira et al., 2019). The diurnal light (cycle of light intensities from dawn to dusk) was simulated with reference to a day in month of May in Guwahati, India (26°11′03″ N and 91°44′44″ E) using a customized unidirectional LED panel for growth of cyanobacteria. To generate automated diurnal light, cool white LED light (6500 K) was controlled through pulse width modulation (PWM) connected with the OPTO-22 control system (Naira et al., 2019). A Lux meter (Sigma Instruments, India) was used to measure diurnal natural sunlight as well as diurnal simulated sunlight intensities. This diurnal lighting system can generate light intensity ranging from 0 to 2200 µE/m^2/s (capable of mimicking sunlight intensities in the laboratory). Light intensities (in lux) were converted to PPFD (photosynthetic photon flux density) in µE/m^2/s by dividing with the conversion factor of 54 and 74 for diurnal natural sunlight and cool white LED respectively (Apogee Instruments, Inc. USA). Fig. 5.1 shows the diurnal light pattern used for all the experiments.

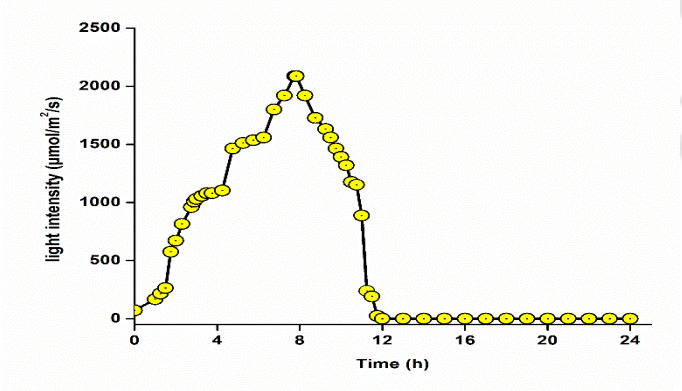

Fig. 5.1: The diurnal simulated sunlight pattern used for cultivation of *C. fritschii* for media optimization.

5.3. Experiments for screening of media composition using Plackett-Burman design

Plackett-Burman design (PBD) was used to screen the significant factors with respect to their main effects on biomass dry cell weight (DCW), PHB (%), and auto-sedimentation factor (SCF) using statistical software Design-Expert 7 (Bhange et al., 2023; Plackett & Burman, 1946). The eight nutrients ($NaNO_3$, K_2HPO_4, $MgSO_4.7H_2O$, $CaCl_2.2H_2O$, $FeCl_3.6H_2O$, Na_2EDTA, TRACE (Micronutrient solution) and Na_2CO_3) of modified BG-11 medium was chosen for the study. Each factor was tested at high (+1) and low (-1) levels (Table 5.1). The low and high levels of nutrients were selected as 10 times lower and 10-fold higher than that of modified BG11 medium (control media) except $NaNO_3$ in Plackett-Burman experiments. Based on PBD, 12 experiments (N+1) were conducted for screening considering eight media components and three dummy variables (N=8+3) (Table 5.2). Flasks were inoculated with a final volume of 200 ml medium under non-sterile conditions and with sparging of 1.5 VVM air containing 1% CO_2 (v/v) using perforated silicone rubber sparger (Fig. 5.2). Diurnal light was used to illuminate cultures for 16 days of the phototrophic growth period. After 16 days of growth period, PHB was induced by the addition of 0.2 % (w/v) acetate in culture media and kept under dark for the next 12 days with a sampling interval of 4 days to measure DCW (g/L), PHB and SCF. It has been seen in earlier study that PHB induction under the dark is higher than in light (Monshupanee et al., 2016). Note that in the transcriptome analysis of cyanobacteria, elevated levels of mRNA of phaE, a subunit of PHB synthase (phaCE) was observed during dark when compared to light (Köbler et al., 2018). The acetate percentage for PHB induction has been chosen based on preliminary experiments (section 4.6.3).

Table 5.1: High and low levels of variables for biomass and PHB production by *C. fritschii* and auto-sedimentation using Plackett-Burman Design.

Coded Factors	*Variables*	*Low level (-1)*	*High level (+1)*
A	$NaNO_3$ (g/L)	0.1	2
B	K_2HPO_4 (mg/L)	4	400
C	$MgSO_4.7H_2O$ (mg/L)	7.5	750
D	$CaCl_2.2H_2O$ (mg/L)	3.6	360
E	$FeCl_3.6H_2O$ (mg/L)	0.6	60
F	TRACE (X)	0.1	10
G	Na_2CO_3 (mg/L)	2	200
H	Na_2-EDTA (mg/L)	0.1	10

Table 5.2: Plackett-Burman experimental design matrix for screening of significant factors for three responses: DCW(g/l), PHB (%) and auto-sedimentation concentration factor (SCF).

Run no.	*A*: $NaNO_3$ g/L	*B*: K_2HPO_4 mg/L	*C*: $MgSO_4.7H_2O$ mg/L	*D*: $CaCl_2.2H_2O$ mg/L	*E*: $FeCl_3.6H_2O$ mg/L	*F*: TRACE X	*G*: Na_2CO_3 mg/L	*H*: Na_2-EDTA mg/L
1	0.1	400	750	360	0.6	0.1	2	10
2	0.1	4	7.5	360	0.6	10	200	0.1
3	2	4	750	360	60	0.1	2	0.1
4	2	400	750	3.6	0.6	0.1	200	0.1
5	0.1	4	750	3.6	60	10	2	10
6	0.1	400	750	3.6	60	10	200	0.1
7	2	4	750	360	0.6	10	200	10
8	2	400	7.5	360	60	10	2	0.1
9	0.1	4	7.5	3.6	0.6	0.1	2	0.1
10	2	4	7.5	3.6	60	0.1	200	10
11	0.1	400	7.5	360	60	0.1	200	10
12	2	400	7.5	3.6	0.6	10	2	10

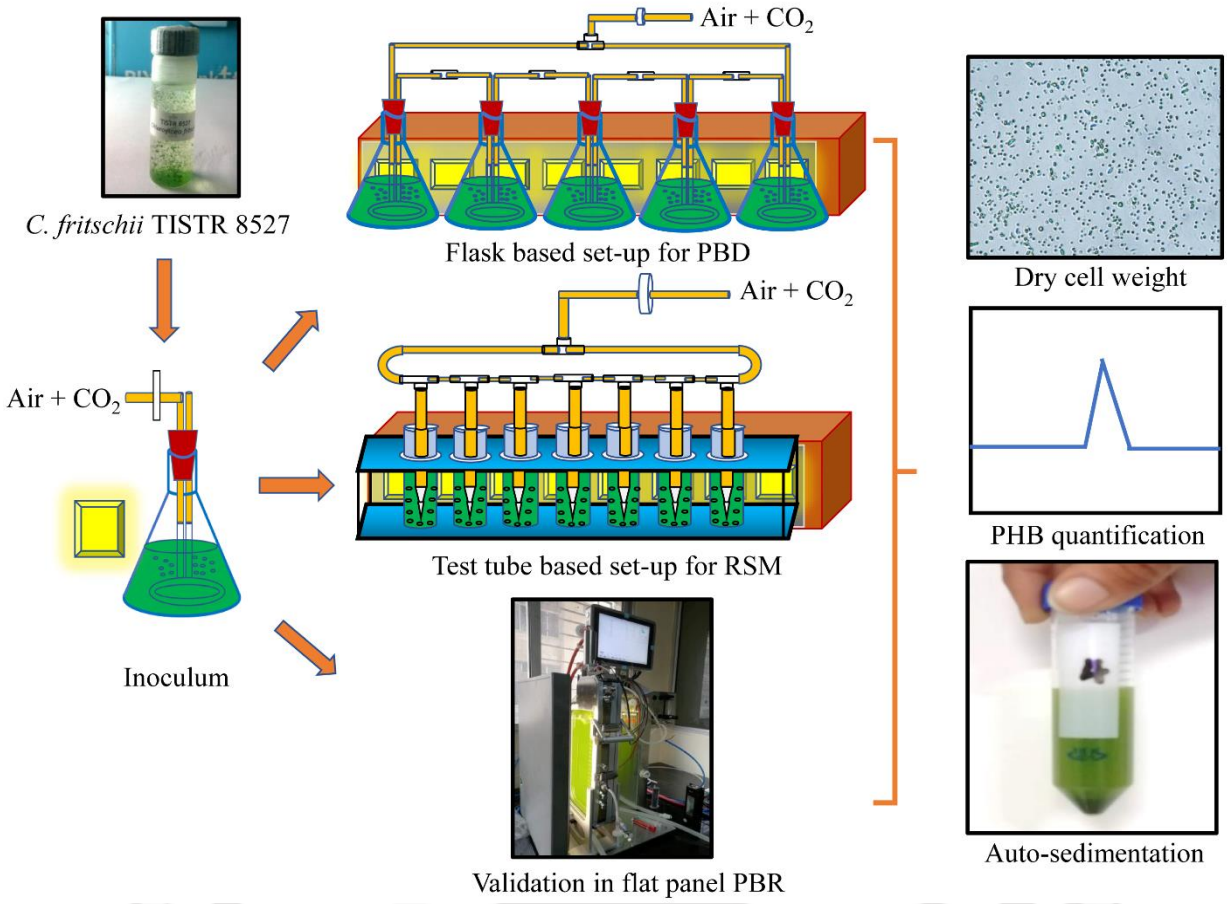

Fig. 5.2: Schematic diagram of the experimental set-up: flask based for PBD, test tube for RSM and flat panel photobioreactor for validation experiment used for the multi-objective media optimization for *C. fritschii* cultivation.

5.4. Development of Response surface-based model for objective functions

After identifying the significant factors based on PBD analysis, five-level Central Composite Design (CCD) was used for designing the experiments to develop the models for three objectives; i) biomass growth (DCW), ii) % of PHB in biomass, and iii) auto-sedimentation factor (SCF). For CCD study components interactions with the levels of $-\alpha$, -1, 0, +1 and $+\alpha$ have been chosen, where $\alpha = 2^{k/4}$ and k is the number of variables (Table 5.3). The design used for parameters in the selected range with coded terms was represented in Table 5.4. For CCD-RSM experiments the factors were

selected in the range as follows: $NaNO_3$ (0.1 to 2 g/L), K_2HPO_4 (4 to 400 mg/L), TRACE (0.1 to 10 X), Na_2EDTA (0.1 to 10 mg/L) and $MgSO_4.7H_2O$ (7.5 to 750 mg/L) (Table 5.4).

All the experiments ($2^k + 2k + m$, where m is the center points) were performed in a 55 mL Borosil test tube containing 35 mL medium with pH 7.5 under diurnal light for growth (12 h:12 h light and dark periods). The concentrations of other nutrients were kept constant. The mixture of air (2 VVM), and CO_2 (1 %) was sparged through 8 mm PU pipes connected in series through 50 mm 0.2 µm PTFE filters (AXIVA) during the autotrophic growth period. The CO_2 flow was turned off during the night period. After 16 days, 0.2 % (w/v) acetate was added to culture media and kept under dark. The sample was taken for analysis at regular intervals. Air without CO_2 was sparged during PHB induction under dark. The schematic of the experimental set-up is shown in Fig. 5.2. Biomass dry cell weight (DCW in g/L), PHB accumulation (% w/w), and SCF were used as responses. Design Expert 7.0 was used for the regression analysis of the experimental data and the second-order polynomial equation was employed for the same. Statistical parameters were estimated using Analysis of Variance (ANOVA).

Table 5.3: Different levels of factors for biomass and PHB production by *C. fritschii* and auto-sedimentation using RSM.

Variable	Coded symbol	Levels				
		-2.3784 (-α)	**-1**	**0**	**1**	**2.3784 (+α)**
$NaNO_3$ (g/L)	**A**	0.1	0.65	1.05	1.45	2
K_2HPO_4 (mg/L)	**B**	4	118.75	202	285.25	400
Trace (X)	**C**	0.1	2.97	5.05	7.3	10
Na_2EDTA (mg/L)	**D**	0.1	2.97	5.05	7.3	10
$MgSO_4.7H_2O$ (mg/L)	**E**	7.5	222.6	378.75	534.84	750

Table 5.4: Design matrix of factors in actual values for experiments using Central Composite Design for development of models of three objectives DCW(g/l), PHB (%) and auto-sedimentation concentration factor (SCF).

Run No.	A $NaNO_3$ g/L	B K_2HPO_4 mg/L	C TRACE X	D Na_2EDTA mg/L	E $MgSO_4.7H_2O$ mg/L	Run No.	A $NaNO_3$ g/L	B K_2HPO_4 mg/L	C TRACE X	D Na_2EDTA mg/L	E $MgSO_4.7H_2O$ mg/L
1	1.45	118.75	2.97	2.97	534.84	**26**	1.45	285.25	2.97	2.97	222.66
2*	1.05	202	5.05	5.05	378.75	**27**	1.05	202	5.05	10	378.75
3	1.05	4	5.05	5.05	378.75	**28**	0.65	285.25	7.13	7.13	534.84
4	1.45	285.25	2.97	7.13	222.66	**29**	0.65	118.75	2.97	2.97	222.66
5	1.45	118.75	7.13	7.13	534.84	**30**	1.05	202	5.05	5.05	750
6*	1.05	202	5.05	5.05	378.75	**31***	1.05	202	5.05	5.05	378.75
7	0.65	285.25	7.13	2.97	534.84	**32**	0.1	202	5.05	5.05	378.75
8	0.65	118.75	7.13	7.13	534.84	**33**	0.65	285.25	2.97	7.13	534.84
9	1.05	202	5.05	0.1	378.75	**34**	0.65	285.25	7.13	2.97	222.66
10*	1.05	202	5.05	5.05	378.75	**35**	1.45	118.75	7.13	2.97	534.84
11*	1.05	202	5.05	5.05	378.75	**36**	0.65	118.75	2.97	2.97	534.84
12	1.45	285.25	2.97	2.97	534.84	**37**	1.45	118.75	2.97	2.97	222.66
13	2	202	5.05	5.05	378.75	**38**	1.45	285.25	7.13	7.13	534.84
14	0.65	285.25	7.13	7.13	222.66	**39**	1.05	400	5.05	5.05	378.75
15	0.65	285.25	2.97	2.97	534.84	**40**	1.05	202	5.05	5.05	7.5
16	0.65	285.25	2.97	2.97	222.66	**41**	1.45	118.75	7.13	2.97	222.66
17	1.45	285.25	7.13	2.97	222.66	**42**	0.65	118.75	2.97	7.13	222.66
18	1.45	285.25	2.97	7.13	534.84	**43**	1.05	202	0.1	5.05	378.75
19	0.65	118.75	2.97	7.13	534.84	**44**	0.65	118.75	7.13	2.97	534.84
20*	1.05	202	5.05	5.05	378.75	**45**	1.45	285.25	7.13	2.97	534.84
21	0.65	285.25	2.97	7.13	222.66	**46***	1.05	202	5.05	5.05	378.75
22	1.45	118.75	7.13	7.13	222.66	**47**	0.65	118.75	7.13	7.13	222.66
23	1.45	285.25	7.13	7.13	222.66	**48***	1.05	202	5.05	5.05	378.75
24	1.45	118.75	2.97	7.13	534.84	**49**	1.45	118.75	2.97	7.13	222.66
25	1.05	202	10	5.05	378.75	**50**	0.65	118.75	7.13	2.97	222.66

'*' represent center points of design matrix.

In this design the independent factors $NaNO_3$, K_2HPO_4, TRACE, Na_2EDTA and $MgSO_4.7H_2O$ are coded as A, B, C, D, and E. The experimental data obtained from the design was subjected to regression analysis and can be represented as second-order polynomial equation as follows:

$$f = \beta_0 + \beta_1 A + \beta_2 B + \beta_3 C + \beta_4 D + \beta_5 E + \beta_{11} A^2 + \beta_{22} B^2 + \beta_{33} C^2 + \beta_{44} D^2 + \beta_{55} E^2 + \beta_{12} AB + \beta_{13} AC + \beta_{14} AD + \beta_{15} AE + \beta_{23} BC + \beta_{24} BD + \beta_{25} BE + \beta_{34} CD + \beta_{35} CE + \beta_{45} DE \quad \text{……. (5.1)}$$

where f is the measured response, β_0 is the offset term, β_1, β_2, β_3, β_4 and β_5 represents the linear term coefficients, β_{11}, β_{22}, β_{33}, β_{44} and β_{55} are quadratic coefficients, β_{12}, β_{13}, β_{14}, β_{15}, β_{23}, β_{24}, β_{25}, β_{34}, β_{35} and β_{45} are the interaction term coefficients.

5.5. Multi-objective media optimization

This study aims to maximize i) DCW in g/L (f_1), ii) % of PHB (f_2), and iii) SCF (f_3) by a composite desirability function approach. In multi-objective optimization, all three responses are optimized together considering the overall desirability (D) function as the objective function to be maximized. The overall desirability (D) is expressed in terms of individual desirability (d_i) of each objective (f_i) according to equations 5.2 and 5.3 (Derringer & Suich, 1980; Konstantinidis et al., 2018)

$$d_i(f_i) = \begin{cases} 0 & for \quad f_i < L_i \\ \left(\frac{f_i - L_i}{U_i - L_i}\right)^w & for \quad L_i \leqslant f_i \leqslant U_i \\ 1 & for \quad f_i > U_i \end{cases} \quad \text{…….. (5.2)}$$

$$D = (d_1 \times d_2 \times d_3)^{\frac{1}{3}} \quad \text{…….. (5.3)}$$

Each desirability value (d_i) is calculated from the corresponding response by scaling to a value between 0 to 1 using equation 5.2. A value of zero indicates the minimized value of response and the value close to 1 indicates the optimized one. The overall desirability function (D) is the weighted geometric mean of individual desirability function d_i , where i= 1, 2, 3 (Eq. 5.3). Here L_i and U_i in equation 5.2 are lower and upper specification limits of i^{th} response and used from RSM experimental data. The weight exponent "*w*" (in Eq. 5.2) determines the relative importance and decides the shape of the d_i from a straight line (w = 1) to convex (w < 1) or concave (w > 1). Weight selection is a critical and challenging task in the desirability approach. To generate a set of feasible solutions, *w* is varied from 1 to 5 with a step change of 1. From those feasible solutions, a set of Pareto points are decided based on a non-dominating approach considering all three objectives. For optimization and generation of all feasible solutions by varying *w*, the popular DoE software package Design Expert® (Stat-Ease, Inc., MN) has been used.

5.6. Experiment with a pareto solution for validation under diurnal light

The experiment has been conducted with one Pareto optimal solution for validation. The compromising programming approach has been used to select Pareto optimal solutions (Deb, 2003). The experiment was conducted in 2 L flat panel photobioreactor (Labfors, INFORS HT, 25.5 × 2 × 50 cm) under diurnal light. The experiment was conducted with a culture volume of 2.0 l with an initial cell density of 0.05 g/L under simulated diurnal light described earlier with a 12 h light:12 h dark cycle for biomass growth. The unialgal culture was aerated with 0.5 VVM air containing 1 % CO_2. The CO_2 flow was turned off during the night period, but the air was sparged continuously to avoid settling of biomass and to maintain O_2 for respiration. The dry cell weight (DCW), phosphate, and nitrate were measured every 24 h till it reached the stationary phase (216 h). PHB production was induced by supplementing 0.2 % acetate (w/v) without medium

replacement at 216 h under completely dark condition. The sampling was done at regular intervals during the induction phase to measure DCW, PHB, and SCF. Model validation experiments and their analysis were performed in duplicates and the average result was reported.

5.7. Results and discussion

5.7.1. Identification of important media components through Plackett-Burman design

The PBD results are shown in Table 5.5 and observed that there was a variation in the DCW (g/L) ranging from 0.24 to 1.22 g/L, PHB content from 0.55 to 29.91 %, and SCF from 9.77 to 48.36. Among eight factors, $NaNO_3$, K_2HPO_4, $MgSO_4$ and Na_2CO_3 showed a positive effect on DCW whereas, $CaCl_2$, $FeCl_3$, Na_2EDTA, and TRACE exhibited a negative effect based on ANOVA analysis (Table 5.6). $NaNO_3$, K_2HPO_4, and $MgSO_4$ led to a negative effect on PHB content (%) and $CaCl_2$, $FeCl_3$, Na_2EDTA, Na_2CO_3, and TRACE exerted a positive effect on PHB accumulation (Table 5.6). $NaNO_3$ and TRACE had a negative effect on SCF and K_2HPO_4, $MgSO_4$, $CaCl_2$, $FeCl_3$, Na_2EDTA, and Na_2CO_3 while had a positive effect on SCF (Table 5.6). $NaNO_3$, K_2HPO_4, TRACE, Na_2EDTA, and $MgSO_4$ were screened as significant factors ($p < 0.1$) considering all three objectives (Table 5.6, Fig. 5.3).

Table 5.5: Experimental and predicted values of responses for Plackett-Burman design of 12 runs with 8 variables.

Run no	DCW (g/L)		PHB (%)		SCF	
	Experimental value	**Predicted value**	**Experimental value**	**Predicted value**	**Experimental value**	**Predicted value**
1	0.97	0.91	1.28	3.72	48.36	46.19
2	0.57	0.43	29.91	24.97	12.83	18.03
3	0.81	1.02	2.66	0.82	18.52	21.06
4	2.82	2.54	0.55	0	20.62	25.44
5	0.24	0	23.66	18.12	32.73	37.56
6	1.22	1.5	10.32	15.86	43.5	38.67
7	0.32	0.45	9.66	14.6	27.33	22.14
8	1.07	0.86	0.56	2.4	11.58	9.04
9	0.84	0.97	2.71	7.65	25.42	20.23
10	1.08	1.02	6.67	9.11	20.22	18.06
11	0.87	0.93	18	15.56	37.75	39.91
12	0.62	0.84	0.68	0	9.77	12.31

Table 5.6: Estimated effects, F-values and p-values for DCW (g/L), PHB (%) and SCF by *C. fritschii* in PBD experiment.

Source	DCW (g/L)						PHB (%)						SCF					
	Effects	Sum of squares	df	Mean Square	F-value	p-value	Effects	Sum of squares	df	Mean Square	F-Value	p-value	Effects	Sum of squares	df	Mean Square	F - value	p-value
Model		4.36	8	0.55	3.72	0.153		898.64	8	112.33	1.744	0.3516		1569.16	8	196.15	3.19	0.184
$NaNO_3$	0.34	0.34	1	0.34	2.32	0.225	-10.85	353.16	1	353.16	5.484	0.099*	-15.42	713.68	1	713.68	11.61	0.042*
K_2HPO_4	0.62	1.16	1	1.16	7.89	0.067*	-7.31	160.45	1	160.45	2.491	0.2125	5.75	99.21	1	99.21	1.61	0.293
$MgSO_4.7H_2O$	0.22	0.14	1	0.14	0.98	0.395	-1.73	9.01	1	9.01	0.139	0.7332	12.25	450.05	1	450.05	7.32	0.073*
$CaCl_2.2H_2O$	-0.37	0.41	1	0.41	2.78	0.193	2.91	25.46	1	25.46	0.395	0.5741	0.68	1.4	1	1.4	0.023	0.889
FeCl3.6H_2O	-0.14	0.061	1	0.061	0.41	0.565	2.85	24.310	1	24.31	0.377	0.5824	3.33	33.21	1	33.21	0.54	0.515
Trace	-0.56	0.94	1	0.94	6.39	0.085*	7.15	153.51	1	153.51	2.384	0.2203	-5.52	91.54	1	91.54	1.49	0.309
Na_2CO_3	0.39	0.45	1	0.45	3.06	0.178	7.26	158.12	1	158.12	2.455	0.2151	2.64	20.95	1	20.95	0.34	0.600
Na_2EDTA	-0.54	0.87	1	0.87	5.92	0.093*	2.21	14.60	1	14.608	0.226	0.6664	7.28	159.11	1	159.11	2.59	0.206
Residual		0.44	3	0.15				193.16	3	64.38				184.34	3	61.45		
Cor Total		4.8	11					1091.81	11					1753.5	11			

* $p<0.1$ were considered as significant factors

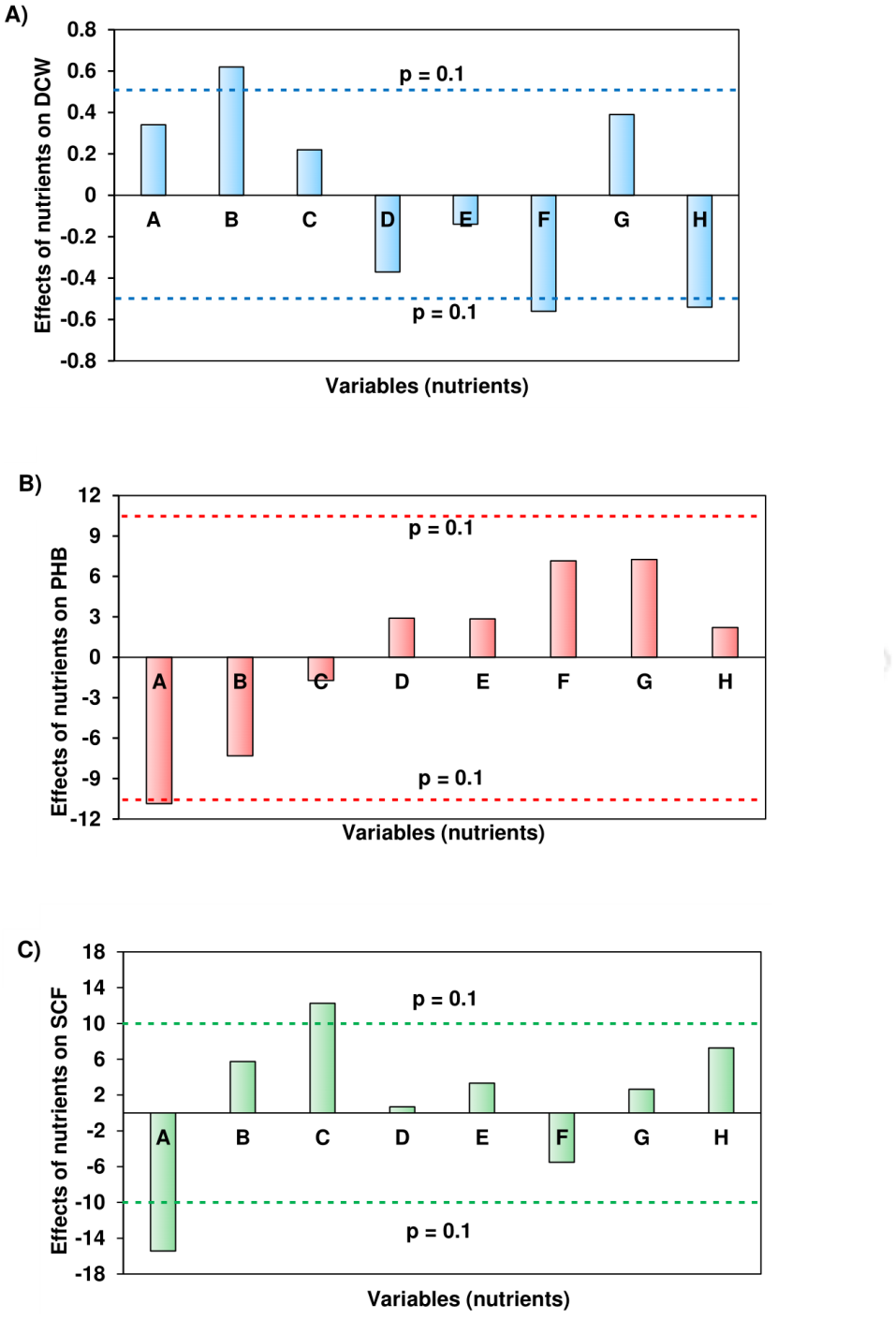

Fig. 5.3: The effects of nutrients resulted from ANOVA of PBD on responses: **A)** DCW (g/L), **B)** PHB (%), and **C)** SCF.

5.7.2. Model development using response surface methodology for optimization

Based on response surface methodology (RSM) 50 experiments ($2^k + 2k + m$, k=5 variables, m=8 center points) have been conducted with various combinations of $NaNO_3$ (A), K_2HPO_4 (B), TRACE (C), Na_2EDTA (D) and $MgSO_4.7H_2O$ (E) (Table 5.4). The experimental results for the DCW (g/L), PHB accumulation (% w/w), and SCF of *C. fritschii* are represented in Table 7. All the experiments with different media combinations resulted in DCW (f_1): 0.056 - 1.59 g/L, PHB (f_2): 0 - 45.7 w/w %, and SCF (f_3): 2.28 - 117.3 (Table 5.7). Using multiple regression analysis, results were fitted to second-order polynomial expressed in terms of coded factors as follows:

$$f_1\,(\text{DCW}, g/l) = 0.73 - 0.016A - 0.033B - 0.065C + 0.04D - 0.022E + 0.026AB - 0.020AC - 0.077AD + 0.000AE - 0.13BC + 0.019BD + 0.007639BE - 0.11CD - 0.041CE + 0.063DE - 0.004233A^2 + 0.006570B^2 + 0.048C^2 - 0.013D^2 - 0.059E^2 \quad \ldots\ldots\ldots (5.4)$$

$$f_2\,(\%\ \text{PHB}) = 3.56 - 3.51A - 0.20B + 1.58C + 0.36D + 1.22E - 3.05AB - 1.38AC - 0.32AD - 2.16AE + 0.96BC + 1.19BD + 1.22BE + 1.31CD - 0.024CE + 0.66DE + 1.51A^2 + 0.98B^2 - 0.43C^2 + 0.44D^2 + 0.87E^2 \quad \ldots\ldots\ldots (5.5)$$

$$f_3\,(\text{SCF}) = 20.80 - 1.03A + 4.27B + 3.01C - 2.39D - 0.89E + 12.36AB + 4.44AC + 4.79AD - 3.04AE - 0.11BC + 1.03BD - 3.52BE + 2.13CD - 1.11CE - 6.18DE - 0.11A^2 + 1.02B^2 + 1.26C^2 + 0.69D^2 + 3.30E^2 \quad \ldots\ldots\ldots (5.6)$$

The ANOVA analysis of the experimental design revealed that interactive terms BC and CD were significant for DCW (g/L) ($p < 0.1$) and interactive term AB was found to be significant for SCF ($p < 0.1$) and PHB ($p < 0.1$). The rest of the other terms were found to be insignificant for all responses (Table 5.8).

Table 5.7: Experimental and predicted values of responses for Response surface design of 50 runs with 5 variables.

Run no	DCW (g/L)		PHB (%)		SCF		Run no	DCW (g/L)		PHB (%)		SCF	
	Expt. value	Predicted value	Expt. value	Predicted value	Expt. value	Predicted value		Expt. value	Predicted value	Expt. value	Predicted value	Expt. value	Predicted value
1	0.78	0.54	0.97	7.08	7.43	9.38	**26**	0.34	0.84	0.66	0	53.21	34.08
2*	0.72	0.73	4.09	3.56	18.86	20.8	**27**	0.61	0.75	6.02	6.92	4.03	19
3	0.31	0.84	21.96	9.55	17.74	16.43	**28**	0.4	0.52	45.7	25.62	3.28	5.68
4	1.28	0.9	2.57	0	12.22	49.04	**29**	0.81	0.53	0	5.87	3.37	34.76
5	0.5	0.57	0.81	4.53	6.07	12.65	**30**	0.32	0.34	21.09	11.36	30.27	37.34
6*	0.72	0.73	4.09	3.56	18.86	20.8	**31***	0.72	0.73	4.09	3.56	18.86	20.8
7	0.44	0.34	1.79	17.96	32.49	26.1	**32**	0.34	0.74	29.76	20.44	2.28	22.61
8	1.59	0.84	0.7	13.17	9.11	27.05	**33**	1.12	1.18	7.91	15.21	32.4	6.73
9	0.68	0.56	12.63	5.21	21.77	30.39	**34**	0.53	0.58	16.96	10.11	26.71	18.7
10*	0.72	0.73	4.09	3.56	18.86	20.8	**35**	0.78	0.78	1.75	2.91	6.98	18.03
11*	0.72	0.73	4.09	3.56	18.86	20.8	**36**	0.71	0.43	5.43	8.93	60.9	60.69
12	0.41	0.77	0	0	31.68	33.76	**37**	0.34	0.64	8.66	12.67	13.25	0
13	1.04	0.66	0.94	3.74	14.44	17.7	**38**	0.2	0.34	0	4.78	64.89	40.7
14	0.56	0.5	13.07	15.15	3.14	23	**39**	1.2	0.69	2.72	8.61	11.85	36.75
15	0.62	0.55	6.61	12.78	27.08	35.65	**40**	0.44	0.44	2.35	5.56	25.04	41.56
16	0.74	0.63	5.15	4.84	54.54	23.8	**41**	1.51	1.04	1.01	8.6	14.92	8.71
17	0.63	0.71	1.7	0	34.05	46.73	**42**	0.99	0.83	1.07	0.92	30.57	26.45
18	1.06	1.08	0	0	19.89	24	**43**	1.18	1.15	7.94	0	13.93	20.79
19	0.83	0.98	4.95	6.61	25.4	27.65	**44**	0.36	0.75	13.33	10.27	88.36	51.58
20*	0.72	0.73	4.09	3.56	18.86	20.8	**45**	0.41	0.48	5.29	0	46.19	41.96
21	0.73	1	3.58	4.65	38.71	19.6	**46***	0.72	0.73	4.09	3.56	18.86	20.8
22	0.33	0.58	25.06	7.6	5.87	28.05	**47**	1.11	0.86	0.43	7.58	71.14	30.29
23	0.056	0.33	0	2.96	117.13	70.19	**48***	0.72	0.73	4.09	3.56	18.86	20.8
24	0.77	0.78	1.22	3.48	10.44	0	**49**	0.73	0.63	0.92	6.45	17.06	6.46
25	0.8	0.84	0.87	4.91	18.38	35.11	**50**	0.93	1.01	7.43	7.31	27.67	30.1

'*' represent center points of design matrix, Expt. Value: Experimental value.

Table 5.8: Estimated F-values and p-values by ANOVA for DCW (g/L), PHB (%) and SCF by RSM-CCD design.

Source	DCW (g/L)					PHB (%)					SCF				
	Sum of Squares	df	Mean Square	F-value	p-value	Sum of Squares	df	Mean Square	F-value	p-value	Sum of Squares	df	Mean Square	F-value	p-value
Model	2.10	20	0.10	1.00	0.490	1632.22	20	81.61	1.06	0.430	10580.74	20	529.04	1.02	0.467
A-$NaNO_3$	0.011	1	0.011	0.10	0.748	533.64	1	533.64	6.96	0.013	46.06	1	46.06	0.089	0.767
B-K_2HPO_4	0.047	1	0.047	0.44	0.510	1.68	1	1.68	0.022	0.883	790.77	1	790.77	1.53	0.226
C-TRACE	0.19	1	0.19	1.76	0.194	108.39	1	108.39	1.41	0.244	392.72	1	392.72	0.76	0.390
D-Na_2EDTA	0.069	1	0.069	0.66	0.423	5.56	1	5.56	0.072	0.789	248.30	1	248.30	0.48	0.493
E-$MgSO_4.7H_2O$	0.021	1	0.021	0.20	0.656	64.30	1	64.30	0.84	0.367	34.23	1	34.23	0.066	0.798
AB	0.021	1	0.021	0.20	0.657	297.70	1	297.70	3.88	0.058*	4885.53	1	4885.5	9.46	0.004*
AC	0.013	1	0.013	0.12	0.727	60.72	1	60.72	0.79	0.381	630.04	1	630.04	1.22	0.278
AD	0.19	1	0.19	1.81	0.188	3.24	1	3.24	0.042	0.838	733.56	1	733.56	1.42	0.243
AE	0.000	1	0.000	0.000	0.999	149.90	1	149.90	1.95	0.172	295.86	1	295.86	0.57	0.455
BC	0.56	1	0.56	5.31	0.028*	29.50	1	29.50	0.38	0.540	0.39	1	0.39	$7.587E^{-4}$	0.978
BD	0.012	1	0.012	0.12	0.736	45.35	1	45.35	0.59	0.448	33.91	1	33.91	0.066	0.799
BE	$1.867E^{-3}$	1	$1.867E^{-3}$	0.018	0.894	47.65	1	47.65	0.62	0.437	396.57	1	396.57	0.77	0.388
CD	0.40	1	0.40	3.86	0.059*	54.55	1	54.55	0.71	0.406	144.64	1	144.64	0.28	0.600
CE	0.054	1	0.054	0.51	0.480	0.018	1	0.018	$2.383E^{-4}$	0.987	39.52	1	39.52	0.076	0.784
DE	0.13	1	0.13	1.22	0.278	13.75	1	13.75	0.18	0.675	1222.20	1	1222.2	2.37	0.134
A^2	$9.959E^{-4}$	1	$9.959E^{-4}$	$9.492E^{-3}$	0.923	126.42	1	126.42	1.65	0.209	0.72	1	0.72	$1.398E^{-3}$	0.970
B^2	$2.398E^{-3}$	1	$2.398E^{-3}$	0.023	0.880	52.92	1	52.92	0.69	0.413	58.17	1	58.17	0.11	0.739
C^2	0.13	1	0.13	1.21	0.280	10.13	1	10.13	0.13	0.718	88.71	1	88.71	0.17	0.681
D^2	$9.496E^{-3}$	1	$9.496E^{-3}$	0.091	0.765	10.91	1	10.91	0.14	0.708	26.32	1	26.32	0.051	0.823
E^2	0.19	1	0.19	1.86	0.183	41.74	1	41.74	0.54	0.466	603.86	1	603.86	1.17	0.288
Residual	3.04	29	0.10			2224.77	29	76.72			14984.60	29	516.71		
Lack of Fit	3.04	22	0.14			2224.77	22	101.13			14984.60	22	681.12		
Pure Error	0.000	7	0.000			0.000	7	0.000			0.000	7	0.000		

*p <0.1 were considered as significant interactions.

5.7.3. Multi-objective optimization

Three polynomial models (eq. 5.4, 5.5, and 5.6) correspond to three objective functions developed using response surface methodology that were used for multi-objective optimization utilizing the composite desirability approach. By giving five different weight importance (w = 1, 2, 3, 4 and 5 in eq. 5.2) for three objectives, 125 feasible solutions (5^3 =125) have been generated considering the overall desirability as an objective function (Fig. 5.4, Table 5.9). From these 125 feasible solutions, non-dominated solutions were considered as Pareto points. To identify the Pareto points all feasible solutions have been plotted in objective space (Fig. 5.4). A set of 9 points have been identified as Pareto points considering f_1 and f_2 (Fig. 4A) and 15 points identified as Pareto points considering f_2 and f_3 (Fig. 5.4B). From the 3-D plot of objectives, a total of 23 points (one point is common for f_1 vs f_2 and f_2 vs f_3) were identified as Pareto points considering all three objective functions (Fig. 5.4C). An increase in f_2 from 18.8 to 45.7 % is accompanied by loss of f_1 from 1.6 to 0.67 g/L; thus, the two objectives, f_1 and f_2 are contradictory to each other (Fig. 5.4A). Similarly, increment of f_3 from 54.9 to 124.3 is associated with decrement of f_2 from 45.7 to 26.1 % across solution points in Pareto front (Fig. 5.4B). These Pareto solutions offer flexibility to operators for choosing the appropriate media to run the process at the most suitable optimal solution with additional considerations. Further, one Pareto optimal solution has been validated experimentally.

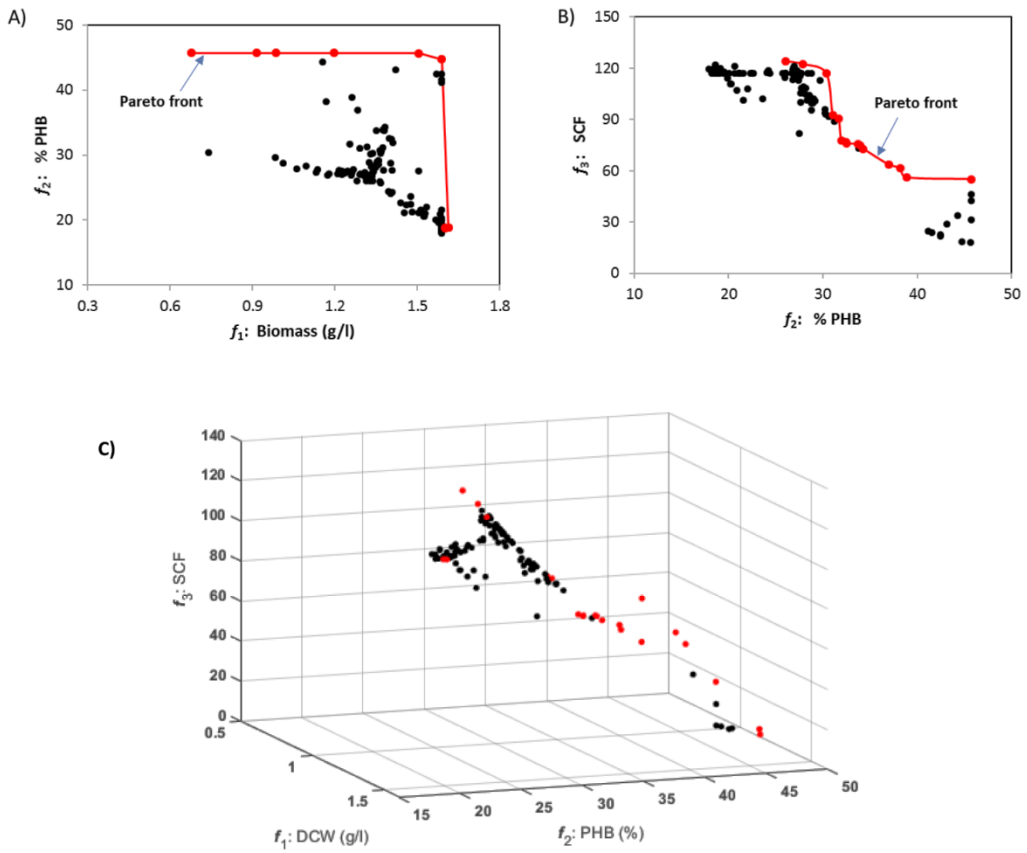

Fig. 5.4: Multi response optimization and pareto solutions to maximize the production of all three responses: DCW, PHB content and SCF. **A)** All feasible solutions and pareto solutions based on DCW and PHB content. **B)** All feasible solutions and pareto solution based on PHB content and SCF. **C)** All feasible solutions and pareto solutions based on all three responses. Points indicated in red color denoted as pareto solution in Fig. A, B and C. Red line denoted as the pareto front in Fig. A and B.

Table 5.9: List of 125 solutions generated using composite desirability function with different weight levels of objective functions.

Sl. No.	Weight (w)			A	B	C	F	H	f_1	f_2	f_3
	DCW (g/L)	PHB (%)	SCF	$NaNO_3$ (g/L)	K_2HPO_4 (mg/L)	$MgSO_4.7H_2O$ (mg/L)	TRACE (X)	Na_2EDTA (mg/L)	DCW (g/L)	PHB (%)	SCF
1	5	5	1	0.11	359.19	750	0.1	5.72	1.58889	44.7455	18.6925
2	5	5	2	0.1	5.12	750	10	7.79	1.36411	30.6606	91.962
3	5	5	3	0.1	6.63	750	10	6.35	1.33264	28.1604	108.215
4	5	5	4	0.1	4	748.36	10	6.78	1.35784	28.5551	104.091
5	5	5	5	0.1	4.43	750	10	7.71	1.36641	30.4292	93.1778
6	5	4	1	0.1	4	749.93	9.99	9.29	1.38012	33.7216	75.4393
7	5	4	2	0.1	4	736.62	10	9.05	1.40511	32.4539	76.7655
8	5	4	3	0.11	4	718.78	10	5.23	1.39619	24.3834	117.129
9	5	4	4	0.11	4	750	10	6.65	1.34716	28.0892	105.183
10	5	4	5	0.1	19.87	651.05	10	3.65	1.452909	21.14102	117.1318
11	5	3	1	0.1	329.96	750	0.11	6.03	1.58889	41.5636	24.0274
12	5	3	2	0.1	4.02	727.14	10	6.87	1.40768	27.64268	99.98411
13	5	3	3	0.1	4	667.62	10	4.54	1.51112	21.5486	117.127
14	5	3	4	0.1	4	738.56	10	6.55	1.37673	27.6554	105.363
15	5	3	5	0.1	4.03	634.65	9.99	4.03	1.57964	19.6756	117.13
16	5	2	1	0.1	4	637.42	9.99	5.05	1.583207	20.90894	107.0067
17	5	2	2	0.1	4	636.91	10	5.61	1.588887	21.56943	101.2599
18	5	2	3	0.1	8.58	618.11	10	3.47	1.588886	18.89739	118.2853
19	5	2	4	0.1	7.7	618.28	10	3.17	1.588885	18.59206	121.88
20	5	2	5	0.1	13.21	600.69	9.97	2.89	1.588894	18.14719	119.2797
21	5	1	1	0.1	4.01	632.28	9.98	4.62	1.588853	20.20803	110.7461
22	5	1	2	0.1	4	658.23	9.96	5.26	1.53264	22.01603	107.9245
23	5	1	3	0.1	7.8	614.99	10	3.55	1.600997	18.73247	117.1291
24	5	1	4	0.1	14.3	601.72	10	2.86	1.588891	18.21906	119.2286
25	5	1	5	0.1	4.25	628.94	10	3.67	1.588894	19.16122	119.9742
26	4	5	1	0.2	400	750	0.1	4.98	1.504995	45.66251	18.14009
27	4	5	2	0.1	5.38	750	9.71	9.45	1.350028	33.79471	73.07716
28	4	5	3	0.1	4.01	750	10	7.07	1.35875	29.16843	100.8458
29	4	5	4	0.11	4.05	744.64	10	5.57	1.337057	26.01218	117.1291
30	4	5	5	0.1	4	750	9.99	5.82	1.331546	27.01795	115.7956
31	4	4	1	0.1	337.61	750	0.1	5.95	1.588767	42.46887	22.73402
32	4	4	2	0.11	4	749.9	10	7.13	1.355078	28.9203	99.54249
33	4	4	3	0.1	4	749.54	9.49	6.49	1.26634	27.74127	108.4134
34	4	4	4	0.1	4	750	10	7.03	1.357884	29.09236	101.3299
35	4	4	5	0.1	6.3	730.94	10	5.59	1.364855	25.9716	114.4618

36	4	3	1	0.1	327.13	750	0.11	6.06	1.58889	41.15885	24.64582
37	4	3	2	0.1	4	737.23	9.93	9.12	1.397087	32.52351	76.13075
38	4	3	3	0.1	9.15	656.52	10	4.17	1.504945	21.08239	117.1284
39	4	3	4	0.1	4	658.48	10	4.03	1.52463	20.62132	121.2436
40	4	3	5	0.11	4.11	748.59	10	5.94	1.334934	26.77169	113.2972
41	4	2	1	0.1	4	681.37	10	8.05	1.50531	27.49992	81.81261
42	4	2	2	0.1	8.4	616.78	10	3.17	1.588882	18.58821	121.2748
43	4	2	3	0.1	9.26	648.11	10	4.03	1.52233	20.61282	117.1284
44	4	2	4	0.1	4.01	657.99	9.98	4.4	1.527637	20.99469	117.1306
45	4	2	5	0.1	4.01	734.14	10	5.49	1.3657	25.7255	117.13
46	4	1	1	0.1	5.04	628.41	10	3.9	1.58889	19.4069	117.141
47	4	1	2	0.1	6.65	618.26	10	3.65	1.60051	18.8378	117.129
48	4	1	3	0.1	4.02	632.62	10	3.93	1.58451	19.523	117.937
49	4	1	4	0.1	16.19	597.77	10	2.92	1.58891	18.2501	117.131
50	4	1	5	0.13	4	627.36	10	3.58	1.5889	18.2616	118.611
51	3	5	1	0.18	400	749.93	0.1	4.06	1.19681	45.701	31.1599
52	3	5	2	0.1	18.66	750	10	7.23	1.29133	31.0499	92.4104
53	3	5	3	0.1	10.62	749.97	10	7.25	1.33023	30.2062	95.7754
54	3	5	4	0.1	4.64	747.26	9.98	5.66	1.32992	26.7017	117.129
55	3	5	5	0.12	35.55	750	10	4.47	1.13105	27.2963	116.804
56	3	4	1	0.14	350.45	750	0.1	5.74	1.57086	42.423	21.7831
57	3	4	2	0.12	4	750	10	7.11	1.3527	28.7709	99.5005
58	3	4	3	0.1	8.37	750	10	5.74	1.30998	27.3396	114.788
59	3	4	4	0.1	4.01	713.94	10	5.09	1.40786	24.2431	118.665
60	3	4	5	0.1	4	749.97	10	6.07	1.33971	27.4438	112.761
61	3	3	1	0.1	4.22	749.84	10	9.51	1.38077	34.2689	72.8899
62	3	3	2	0.1	4	750	10	6.01	1.33809	27.3385	113.564
63	3	3	3	0.1	4.18	750	10	6.97	1.35656	29.0011	101.978
64	3	3	4	0.1	6.86	750	9.7	5.65	1.2606	26.9087	117.129
65	3	3	5	0.1	7.55	750	10	5.43	1.30564	26.7713	119.02
66	3	2	1	0.1	4	732.81	10	8.92	1.4119	31.9609	77.7926
67	3	2	2	0.1	4.01	732.68	10	7.35	1.40151	28.7778	95.323
68	3	2	3	0.1	4	683.4	10	4.78	1.477	22.4916	117.129
69	3	2	4	0.1	13.24	656.85	10	4.01	1.48011	21.2406	117.13
70	3	2	5	0.1	11	681.68	10	4.48	1.43973	22.6298	117.129
71	3	1	1	0.1	4.48	633	10	4.62	1.5889	20.2735	110.634
72	3	1	2	0.1	4	633.1	10	4.3	1.58812	19.9015	114.181
73	3	1	3	0.1	16.8	594.52	10	2.6	1.58891	17.9489	119.541
74	3	1	4	0.11	4.03	688.67	10	4.77	1.46046	22.3048	117.129
75	3	1	5	0.1	13.6	604.96	10	3.15	1.58889	18.5082	117.132
76	2	5	1	0.2	400	750	0.1	3.9	1.15626	44.3147	34.0034
77	2	5	2	0.1	49.86	750	10	8.74	1.16752	38.1674	61.6086

78	2	5	3	0.11	4	749.73	10	6.94	1.3552	28.7518	102.133
79	2	5	4	0.1	23.19	749.95	10	5	1.21526	27.6087	117.113
80	2	5	5	0.1	4	749.94	10	5.95	1.3362	27.1762	114.115
81	2	4	1	0.1	345.98	750	0.11	5.34	1.42062	43.113	28.7963
82	2	4	2	0.1	5.56	750	10	9.29	1.37356	33.921	74.7353
83	2	4	3	0.1	5.87	749.9	9.85	7.61	1.33816	30.2287	93.7346
84	2	4	4	0.12	4	750	9.96	5.6	1.31384	26.0187	117.129
85	2	4	5	0.1	19.72	750	10	4.79	1.22589	26.9735	121.241
86	2	3	1	0.1	25.72	750	10	9.51	1.28297	36.9497	63.6479
87	2	3	2	0.1	4.71	749.97	10	6.92	1.35319	28.9679	102.284
88	2	3	3	0.1	8.3	749.99	9.92	5.56	1.29033	27.0186	117.13
89	2	3	4	0.1	21.01	749.73	9.98	5.08	1.2249	27.5032	117.129
90	2	3	5	0.1	19.02	750	10	5.03	1.2372	27.2637	118.61
91	2	2	1	0.1	4	749.95	10	7.84	1.37015	30.6364	91.8604
92	2	2	2	0.12	4	750	9.95	6.96	1.34039	28.3439	101.163
93	2	2	3	0.1	4.39	750	10	6.35	1.34351	27.9363	109.232
94	2	2	4	0.1	38.1	743.51	10	4.35	1.13587	27.7218	117.13
95	2	2	5	0.1	6.29	747.19	10	5.59	1.32364	26.7457	117.129
96	2	1	1	0.12	6.98	680.98	10	5.89	1.47687	23.6261	102.165
97	2	1	2	0.1	4	641.1	10	4.14	1.56782	20.0471	117.172
98	2	1	3	0.1	5.31	632.84	10	3.96	1.57792	19.6501	117.129
99	2	1	4	0.1	4	619.41	10	3.78	1.61372	18.8905	117.355
100	2	1	5	0.1	4	622.32	9.92	3.86	1.58889	19.0783	117.136
101	1	5	1	0.1	376.58	747.81	0.1	3.71	0.984328	45.701	42.7004
102	1	5	2	0.12	388.93	750	0.1	2.68	0.678439	45.701	54.993
103	1	5	3	0.1	61.2	750	10	3.93	0.984118	29.6673	113.057
104	1	5	4	0.1	85.84	750	9.66	2.8	0.739117	30.3494	117.124
105	1	5	5	0.1	10.61	749.78	10	5.46	1.29226	27.109	117.129
106	1	4	1	0.1	31.02	749.79	10	10	1.26112	38.8838	56.0394
107	1	4	2	0.1	26.24	750	10	7.11	1.25285	31.6547	90.3592
108	1	4	3	0.1	44.89	750	10	3.77	1.06082	27.8536	122.44
109	1	4	4	0.1	19.05	748.65	10	5.26	1.24745	27.555	115.526
110	1	4	5	0.1	51.55	750	9.88	3.97	1.01147	28.7504	117.129
111	1	3	1	0.1	376.14	750	0.1	3.52	0.914892	45.7011	46.1408
112	1	3	2	0.1	14.62	750	10	7.58	1.31612	31.299	90.1274
113	1	3	3	0.1	15.38	750	10	5.29	1.26301	27.3067	117.129
114	1	3	4	0.1	42.05	749.99	10	4.3	1.09604	28.364	117.129
115	1	3	5	0.1	17.11	750	9.79	5.26	1.21425	27.3406	117.129
116	1	2	1	0.1	4	750	10	8.12	1.37311	31.1977	88.6823
117	1	2	2	0.1	4	750	9.79	6.98	1.32489	28.806	102.074
118	1	2	3	0.1	27.83	740.04	10	4.68	1.2087	27.0842	117.129
119	1	2	4	0.1	12.93	750	9.44	5.46	1.17916	27.0849	117.129

120	1	2	5	0.1	15.04	750	9.54	5.12	1.17257	26.8529	120.258
121	1	1	1	0.1	4	749.88	9.99	6.93	1.35415	28.7847	102.327
122	1	1	2	0.1	5.83	750	10	5.65	1.32045	26.9507	117.073
123	1	1	3	0.1	10.25	734.5	10	5.27	1.32842	26.0287	117.129
124	1	1	4	0.1	6.43	707.35	9.96	5.01	1.40268	24.0453	117.416
125	1	1	5	0.11	9.39	749.99	10	4.91	1.28069	26.019	124.246

Note: The solutions in red color are Pareto solutions considering all the three objective functions.

5.7.4. Experimental validation of pareto optimal solution

To select one of the Pareto optimal solution for validation "Compromising programming approach" (also termed as the "global criteria method") has been used (Deb, 2003). For this purpose, a reference point was chosen which corresponds to the maximum possible values of all three objectives. The Pareto optimal solution closest to this reference point determined using the normalized Euclidean distance was chosen as best and considered for experimental validation. This Pareto solution corresponds to the initial substrates concentrations as follows: $NaNO_3$: 0.1 g/L, K_2HPO_4: 26.24 mg/L, TRACE:10 X, Na_2EDTA: 7.11 mg/L and $MgSO_4.7H_2O$: 750 mg/L (Table 5.10). PHB production with the above media composition has been carried out in 2 l flat panel photobioreactor under diurnal light with 1 % CO_2 with air (0.5 VVM) described in the material and method section. Other media components remained the same as the modified BG-11 media. The validation experiment has been done in duplicates with duplicate sampling ($n = 2 \times 2 = 4$). Extracellular nitrate and phosphate have been exhausted at 48 h and 72 h respectively (Fig. 5.5A). Dissolved oxygen (DO) and pH both are increased with the increase of light during the growth period within a day due to enhancement of metabolic activity at higher intensity of light (Fig. 5B). Similarly, temperature also increased with the increase of light within a day conceivably due to high metabolic activity as well as high light intensity (Fig. 5.5B). When the culture reached stationary condition (216 h) 0.2 % acetate was added to induce PHB accumulation under continuous dark condition. Note that the pH level gradually increased to 10 from 8 under the dark period. After 4 days of induction (at 312 h) 31.78 % PHB was achieved with 1.23 g/L of DCW having 90.36 SCF (Fig. 5.5A). This is well agreed with predicted values; DCW of 1.25 g/L, PHB content of 31.65 % and SCF value of 90.36 (Table 5.10). A comparison of DCW, PHB production, and SCF using modified BG-11 medium (control) and multi-objective optimization-based medium

were tabulated in Table 5.10. Optimized medium resulted in 0.055 g PHB/day in 13 days whereas non-optimized medium resulted in 0.03 g PHB/day in 14 days. There is a 2.72-fold increment in % of PHB and 1.63-fold increment of SCF was recorded with optimized media in comparison to control. But it is clearly shown that the trade-off scenario between the objectives as there is a decrement of DCW to some extent with optimized media. Note that ultimately the amount of PHB (g/L) increases 69 % in optimized media as the PHB amount are 0.396 g/L and 0.234 g/L with optimized media and non-optimized BG-11 media (control) respectively. In an earlier study, *C. fritschii* TISTR 8527 produced 30.7 % (w/w) PHB under both nitrogen and phosphate starvation with 0.2 % (w/v) acetate under the dark condition with a two-stage cultivation strategy (Monshupanee et al., 2016). The optimized media developed in the current study shows the capability of production of cellular PHB with a similar % using single-stage cultivation but with a higher auto-sedimentation rate which decreased the cost of the process. Previous study reports the auto-sedimentation of biomass having very less PHB (non-induced biomass) instead of biomass with higher % of PHB (induced biomass) via two-stage cultivation method (Monshupanee et al., 2016). Whereas the current work reports auto-sedimentation of biomass having high PHB content since there is a clear trade-off between % of PHB in biomass and auto-sedimentation concentration factor. In an another study, *Synechocystis* sp. accumulated the biopolymer of 26.1 % in 3 d of incubation with 1.23 g/L acetate, 0.05 g/L $NaHCO_3$ and salinity of 9 g/L with two stage cultivation (Rueda et al., 2022).

Table 5.10: Comparison of DCW (g/L), PHB content (%) and SCF for different medium constituents.

Conditions	Media					Objectives		
	$NaNO_3$ (g/L)	K_2HPO_4 (mg/L)	TRACE (X)	Na_2EDTA (mg/L)	$MgSO_4.7H_2O$ (mg/L)	DCW (g/L)	PHB (%)	SCF
Modified BG-11 medium (control) (experiment)	1.5	40	1	1	75	2.0 ± 0.094	11.7 ± 3.53	57.04 ± 2.85
Multi-objective optimization (prediction)	0.1	26.24	10	7.11	750	1.25	31.65	90.36
Multi-objective optimization (experiment)	0.1	26.24	10	7.11	750	1.23 ±0.004	31.78 ± 0.276	93.63 ± 2.9

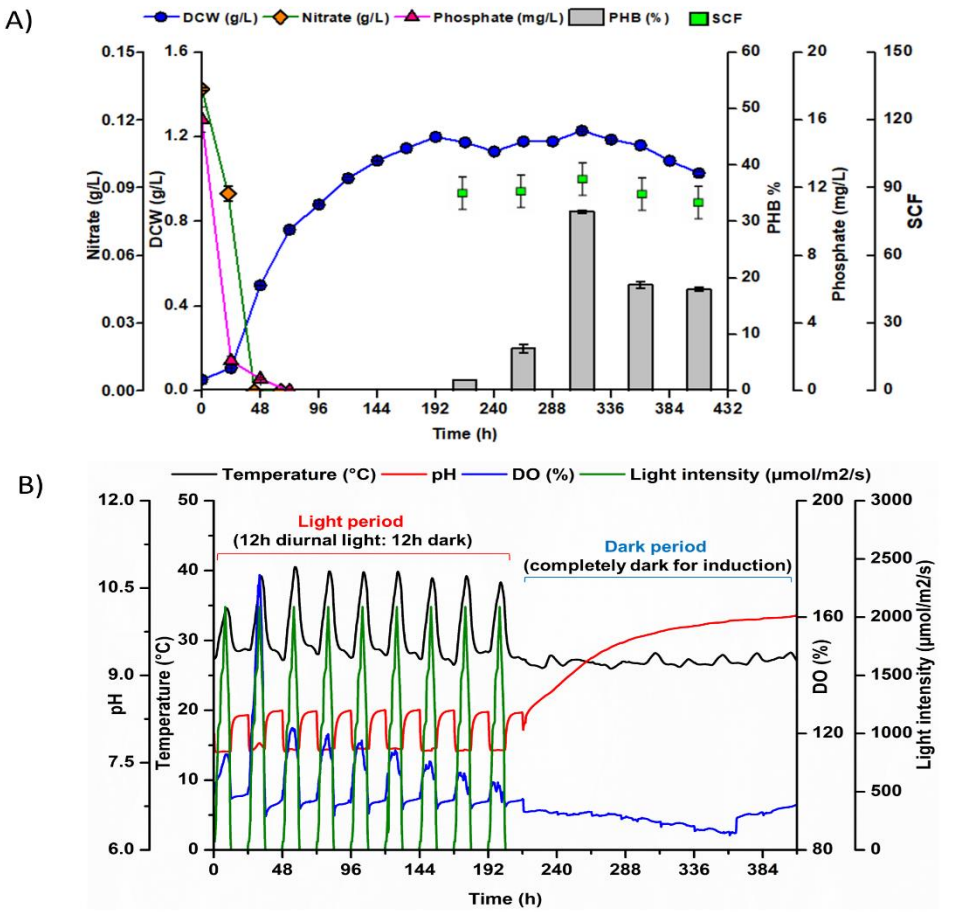

Fig. 5.5: Production of PHB via *C. fritschii* under diurnal light in flat panel PBR using optimized media selected from many pareto solution for validation. **A)** DCW (g/L), PHB (%) and SCF profile with nitrate and phosphate consumption, **B)** Culture parameters such as temperature (°C), pH and DO (%) along with diurnal light intensity (µmol/m^2/s). The phototrophic growth period was up to 216 h from start of the experiment and dark period for PHB induction was from 216 to 408 h. The experiment has been done in duplicates with duplicate sampling (n = 4).

Table 5.11 compares various harvesting methods based on cost, energy and efficiency. The selection of appropriate harvesting techniques depends on the specific characteristics of the microalgal or cyanobacterial species and the end product. Auto-sedimentation is species specific and involves negligible cost involved in operation with high settling rates. *C. fritschii* has unique nature of autosedimentation which makes the process more feasible. Apart from these the cost of autosedimentation per Kg of PHB was $ 0.13/Kg of PHB which was cheaper when compared to other harvesting techniques (Table 5.11). Hence auto-sedimentation has been used as a cost-economic harvesting strategy.

Table 5.11: Cost analysis of different harvesting methods for PHB recovery from *C. fritschii* in photobioreactor using optimal medium.

Basis for cost analysis:

Volume of the photobioreactor: 10^6 L

Biomass concentration: 1.23 g/L

Total Biomass: 1230 Kg

PHB: 31 % in biomass

Electricity cost: $ 0.1 /kWh

Method	Efficiency (% biomass recovery) *	Biomass recovered (Kg)	PHB recovered (Kg)	Energy consumption (kWh/m^3) *	Total Energy Consumption (kWh)	Total Cost ($)	Cost/PHB recovered ($/Kg)	Remarks
Sedimentation	10	123	38.13	0.3	300	30	0.79	Low efficiency of biomass recovery
Flocculation	80	984	305.04	0.8	800	80	0.26	Cannot reuse water, chemical cost, pollution issue and bio-flocculants are very costly
Flotation	70	861	266.91	2.75	2750	275	1.03	Energy intensive
Centrifugation	90	1107	343.17	12.5	12500	1250	3.64	High energy consumption
Filtration	85	1045.5	324.105	6	6000	600	1.85	Frequent cleaning of membranes and expensive membranes
Auto-sedimentation (Current study)	60 (with high PHB)	738	278.078	0.3	300	30	0.13	Negligible cost

*See Table 2.2 for recovery efficiency and energy consumption of various harvesting methods. The mean values are chosen from the range of values in the table.

5.8. Conclusions

Desirability based multi-objective optimization approach has been used to develop media for single-stage cultivation of *Chlorogloea fritschii* TISTR 8527 to increase PHB, biomass concentration and auto-sedimentation of biomass under diurnal light mimic to sunlight. The model used for multi-objective optimization has been developed using Response surface methodology. A set of Pareto points has been generated in multi-objective optimization which presents flexibility to choose suitable media composition for profitability. An optimized medium selected from the pareto set enhances the bioplastic PHB content and SCF by 2.72 (31.78 % PHB) and 1.64-fold (93.63) respectively with a loss of biomass concentration compared to non-optimal media under autotrophic conditions. But ultimately the amount of PHB (g/L) enhanced by 69 % using optimized media. This multi-objective approach developed here with *C. fritschii* TISTR 8527 can be used for other cyanobacteria to optimize value added products.

CHAPTER 6

Effect of CO_2 and acetate inducer on PHB accumulation of *C. fritschii* using optimal media under diurnal light with single stage cultivation

6.1. Background and motivation of the study

A key factor contributing to the significant changes in our global climate is the increase in atmospheric CO_2 concentration. Prior to the industrial revolution, atmospheric CO_2 was stable at 280 parts per million (ppm). However, because of the burning of fossil fuels CO_2 levels rose by 40 % and have reached more than 400 ppm (Ma & Wang, 2021). Increased solubility of free CO_2 in water bodies is expected to alter the chemical and physical characteristics of aquatic environments, hence influencing the microorganisms' community structures and activities and, eventually, the higher-ranking creatures in the food chain (Verspagen et al., 2014). Since rising atmospheric CO_2 levels can impact cyanobacterial growth by redistributing resources and energy within cells, they can also encourage photosynthesis of cyanobacteria by easing their carbon constraints (Ma & Wang, 2021). Freshwater works as atmospheric CO_2 sinks or high primary productivity zones because they support algae or cyanobacterial blooms with absorption of a significant amount of CO_2 from the water. In these situations, one of the main carbon sources for cyanobacteria and microalgae that encourage algal growth is the CO_2 exchange at the air-water interface (Balmer & Downing, 2011). Elevated pH levels have been linked to increased primary production and algal/cyanobacterial blooms, resulting in OH^- interactions with CO_2 in the following formula: $OH^- + CO_2 = HCO_3^-$. This procedure raises the mass transfer coefficient of CO_2, which increases the uptake of CO_2 by the water from the atmosphere (Bade & Cole, 2006).

In the current study, *C. fritschii* has been cultivated in flat panel PBR under simulated sunlight with various concentrations of CO_2. The present study focuses on the utilization of nutrients, mainly nitrate and phosphate in the media in the presence of elevated levels of CO_2. The study

investigates the biomass accumulation along with auto-sedimentation and PHB accumulation with acetate as an inducer under single-stage cultivation. The study examines whether PHB accumulation in the dark may be influenced by the CO_2 selected for phototrophic growth. Apart from this effect, the role of intracellular phosphate quota was studied with acetate feeding which may affect growth and PHB synthesis of *C. fritschii*.

6.2. Cultivation of *C. fritschii* in flat panel PBR with different CO_2 concentrations

The experiment was performed with an initial cell density of 0.05 g/L of *C. fritschii* in flat panel PBR (Labfors, Infors HT, 25.5 × 2 × 50 cm) using optimized BG-11 medium by multi-objective optimization (Chapter 5) (Yashavanth & Maiti, 2024). The culture was mixed through aeration of 0.5 VVM air mixed without or with CO_2 resulting in different concentrations of CO_2 (v/v) namely 0.04 (air), 1, 3 and 5 % (v/v) (Nayak & Das, 2013). CO_2 was supplied during the light period and only air was sparged during the night period. The diurnal light (cycle of light intensities from dawn to dusk) was simulated with reference to a day in May in Guwahati, India (26°11′03″ N and 91°44′44″ E) using a customized unidirectional LED panel for growth of cyanobacteria (Naira et al., 2019). The culture temperature (°C), pH, dissolved oxygen (DO, %), and light intensity (µmol/m^2/s) were recorded throughout the study. Note that during cultivation in flat-panel PBR, the temperature was not controlled either during growth or induction. The sampling was done at regular intervals to measure DCW, and phosphate in the supernatant were estimated (section 3.3 and 3.6). The specific growth rate during the growth period was calculated using Eq. 3.1. The stored intracellular phosphate was extracted and estimated according to section 3.12.

After phototrophic period of cultivation, 0.2 % (w/v) acetate was supplemented to induce the PHB accumulation in the dark (section 6.5.1). The sampling was done to measure the PHB from the

dried biomass as mentioned in section 3.7. An appropriate volume of experimental culture was subjected to autosedimentation studies (section 3.8). Auto-sedimentation concentration factor (SCF) was calculated using Eq. 3.4 and 3.5.

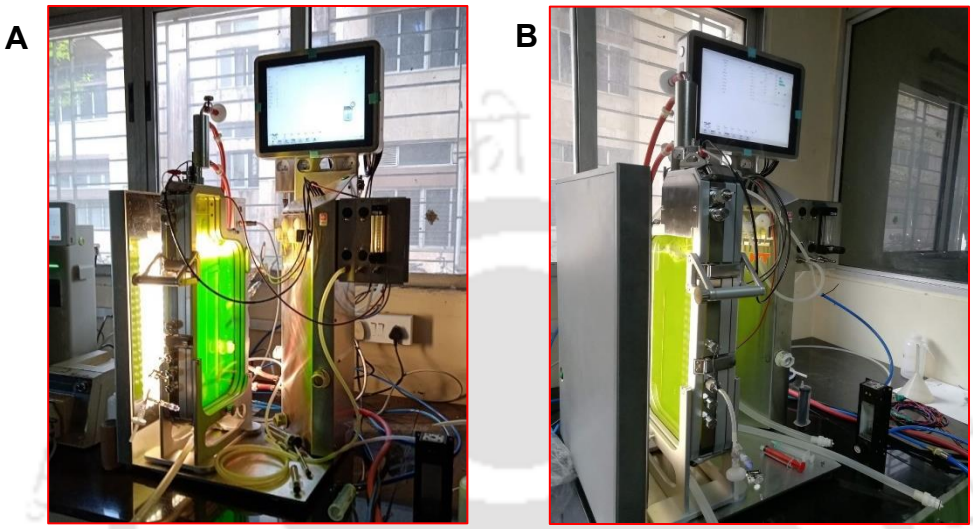

Fig. 6.1: Single stage cultivation of *C. fritschii* under diurnal light using optimal medium with various CO_2 concentrations in flat panel PBR. **A)** Nutrient sufficient and **B)** nutrient limiting conditions**.**

6.3. Characterization of clump cell nature of *C. fritschii* by Field emission scanning electron microscopy

C. fritschii culture during PHB induction stage was collected and washed in 0.1 M phosphate buffer of pH 7.4. Before being inspected with a field emission scanning electron microscope (FESEM), the biomass of cyanobacteria was fixed in equal volume of 2.5 % glutaraldehyde (w/v) in phosphate buffer and kept overnight at 4 °C before washing it with PBS for three times. The dehydration process in a graded ethanol series (30, 40, 50, 60, 70, 80, 90 and 95 %) was carried out in step-by-step manner (Debnath & Bhadury, 2016). The final biomass was suspended in an appropriate volume of 95 % ethanol. On a 0.4 x 0.4 cm glass piece covered by aluminum foil, samples were dropped cast and allowed to air dry. Following gold sputtering, the samples were scanned using a 5 kV FESEM (Zeiss, GEMINI).

6.4. Effect of acetate feeding on growth, PHB and auto-sedimentation of *C. fritschii*

The optimized BG-11 media was used for the current study with 1 % CO_2 and diurnal light setup. Experimental conditions were similar to section 6.2 i.e. single-stage cultivation in flat panel PBR under diurnal light with the usage of 1 % CO_2. The experiment was performed with an initial cell density of 0.05 g/L. Once the culture reached the stationary phase 0.2 % acetate was added on 9^{th} day for PHB induction under dark. After 13^{th} day, 0.2 % acetate was fed again to avoid the acetate limitation during PHB accumulation. Sampling was done at regular intervals for DCW, chlorophyll, nitrate, and phosphate estimation (section 3.3-3.6). The PHB from the dried biomass was measured as mentioned in section 3.7. An appropriate volume of experimental culture was subjected to autosedimentation studies (section 3.8). The culture pH, DO concentration, culture temperature and light intensity were monitored (section 3.11). The stored intracellular phosphate ($P_{intra)}$ was extracted from biomass and estimated according to section 3.12.

6.5. Results and Discussion

6.5.1. Effect of CO_2 on growth of *C. fritschii*

The batch-wise experiments using optimized BG-11 medium were started with selected levels of CO_2 in flat panel PBR using diurnal light with an initial cell density of 0.05 g/L. In the culture aerated with only air (0.04 % CO_2), the DCW of 0.81 g/L at the end of stationary phase of growth period (312 h). The culture with 1, 3 and 5 % CO_2 resulted in biomass concentration of 1.17 g/L at 216 h, 1.09 g/L at 168 h and 1.38 g/L at 120 h respectively (Fig. 6.2A). Increase in the CO_2 level resulted in the early arrival of stationary phase i.e. reduction in the phototrophic cultivation period. Following the PHB induction with 0.2 % acetate under dark conditions, the highest DCW of 1.205 g/L was obtained at 432 h with 0.04 % CO_2, 1.23 g/L at 312 h with 1% CO_2, 1.303 g/L at 264 h with 3% CO_2, and 1.65 g/L at 312 h with 5% CO_2, respectively (Fig. 6.2A). The initial extracellular phosphate (P_{extra}) of 26.24 mg/L was consumed within 144, 72, 48, and 48 h from the start of the experiment with 0.04, 1, 3 and 5 % CO_2 respectively (Fig. 6.2B). The P_{extra} consumed is stored as an initial intracellular phosphate (P_{intra}) concentration of 109.88 ± 0.827, 112.54 ± 1.5, 103.72 ± 3.74, 96.053 ± 4.42 mg of P/g of dry cell weight with 0.04, 1, 3 and 5 % CO_2 respectively. Stored P_{intra} was utilized for cellular growth and various metabolic processes. Once the culture reached the stationary phase, the stored P_{intra} reduced to values of 6.11, 10.97, 12.84 and 9.33 mg of P/g of cell with 0.04, 1, 3 and 5 % CO_2 respectively (Fig. 6.2C). The specific growth rates were calculated till 5 d of cultivation. The growth rates of 0.302, 1.538, 1.34 and 1.113 d^{-1} were observed for experiments with 0.04, 1, 3 and 5 % CO_2 respectively (Fig. 6.2D). Among the different percentages of CO_2 selected, 1 % CO_2 resulted in the highest specific growth rate of 1.538 d^{-1} on 2 d of cultivation.

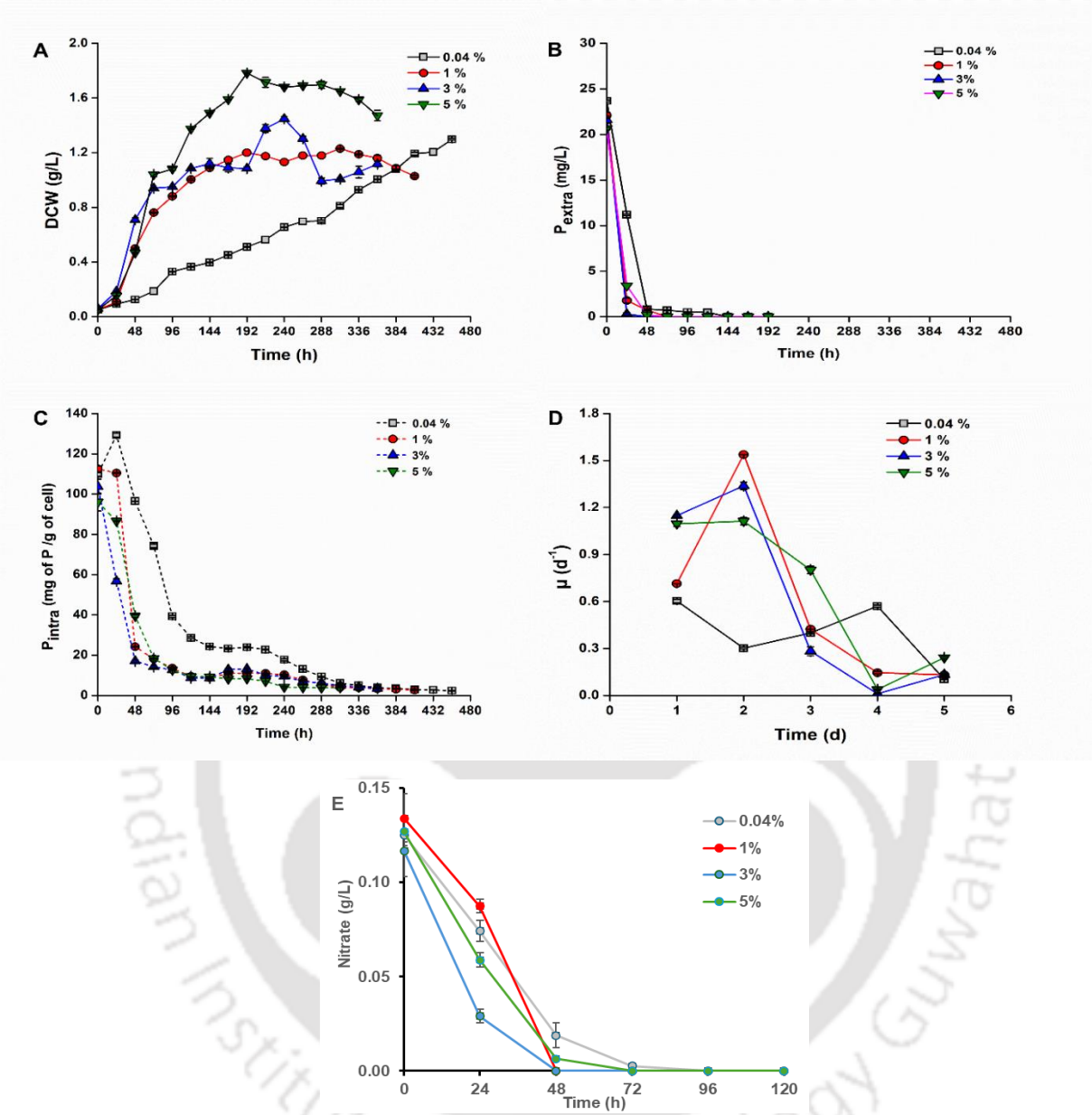

Fig. 6.2: Effect of CO_2 on growth of *C. fritschii* under diurnal light. **A)** Dry cell weight measured during course of cultivation in flat panel PBR, **B)** Phosphate consumption, **C)** Intracellular phosphate present in the cell during course of cultivation, **D)** Specific growth rates of *C. fritschii* under different CO_2 concentrations (0.04, 1, 3 and 5 % CO_2), and **E)** Nitrate consumption. The experiments have been done in duplicates with duplicate sampling (n = 4).

6.5.2. Effect of CO_2 on PHB accumulation of *C. fritschii*

The PHB induction with 0.2 % (w/v) acetate under dark conditions was initiated when the culture reached stationary phase i.e. 312, 216, 168 and 120 h for 0.04, 1, 3 and 5 % CO_2 respectively. The culture with air (0.04 % CO_2) resulting in the PHB accumulation of 19.85 % (w/w) at 432 h of cultivation (Fig. 6.3A). Whereas the experiment with 1 % CO_2 resulted in a maximum PHB content of 31.78 % at 312 h or 13 d of cultivation (Fig. 6.3B). The experimental conditions with 3 % and 5 % CO_2 used for phototrophic cultivation resulted in PHB accumulation of 28 % at 264 h and 18 % at 312 h of cultivation under dark (Fig. 6.3C and 6.3D). Note that the increase in % CO_2 after 3 % for cultivation of *C. fritschii* using optimal medium didn't enhance the PHB synthesis. In a study of phototrophic PHB accumulation using elevated levels of CO_2 with *Thermosynechococcus elongatus*, low level of CO_2 resulted in 14.5 % PHB which was higher when compared to PHB resulted from 5 - 20 % CO_2. This was due to trigger of PHB accumulation by carbon limitation. PHB production can be decreased at a high carbon level (Eberly & Ely, 2012). Same was observed in the current study with *C. fritschii*, where 1 and 3 % CO_2 resulted in PHB content of 31.78 % and 28 % respectively with acetate as PHB inducer. Whereas the increase in CO_2 to 5 % reduced PHB content to 18 %. The supply of adequate or lower amounts of CO_2 may trigger the condition required for PHB synthesis with acetate supplementation. Supplementation of excess CO_2 may result in higher biomass production with lower PHB accumulation.

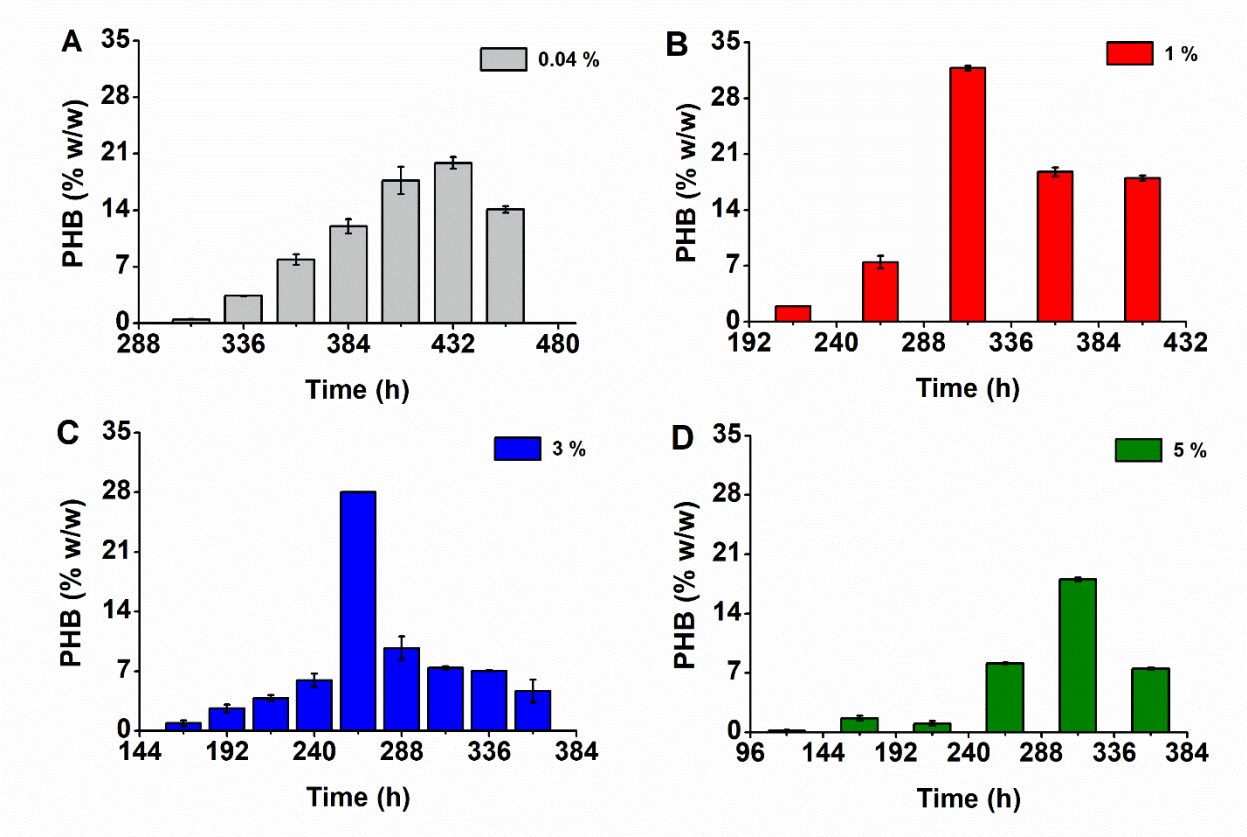

Fig. 6.3: PHB accumulation using *C. fritschii* under dark with 0.2 % acetate with cultures pregrown phototrophically in optimized medium using diurnal light in flat panel PBR using various CO_2 concentrations. **A)** 0.04 % or air, **B)** 1 %, **C)** 3 %, and **D)** 5 %.

6.5.3. Effect of pH on PHB accumulation

The pH in the experimental cultivation were recorded using eve software (INFORS, HT). The initial pH of optimized BG-11 media was 7.5 before inoculation of *C. fritschii*. After inoculation with cells, the pH of experimental cultures rose to 7.8 – 8.0. During daytime supplied CO_2 resulted in drop in pH value less than 8.0 in cultures with 1, 3 and 5 % CO_2 and during night only air was sparged which raised the pH to 8.2 - 8.4 (Fig. 6.4). The presence of 20 mM HEPES didn't cause a drop or rise in pH values in cultures even after without or with supply of various concentrations of CO_2. During induction with 0.2 % acetate under dark only air was sparged for the respiration and

metabolic activity of cells. During induction, pH was not maintained with acid addition after acetate supplementation. The uptake of acetate by *C. fritschii* resulted in the increment of pH value up to 10 (Fig. 6.4). From PHB content measured using *C. fritschii* with various CO_2 it can be concluded that alkaline pH of 9.5 to 10.2 favored the PHB accumulation.

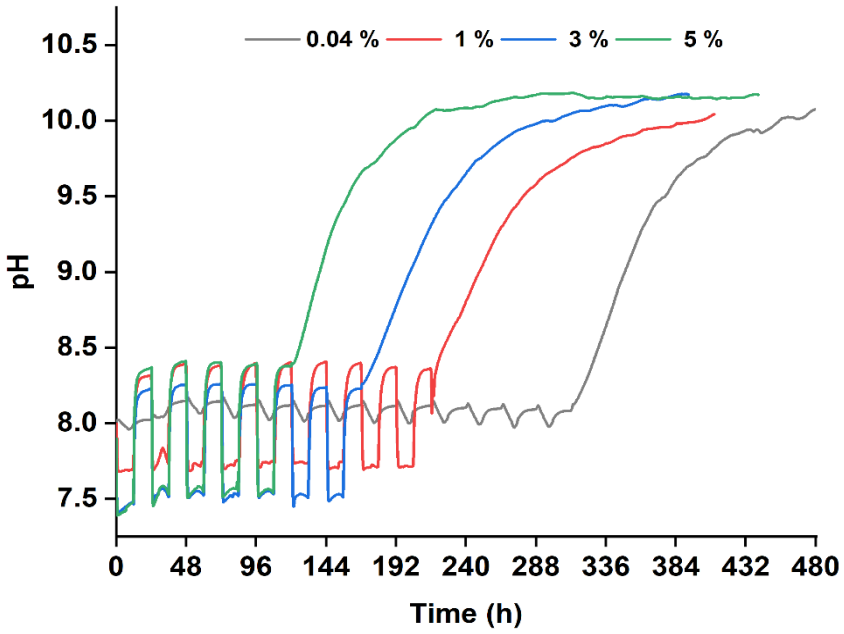

Fig. 6.4: pH values of *C. fritschii* cultures during the batch process under diurnal light using various CO_2 concentrations and acetate as PHB inducer.

6.5.4. Effect of CO_2 on PHB productivity

Polymer production was evaluated in terms of PHB productivity calculated on different days of induction. PHB productivity of 13.28 mg/L/d at 18th d, 30.07 mg/L/d at 13th d, 33.15 mg/L/d at 11th d and 22.88 mg/L/d at 13th d were observed with 0.04, 1, 3 and 5 % CO_2 respectively (Fig. 6.5). In a study with *Synechococcus* 2973-*phaCAB* using average light intensity of 400 µmol/m^2/s and 5 % CO_2 resulted in PHB productivity of 27.8 mg/L/d after 10 d with 21.1 % PHB (Roh et al., 2021). In a study with two stage cultivation under salinity stress, *Synechocystis* sp. produced biopolymer with a productivity of 15.7 mg/L/d (Rueda et al., 2022). In the current study, single stage cultivation

of *C. fritschii* TISTR 8527 using 3 % CO_2 under diurnal light and minimal acetate concentration of 0.2 % under dark resulted in a higher PHB productivity of 33.15 mg/L/d at 11th d with polymer content of 28 %.

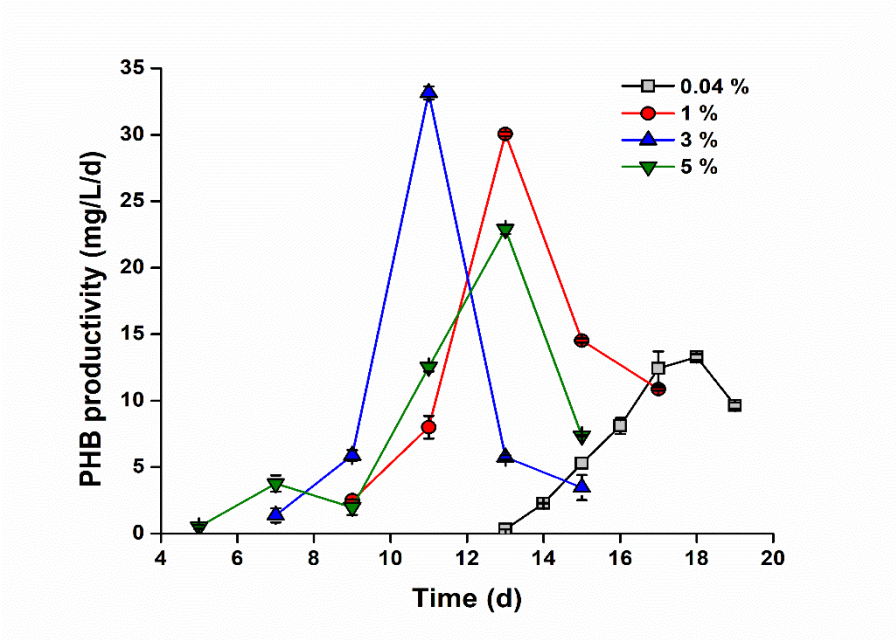

Fig. 6.5: PHB productivities of *C. fritschii* under dark with cultures pregrown under diurnal light in optimized media using various CO_2 concentrations (v/v) of 0.04 % or air, 1 %, 3 %, and 5 % respectively in flat panel PBR.

6.5.5. Effect of CO_2 on auto-sedimentation of *C. fritschii*

SCF values resulted from autosedimentation studies during induction phase were studied. Maximum SCF value of 148 was obtained with air at 360 h. With 1 % CO_2, SCF of 93.63 resulted at 312 h and it was almost constant during induction phase (Fig. 6.6). SCF of 77.89 was obtained with 3 % CO_2 at 264 h. For the culture with 5 % CO_2, auto-sedimentation values of 146.54 at the start of PHB induction and later ceased to 77.27 at 336 h (Fig. 6.6). Exopolysaccharides (EPS) produced by cyanobacteria or microalgae binds with other cells to create flocs or sediments which

later results in autosedimentation by clustering of cells based on bridging charge mechanism (Patyna et al., 2018). Generally, the concentration of exopolysaccharides (EPS) production requires a high carbon in the medium with nitrogen starvation condition (Netrusov et al., 2023). *C. fritschii* used in current study has capability of EPS production (measured, data not shown). Probably the presence of bound EPS was more when *C. fritschii* was cultivated using 5 % CO_2, than with air (CO_2 is 0.04%) due to high carbon supply. Nitrogen was limiting in both the conditions before induction (Fig. 6.2). Note that the induction time was 120 h for 5 % CO_2 and 312 h for air. This high EPS causes the clumping of cells and higher SCF values of 146.54 at starting of PHB induction (120 h) for 5 % CO_2 (Fig. 6.6). In case of pre grown with air, SCF value of 63 was observed at 312 h (starting of induction) which may be due to low EPS production due to carbon limitation. At the start of induction, acetate (0.2 %, w/v) was added. Note that CO_2 supply was stopped and air was sparged during induction period. Generally, the addition of acetate to the culture medium increased EPS synthesis in cyanobacteria (Alvarez et al., 2021). Due to excess production of EPS in pre-grown with 5 % CO_2, EPS was detached from cells and become unbound EPS in culture liquid which increase viscosity of the liquid (Prathyusha et al., 2018). Due to the increase of liquid viscosity the SCF gradually decreased to 60 at 360 h in case of cell pre-grown with 5 % CO_2. EPS production was also increased due to acetate addition in case of cell pre-grown with air and therefore SCF was increased to 148 at 360 h from 63 (at 312 h, starting of induction). But probably the total EPS was not that high which can lead to detachment of EPS due to low EPS at induction time. Later after 360 h detachment of EPS may be started and increase the liquid viscosity which leads to decrease of SCF. In the case of cultures pre-grown with 1 % and 3 % CO_2 almost constant SCF values (Fig. 6.6) were observed due to settling force created by bound EPS was counterbalanced by increase of viscosity caused by unbound EPS in media.

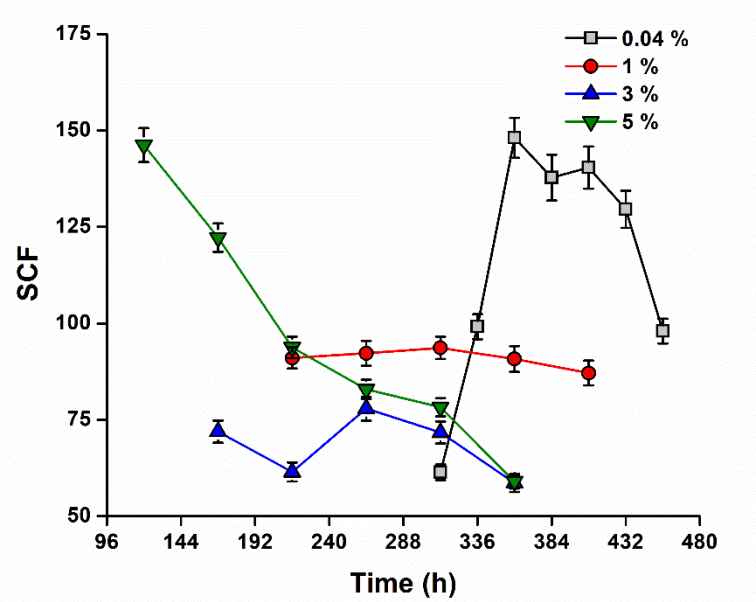

Fig. 6.6: SCF values of *C. fritschii* subjected to autosedimentation during PHB induction. *C. fritschii* pregrown under diurnal light in optimized media using various CO_2 concentrations (v/v) of 0.04 % or air, 1 %, 3 %, and 5 % respectively in flat panel PBR.

6.5.6. Effect of acetate feeding on growth, PHB and auto-sedimentation

The experiment was started with optimized BG-11 using 1 % CO_2 under diurnal light in flat panel PBR since 1 % CO_2 resulted in higher PHB content. The fed-batch was started with an initial cell density of 0.05 g/L. The nitrate and phosphate (P_{extra}) present were consumed within 72 h of the experiment. Dry cell weight of 1.16 g/L was obtained with chlorophyll content of 0.71 µg/mL on 216 h with culture reaching the stationary phase (Fig. 6.7A). At 216 h, 0.2 % acetate was added to the culture for PHB induction under dark without medium replacement. The maximum DCW of 1.19 g/L was obtained after 3 days of feeding of acetate (Fig. 6.7A). After 13 d or 312 h, a second feeding of acetate was done to minimize the acetate limitation during PHB induction. At the initial stage of cultivation P_{intra} of 114.6 mg/g of cell was obtained. During cultivation, the stored P_{intra}

was consumed for the cellular growth and value of P_{intra} of 8.74 mg/g of cell was resulted at stationary phase. Feeding of acetate at 312 h (13 d) resulted in DCW of 1.17 g/L and later the dry cell weight decreased during PHB induction (Fig. 6.7A). The pH decreased by the CO_2 supplied during the light period, and during the dark hours only air was sparged for cellular respiration which caused pH to rise to 8.4. The metabolic activity of the cells was causing the culture's temperature to rise during the day. The photosynthetic uptake of CO_2 provided during the daytime was responsible for the rise in DO percentage (Fig. 6.7B). There was a drop in DO % during the PHB induction due to cellular respiration and metabolism after acetate supplementation. The acetate was up taken by cells along which caused the rise in pH up to 10 during dark (Fig. 6.7B). The cells were subjected to autosedimentation during induction period. At the start of induction SCF values of 129.1 and 140.6 were obtained at 216 h and 240 h respectively and during PHB induction, SCF value of 124.1 resulted at 312 h (Fig. 6.7C). The maximum PHB of 29.62 ± 0.9 % was obtained with DCW of 1.14 g/L at 312 h. The supplied acetate of 2 g/L (0.2 %) was almost utilized completely at 312 h and the second feeding of acetate didn't enhance the PHB accumulation (Fig. 6.7D). PHB productivity of 25.46 mg/L/d resulted due to a P_{intra} of 3.76 mg/g of cell (0.04 mmol/g of the cell) at 312 h which is close to 0.043 mmol per g of cell required for PHB accumulation (Nishioka et al., 2001). Feeding of acetate at the second time neither enhanced biomass nor the PHB accumulation whereas SCF value of 124.1 was obtained which was 1.3-fold higher than control. After the initial feeding of acetate, the cells might have already reached a saturation point where additional acetate does not further stimulate PHB synthesis. While studying the effect of acetate on PHB induction, it was found that second feeding of acetate didn't enhance PHB. In PHB production pathway due to multi addition of acetate conversion of acetyl-CoA to acetoacetyl-CoA (phaA) may be increased but the enzyme activities of next two steps (phaB and

phaC/E may not be increased. Hence multi feeding of acetate may not be increased PHB production. Table 6.1 is a summary of comparison of PHB production from *C. fritschii* with various reported cyanobacteria.

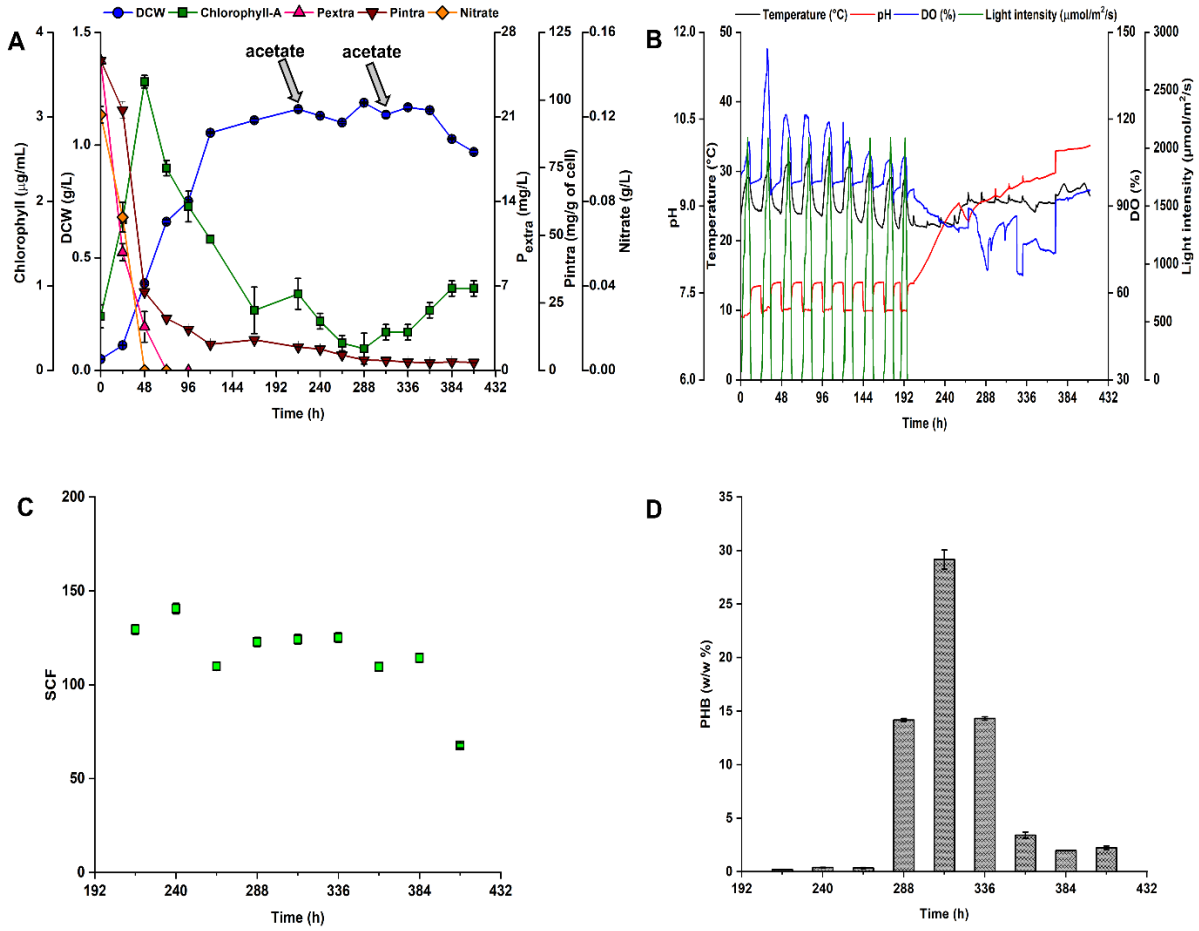

Fig. 6.7: PHB production by *C. fritschii* by acetate feeding in optimal medium. **A)** Growth behavior of *C. fritschii*: DCW, nitrate consumption, chlorophyll content, phosphate uptake rate (P_{extra}) and intracellular phosphate (P_{intra}), Induction was started by addition of 0.2 % acetate on 216 h and 312 h under dark. **B)** Parameters such as pH, temperature, DO, and light intensity were recorded online, **C)** SCF measured during PHB induction, and **D)** PHB accumulation under dark.

Table 6.1: Comparison of PHB production from *C. fritschii* with various reported cyanobacteria

Cyanobacteria	Conditions	PHB (%)	Biomass productivity (g/L/d)	References
Spirulina subsalsa	Two stage, ASN-III, salinity 5 %, nitrogen starvation, phototrophic	7.45	0.078	(Shrivastav et al., 2010)
Synechocystis PCC 6803 (recombinant)	Two stage, BG-11, nitrogen starvation, mixotrophic 0.4 % acetate	35	-	(Khetkorn et al., 2016)
Synechocystis sp.	Two stage, BG-11, salinity 9 g/L 0.123 % acetate 0.05 g/L $NaHCO_3$ dark	26.1 ± 7.0	-	(Rueda et al., 2022)
C. fritschii TISTR 8527	Two stage, modified BG11 medium, Nitrogen and phosphate starvation 0.2 % acetate Dark	30.7 ± 2.8	-	(Monshupanee et al., 2016)
C. fritschii TISTR 8527	Single stage, modified BG11 medium, shake flask equipped with sparger, 0.2 % acetate dark	16.4 ± 0.984	0.115	Current study
C. fritschii TISTR 8527	Single stage, multi-objective optimization, flat panel PBR, 1% CO_2, diurnal 0.2 % acetate dark	31.78 ± 0.276	0.095	Current study

6.5.7. Visualization of clump cell nature of *C. fritschii*

The clump cell nature of *C. fritschii* resulted in higher SCF values during PHB induction under dark with *C. fritschii* cultivated using 0.04 % CO_2 or air (Fig. 6.6). Once the cells settled to bottom, they were visualized using FESEM after fixation and dehydration with graded ethanol (section 6.3). The clump cells of *C. fritschii* were observed under magnification order of 1000X (Fig. 6.8A and 6.8B) after auto-sedimentation.

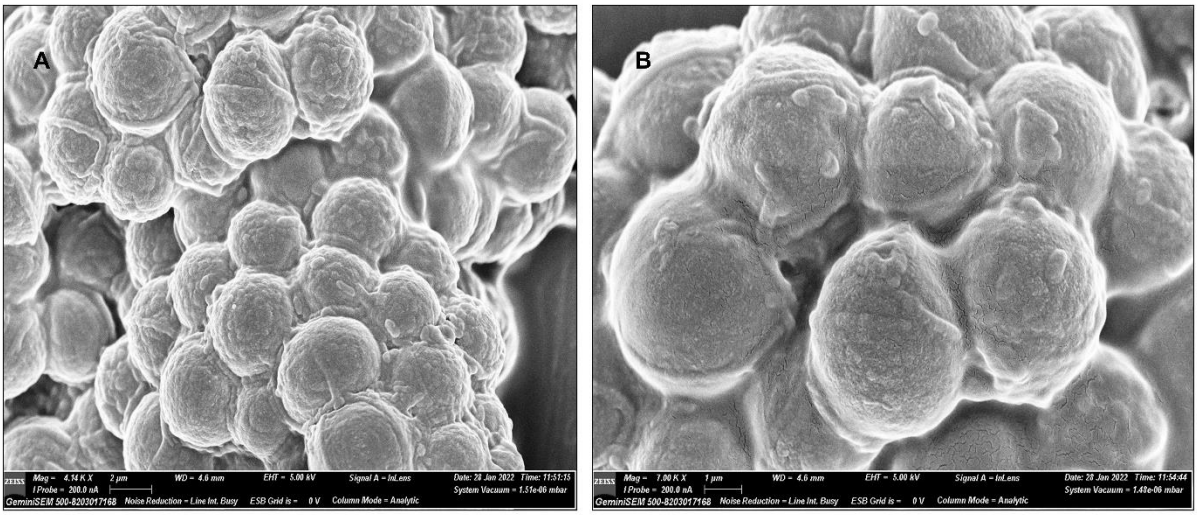

Fig. 6.8: Clump cell nature of *C. fritschii* TISTR 8527 visualized by FESEM. **A)** 4.14 kX magnification and **B)** 7 kX magnification.

6.6. Conclusions

C. fritschii was cultivated in flat panel PBR using optimized BG-11 medium under diurnal simulated sunlight with various levels of CO_2 starting from air to 5 %. A higher specific growth rate of 1.538 d^{-1} was resulted with 1 % CO_2 with PHB accumulation of 31.78 % in single stage cultivation. The maximum PHB productivity of 33.15 mg/L/d with polymer production of 28 % was observed with 3 % CO_2. Air resulted in higher SCF values of 148 and PHB content of 19.85 % due to lower repulsion caused by EPS of *C. fritschii* and carbon stress respectively. Lower levels of CO_2 resulted in higher polymer content and SCF values. The supplementation of 1 and 3 % CO_2 resulted in higher PHB production which in turn affect SCF values. Intracellular phosphate plays a significant role in cellular growth and carbon flow towards PHB accumulation. At the initial stage of cultivation, an average intracellular phosphate concentration (P_{intra}) of approximately 105.6 mg/g was observed which was utilized during cultivation process for cellular growth and later for carbon trafficking of supplemented acetate for PHB synthesis. PHB productivity of 30.3 mg/L/d and 33.15 mg/L/d had resulted due to P_{intra} of 4.024 ± 0.03 mg/g (0.042 mmol/g) and 6.96 ± 0.2 mg/g (0.073 mmol/g) with 1 and 3 % CO_2 respectively. Fed-batch studies with acetate during induction didn't enhance the PHB productivity after second feeding due to substrate inhibition or limitation of other nutrients which favor PHB accumulation.

CHAPTER 7

Recovery and characterization of polyhydroxybutyrate from *Chlorogloea fritschii* TISTR 8527 using halogenated and green solvents

7.1. Background and motivation of the study

PHB is stored as an intracellular product by cyanobacteria under nutrient limitations. PHB has to be recovered and purified by various methods such as solvent extraction, surfactants, non-PHB cellular material (NPCM) removal using hypochlorite, dispersion of hypochlorite and chloroform, and enzymatic digestion (Yashavanth et al., 2021). Recovering PHB from cytoplasm increases production cost by up to 50 % cost of the polymer since PHB has to be purified in multiple steps (Samorì et al., 2015b). The molecular weight of the recovered polymer may decrease because of NPCM digestion with hypochlorite. Hypochlorite and chloroform dispersion can decrease the loss in molecular weight of recovered PHB while raising the yield and purity.

Solvent recovery is the most used method by industries due to its high recovery efficiency resulting in polymer of high molecular weight along with the removal of endotoxins (Lee et al., 1999). Cyanobacteria contain pigments that affect material properties of PHB after extraction. Therefore, pigment removal from cyanobacteria is essential before PHB recovery with a minimum number of solvents and steps involved (Troschl et al., 2017). Methanol can be used for pigment removal at 4 °C before PHB extraction (Gopi et al., 2014; Zavřel et al., 2015). The combination of hypochlorite and chloroform may result in higher recovery with pigment removal, but both are toxic to humans and the environment. Therefore, the selection of solvents based on safety and reusability has significance in the evaluation of the extraction process (Mongili et al., 2021). Dimethyl carbonate (DMC) is a solvent of industrial importance and is used as a reagent in various processes. DMC is considered a green solvent since it is biodegradable and less toxic to humans

and the environment (Delledonne et al., 2001) and could be used as an alternative to halogenated solvents (Mongili et al., 2021). Previously, DMC was used for the extraction of homopolymer PHB and copolymer poly-hydroxybutyrate-hydroxyvalerate (PHBHV) from single strains and mixed consortia (Elhami et al., 2022; Samorì et al., 2015a; Samorì et al., 2015b).

The present study focuses on the recovery of PHB from *Chlorogloea fritschii* TISTR 8527 using various extraction methods. PHB was extracted with pigment removal using the dispersion method. Dispersion involves a two-phase extraction procedure using hypochlorite (for biomass digestion) and chloroform (solvent for PHB extraction). Various halogenated such as chloroform and dichloroethane and non-halogenated solvents namely propylene carbonate, dioxolane, DMC and acetic acid were selected for PHB recovery based on the capabilities of solvents to dissolve PHB (Terada & Marchessault, 1999). after hypochlorite pretreatment. A suitable solvent is selected based on the performance and environmental concerns. DMC is employed as a green solvent in the current investigation to recover PHB after pigments removal from cyanobacteria using methanol. The selection of a suitable biomass-to-solvent ratio, extraction temperature and mixing time are critical factors as they affect the recovery yield. Once the PHB is extracted from the biomass, it is recovered by evaporation of the solvent. Comparison of thermal properties of recovered PHB are shown to decide the most suitable method based on polymer characteristics.

7.2. Conditions for PHB accumulation.

The experiment was performed with an optimized BG-11 medium resulting from multi-objective optimization under diurnal simulated sunlight in flat panel photobioreactor (PBR) with 3 % CO_2 (v/v) and 0.5 VVM air. The high cell-density biomass pre-grown under autotrophic mode was subjected to biopolymer production under the dark with 0.2 % (w/v) acetate as an inducer at the stationary phase (section 6.2). The sampling was done at regular intervals to measure the dry cell

weight (DCW) after centrifugation (section 3.3). The biomass harvested by centrifugation was freeze-dried and used for recovery of stored PHB (Farinacci & Laurent, 2023). The experiment was performed in duplicates with duplicate sampling and an average of result were reported with standard deviation. PHB content of the sample was quantified using gas chromatography (section 3.7).

7.3. Extraction of intracellular PHB

7.3.1. PHB recovery by single-step hypochlorite-chloroform dispersion method

The commercially available hypochlorite (4 w/v %) was purchased from Himedia and diluted to different concentrations (10, 20, 30, 50, 70 and 100 % (v/v)). In the current study, 1 % (w/v) of lyophilized biomass (i.e. 10 mg of biomass per 10 mL solvent) was subjected to PHB recovery using the dispersion method with equal volumes of hypochlorite and chloroform at 30 °C for 1 h. After the dispersion, the mixture was centrifuged to separate the layers i.e., the upper layer contains NPCM, the middle layer contains cell debris, and the bottom chloroform layer contains PHB. The lower bottom phase was collected to concentrate the biopolymer by evaporation of solvent (Hahn et al., 1995) and the percentage recovery was calculated by using Eq. 3.4 after quantification by GC.

7.3.2. PHB recovery using two-step method using hypochlorite pretreatment followed by extraction with different solvents

Solvent extraction is widely used in the recovery of PHB due to the efficient recovery of PHB with integrity of the polymer characteristics. Various solvents used for our study were chloroform (boiling point: 61.2 °C), dichloroethane (84 °C), propylene carbonate (242 °C), acetic acid (118 °C), dioxolane (74 °C) and dimethyl carbonate (90 °C). Previous studies showed that the above

solvents resulted in a higher PHB recovery (Terada & Marchessault, 1999). In the present study, 200 mg of lyophilized biomass was subjected to pretreatment with 20 mL of 4 % (w/v) hypochlorite (Himedia) for 15 min at room temperature (Kanzariya et al., 2023). The pellet was collected by centrifugation after discarding the supernatant. The pellet was subjected for PHB recovery at 100 °C for 1 h with the biomass-to-solvent ratio of 1 % (w/v) for the above-mentioned solvents. After extraction, the suspension was centrifuged to collect the solvent phase. The polymer was recovered by evaporation of solvents and the percentage recovery was calculated by using Eq. 3.4 after quantification by GC.

7.3.3. PHB recovery by two-step method using pigment removal by methanol followed by extraction with green solvent dimethyl carbonate (DMC)

7.3.3.1. Effect of biomass loading on PHB recovery by DMC

Lyophilized biomass was used for the extraction of PHB using a green solvent DMC. At first, the freeze-dried biomass was subjected to pigment removal using chilled methanol at 4 °C overnight in 50 mL falcons. The biomass used for extraction varied at different concentrations. Lyophilized biomass of 50, 100, 150, and 200 mg were suspended in 4 mL of DMC to get biomass concentrations of 12.5, 25, 37.5, and 50 g/L. The extraction was performed at 90 °C while mixing at regular intervals till 4 h. After extraction, the mixture was centrifuged at 4696 ×g for 10 min to collect the DMC containing PHB. The solvent was subjected to evaporation to recover the polymer (Mongili et al., 2021; Samorì et al., 2015b). The recovery percentage was calculated using Eq. 3.4.

7.3.3.2. Effect of pigment removal on PHB recovery by DMC

The biomass-to-methanol ratio played an important role as pigments interfere with the recovery of biopolymer. The biomass in methanol used for pigment removal was 0.1, 0.25, 0.5, and 1 % (w/v).

Biomass of 100 mg was suspended in chilled methanol of different volumes (10, 20, 40, and 100 mL) to get the above concentrations. After the incubation at 4 °C, biomass was separated by centrifugation at 8000 rpm for 10 min (Ansari & Fatma, 2016). Then the pellet was suspended in 4 mL of DMC for PHB extraction at 90 °C with mixing at regular intervals up to 4 h. Then the mixture was centrifuged at 4696 ×g for 10 min to collect the DMC containing PHB. The solvent was subjected to evaporation to recover the polymer (Mongili et al., 2021; Samorì et al., 2015b). The recovery percentage was calculated as before using Eq. 3.4.

7.3.3.3. Effect of incubation time on PHB recovery

To optimize the time required for extraction of PHB, 100 mg of biomass per 4 mL of DMC was selected after pigment removal with 0.5 % (w/v) and 0.25 % (w/v) biomass in methanol. The experiment was performed at different time points from 2, 4, 6, and 8 h (Mongili et al., 2021; Samorì et al., 2015b). The percentage polymer recovery was calculated after the evaporation of DMC and quantification by GC using Eq. 3.4.

7.4. Characterization of recovered polymer

The recovered polymer from *C. fritschii* using hypochlorite-chloroform dispersion and DMC were subjected for characterization using various techniques such as FTIR for characteristic peaks identification (section 3.9.1), TGA analysis and DSC analysis for thermal properties determination (section 3.9.2 – 3.9.3), Powder XRD analysis for crystallinity (section 3.9.4), GPC for molecular weight determination (section 3.9.5) and UTM for mechanical properties (section 3.9.6). Standard PHB from Sigma-Aldrich (standard) was used as a reference to PHB recovered using both methods from *C. fritschii* TISTR 8527.

7.5. Statistical analysis

All experiments were conducted in duplicates with triplicate sampling measurements and average results were reported with standard deviation. One-way ANOVA was performed followed by Tukey's post hoc tests using the OriginPro 2021 software (OriginLab). A p-value of < 0.05 was considered statistically significant.

7.6. Results and Discussion

7.6.1. PHB production from *C. fritschii*

C. fritschii was cultivated in flat-panel PBR using optimized BG-11 medium with 3 % CO_2 under diurnal light. The initial cell density of *C. fritschii* was 0.05 g/L. After 7 days of cultivation the culture reached the stationary phase with a DCW of 1.084 g/L (Fig. 6.2A). PHB was induced under dark with 0.2 % acetate (w/v) after 7 days. PHB of 28 ± 0.08 % was obtained with DCW of 1.3 ± 0.02 g/L after 4 days of induction under dark (Fig. 6.3C). The biomass with a polymer content of 28 % was collected by centrifugation, freeze dried and used for recovery of intracellular PHB by various methods. Previously *C. fritschii* TISTR 8527 has been reported to produce 31.78 % of polymer using optimized BG-11 medium with 1 % CO_2 under diurnal light (Yashavanth & Maiti, 2024). Increase in CO_2 may reduce the carbon stress required for PHB accumulation.

7.6.2. PHB extraction by single-step hypochlorite-chloroform dispersion method

Firstly, the lyophilized biomass was subjected to the hypochlorite-chloroform dispersion method. It was observed that the percentage recovery of biopolymer increased with an increase in the hypochlorite percentage used for cell lysis. Use of 10 % (v/v) hypochlorite was inefficient in cell lysis and resulted in lower PHB recovery of 4.44 ± 0.574 % (w/w). Gradual increase in hypochlorite concentrations from 20 to 70 % (v/v) led to the improvement in PHB recovery from

42.88 ± 4.09 % to 90.50 ± 3.26 % (w/w). Direct usage of commercial hypochlorite from Himedia (100 % v/v or 4 % w/v) with an equal volume of chloroform resulted in the recovery of 95.51 ± 3.164 % PHB (Fig. 7.1A). The PHB recovery was found to be significant with increase in hypochlorite concentrations ($p < 0.05$). Hahn et al. also showed that increase in the hypochlorite concentration increase the percentage recovery of the polymer (Hahn et al., 1994).

7.6.3. PHB recovery by two-step method using hypochlorite pretreatment followed by extraction with different solvents

Various organic solvents used for our study were chloroform, dichloroethane (DCE), propylene carbonate, acetic acid, dioxolane, and dimethyl carbonate (DMC) (Terada & Marchessault, 1999). These solvents were screened for recovery of PHB at 100 °C for 1 h from *C. fritschii* after pretreatment of 200 mg of lyophilized biomass with 4 % (w/v) hypochlorite for 15 min at room temperature. The recovered polymer content varied with different solvents employed (Fig. 7.1B). Propylene carbonate, chloroform, DCE, dioxolane, DMC and acetic acid resulted in PHB recovery of 29.2 ± 0.714, 73.1 ± 3.053, 51.61 ± 0.805, 48.62 ± 1.605, 74.79 ± 5.134, 34.9 ± 0.3 % (w/w) respectively at 100 °C (Fig. 7.1B). The maximum recovery of 74.79 ± 5.134 % was achieved with green solvent DMC after digestion of biomass with hypochlorite which aided in cell lysis along with pigment removal. Apart from DMC, chloroform also resulted in PHB recovery of 73.1 %.

Generally, extraction of PHB using solvent depends on the solubility of PHB and the combination of the boiling point of the solvent and operating temperature. In the current extraction process, the operating temperature was 100 °C. The boiling points of propylene carbonate and acetic acid are 242 °C and 118 °C respectively, which were much higher than the operating temperature. The boiling points of chloroform, DCE, dioxolane, and DMC were lower than the operating

temperature. Therefore, the PHB recovery was lesser with propylene carbonate and acetic acid (Aramvash et al., 2018). According to the Hansen solubility parameter the distance of DMC from the center of solubility radius of PHB (R_{PHB} = 8.5) is lowest (5.12) compared to other solvents used in this study (Terada & Marchessault, 1999). As the solubility of PHB in DMC is very high and the operating temperature is close to the boiling point, the recovery using DMC is higher.

In a study, *Cupriavidus necator* biomass was subjected to PHB recovery using propylene carbonate at 100 °C for 45 min resulting in a percentage recovery of 45 % (Fiorese et al., 2009). In the present study, a low operating temperature of 100 °C resulted in PHB recovery of 29.2 % using propylene carbonate in *C. fritschii*. Aramvash et al. showed that acetic acid can recover the PHB to 36.71 % using *C. necator* (Aramvash et al., 2018). In the current study, acetic acid demonstrated a recovery of 34.9 % from *C. fritschii*. Previously, *Synechococcus* and *Synechocystis* biomass were subjected to a recovery of biopolymer using DMC without pigment removal resulting in the low recovery of 21.5 and 27.3 % respectively (Scholz & Björke). Samori et al. reported PHB recovery of 20 % from mixed culture using DMC (Samorì et al., 2015b). In this study, DMC could recover PHB from *C. fritschii* with a high recovery yield of 74.79 % after hypochlorite pretreatment. Dioxolane was capable of PHB recovery of 60 % from *C. necator* at 100 °C for 4 h (Yabueng & Napathorn, 2018). However, in this work dioxolane resulted in a recovery of 48.62 % of PHB which was due to lower contact time (1 h) of solvent with biomass at 100 °C. Chloroform and DCE recovered PHB of 73.1 % and 51.61 % at 100 °C after hypochlorite pretreatment. Chloroform and DCE are well known for good recovery of polymer due to high solubility of PHB (Hahn et al., 1995; Monshupanee et al., 2016; Terada & Marchessault, 1999). At high temperatures, these solvents are highly volatile, and continuous exposure to their fumes by human were proven to be carcinogenic (Sekar et al., 2023). These solvents are not eco-friendly.

Hence, DMC was selected for further experiments based on its capability to solubilize PHB along with health and environmental concerns (Mongili et al., 2021).

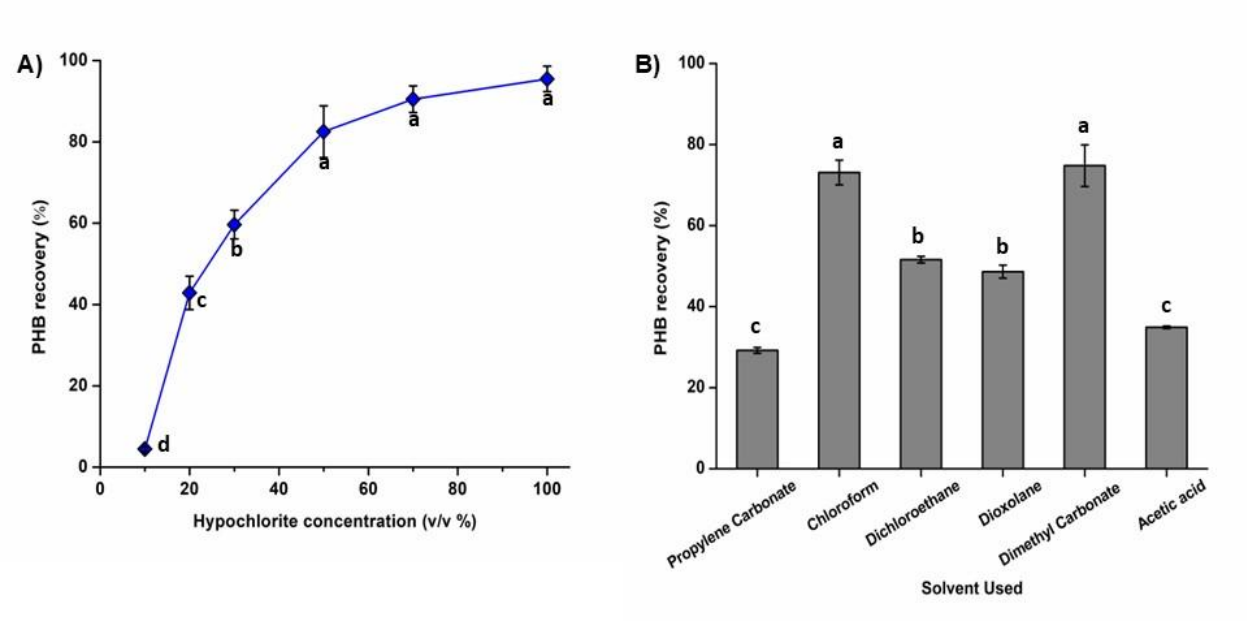

Fig. 7.1: PHB recovery with hypochlorite for cell lysis. **A)** PHB recovery (%) from *C. fritschii* using hypochlorite-chloroform dispersion method with increase in hypochlorite concentrations (v/v %). **B)** PHB recovery (%) from *C. fritschii* using solvent extraction with different halogenated and non-halogenated solvents after hypochlorite pretreatment. The experiments were conducted in duplicates with triplicate sampling measurements and average results were reported. Different letters indicate significant differences between the groups with $p \leq 0.05$.

7.6.4. PHB recovery by two-step method using pigment removal by methanol followed by extraction with green solvent DMC

Being an industrially important solvent, DMC recovered 19.62 % PHB directly from *C. fritschii* biomass without removal of pigments (data not shown). Pigments were also extracted with PHB when the biomass was heated with DMC. This resulted in a lower recovery of polymer. Hence

biomass was subjected to pigment removal using chilled methanol followed by PHB extraction with DMC. The % recovery was found to be 41 ± 0.97, 53.52 ± 0.47, 50.51 ± 0.64 % and 19.574 ± 0.15 % with 50, 100, 150 and 200 mg biomass per 4 mL of DMC, respectively (Fig. 7.2A). It was found that 100 mg biomass per 4 mL DMC i.e. 25 g/L biomass resulted in maximum recovery of 53.52 % polymer in biomass variation experiment with an incubation period of 4 h. The decrease in the % recovery with an increase in the biomass was due to the limitation of solvent. Therefore 25 g/L of biomass in DMC was selected for further studies (Fig. 7.2A).

The biomass-to-methanol ratio varied from 1, 0.5, 0.25, and 0.1 % (w/v) to study the effect of pigment removal on PHB recovery. After pigment removal, the pelleted biomass was subjected to PHB recovery with 100 mg of biomass per 4 mL of DMC (i.e. 25 g/L) for 4 h at 90 ºC. The percentage recoveries of PHB were 9.98 ± 0.83, 53.63 ± 1.38, 81.88 ± 0.91 and 82.93 ± 0.37 % respectively (Fig. 7.2B). Still there was scope to enhance the percentage recovery by increasing the biomass contact time of biomass with DMC. Hence 0.5 % w/v biomass in methanol was selected for pigment removal followed by extraction with DMC resulted in the polymer recoveries of 10.77 ± 0.28, 54.42 ± 1.19, 68.87 ± 0.125, and 42.28 ± 1.11 % with an incubation time of 2, 4, 6, and 8 h respectively (Fig. 7.2C). Using 0.25 % w/v biomass in methanol for pigment removal and PHB recovery using DMC with 2, 4, 6, and 8 h contact time gave recovery yields of 22.97 ± 0.18, 83.34 ± 0.76, 62.2 ± 1.59 and 57.17 ± 0.54 % respectively (Fig. 7.2D). PHB recovery using DMC with considering biomass variation, effect of biomass to methanol for pigment removal on PHB recovery and contact time studies on PHB recovery with 0.25 % and 0.5 % biomass to methanol were statistically significant with $p < 0.05$ (Fig. 7.2C and D). Previously *C. necator* biomass was used and DMC was capable of resulting in a recovery yield of 88 % (Samorì et al., 2015b). It's interesting to note that in the current work with *C. fritschii*, pigment removal

employing a biomass-to-methanol ratio of 0.25 % (w/v) achieved 83.34 ± 0.76 % of PHB recovery and purity of 75 % with same incubation period of 4 h.

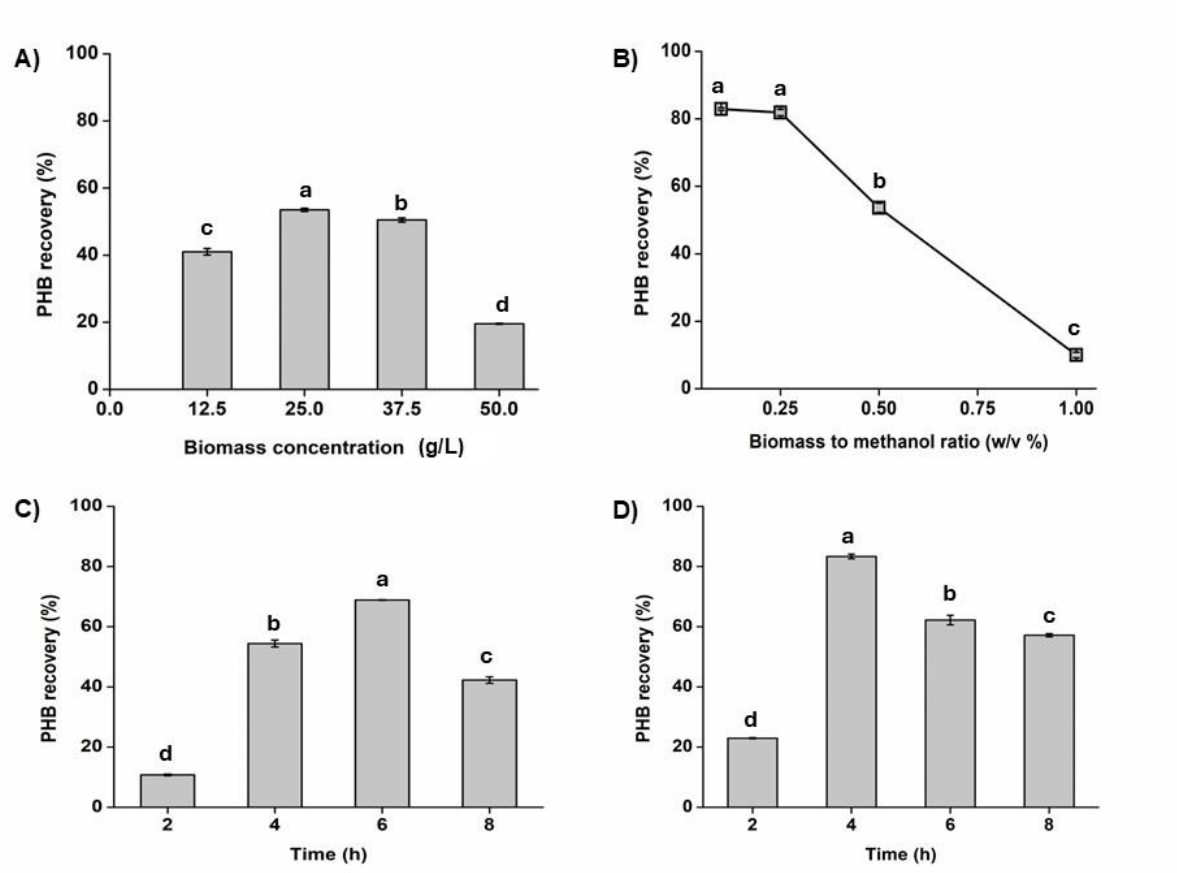

Fig. 7.2: PHB recovery (%) from *C. fritschii* using DMC with pigment removal with chilled methanol. **A)** Effect of biomass amount for PHB recovery using DMC, **B)** Effect of pigment removal by varying biomass to methanol ratio on PHB recovery by DMC, **C)** Effect of contact time on PHB recovery with 0.5 % (w/v) biomass to methanol ratio for pigment removal, and **D)** Effect of contact time on PHB recovery with 0.25 % (w/v) biomass to methanol ratio for pigment removal. The experiments were conducted in duplicates with triplicate sampling measurements and average results were reported. Different letters indicate significant differences between the groups with $p \leq 0.05$.

7.6.5. Characterization of biopolymer

PHB recovered from *C. fritschii* using the hypochlorite-chloroform dispersion method and the DMC method was characterized using various techniques with a reference to the standard PHB (Sigma-Aldrich).

7.6.5.1. Fourier Transformed Infrared Spectroscopy

PHBs from both methods were subjected to FTIR analysis by the pellet method. The FTIR spectra of PHB from both methods were similar. The -CH group was represented by 2930 to 2975 cm^{-1}. The characteristic peak at 1728 cm^{-1} represents the -C=O group. The bands from 1058 - 1281 cm^{-1} represented the C-O-C stretching vibration. The FTIR peaks of standard (Fig. 7.3A and Table 7.1) and samples (Fig. 7.3B and Fig. 7.3C) were similar. These results were in agreement with previous studies (Ansari & Fatma, 2016; Pradhan et al., 2018).

Table 7.1: Comparison of characteristic FTIR peaks of PHB recovered from *C. fritschii* using hypochlorite-chloroform dispersion and DMC based recovery with standard (Sigma-Aldrich).

Groups	**Standard PHB (Sigma-Aldrich)**	**PHB (DMC)**	**PHB (hypochlorite-chloroform dispersion)**
	wavenumber (cm^{-1})	**wavenumber (cm^{-1})**	**wavenumber (cm^{-1})**
C=O	1728	1728	1727
C-O-C	1287-1058	1281-1059	1281-1057
-CH	2935-2977	2930-2960	2927-2973

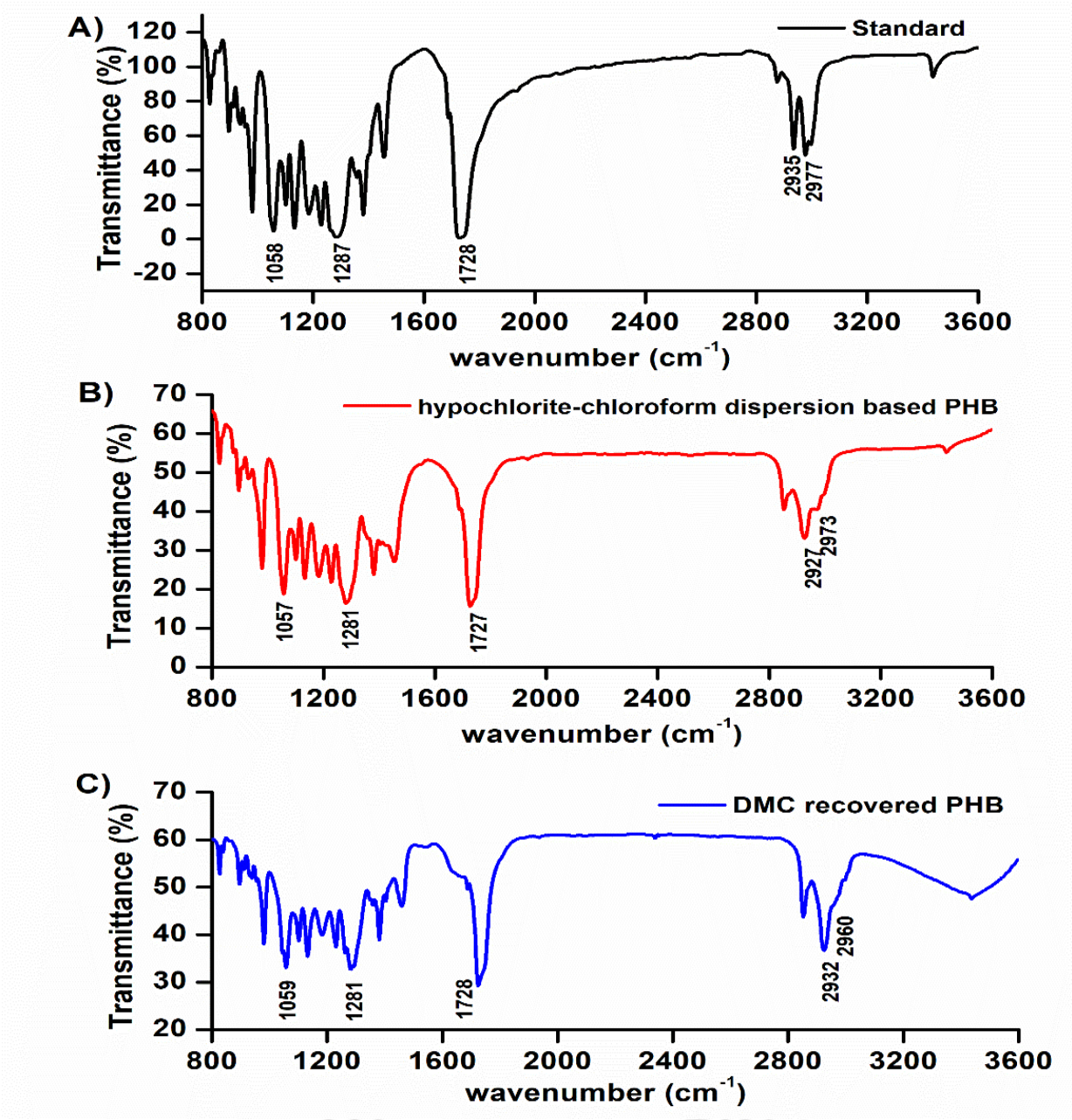

Fig. 7.3: FTIR spectra of PHB recovered from *C. fritschii* for the identification of functional groups. A) Standard PHB from Sigma-Aldrich, B) Hypochlorite-chloroform dispersion based PHB, and C) DMC recovered PHB.

7.6.5.2. Thermogravimetric Analysis

PHB derived from the hypochlorite-chloroform dispersion method and DMC method were subjected to thermal degradation under an inert atmosphere. Initial mass loss corresponds to the loss of solvents adsorbed to the film (i.e. chloroform and DMC). The standard PHB was degraded in a single step since it is highly pure. PHB derived from both methods was degraded in two steps. The loss is due to the random chain scission by β-elimination reaction and conversion of cleaved chains to crotonic acid or oligomers of crotonic acid (Ariffin et al., 2008). The former showed 49.6 % degradation in the first phase, followed by 37 % degradation in the second phase with a residual mass of 12.5 %. Later one showed a mass loss of 33.8 % in the first step and 56.2 % in the second step with a residual of 10.8 % (Fig. 7.4A). The characteristic decomposition temperatures, i.e. temperature at 5 % (T_5) and temperature at 10 % weight loss (T_{10}) were determined using TGA curve (Fig. 7.4A). The maximum decomposition temperature (T_{max}) was determined by the DTG curve (Fig. 7.4B). The T_5, $T_{10,}$ and T_{max} of PHB recovered using the hypochlorite-chloroform dispersion method were 232.7, 238, and 250 °C respectively. Whereas T_5, $T_{10,}$ and T_{max} of PHB recovered using DMC are 261.6, 274.2, and 289 °C respectively (Fig. 7.4A and 7.4B). The standard PHB from Sigma-Aldrich showed T_5, $T_{10,}$ and T_{max} of 270, 274, and 285 °C respectively (Table 7.2). The characteristic decomposition temperatures of PHB recovered using DMC were matching with that of standard PHB. In a study with *Nostoc muscorum*, a T_{max} of 284 °C was reported (Ansari & Fatma, 2016) which is close to the T_{max} of PHB recovered from *C. fritschii* using DMC (289 °C) in the current study. Other fossil-based biopolymers such as PLA have a T_{max} of 366 ºC which is higher than the T_{max} of PHB (285 ºC) (Arrieta et al., 2014).

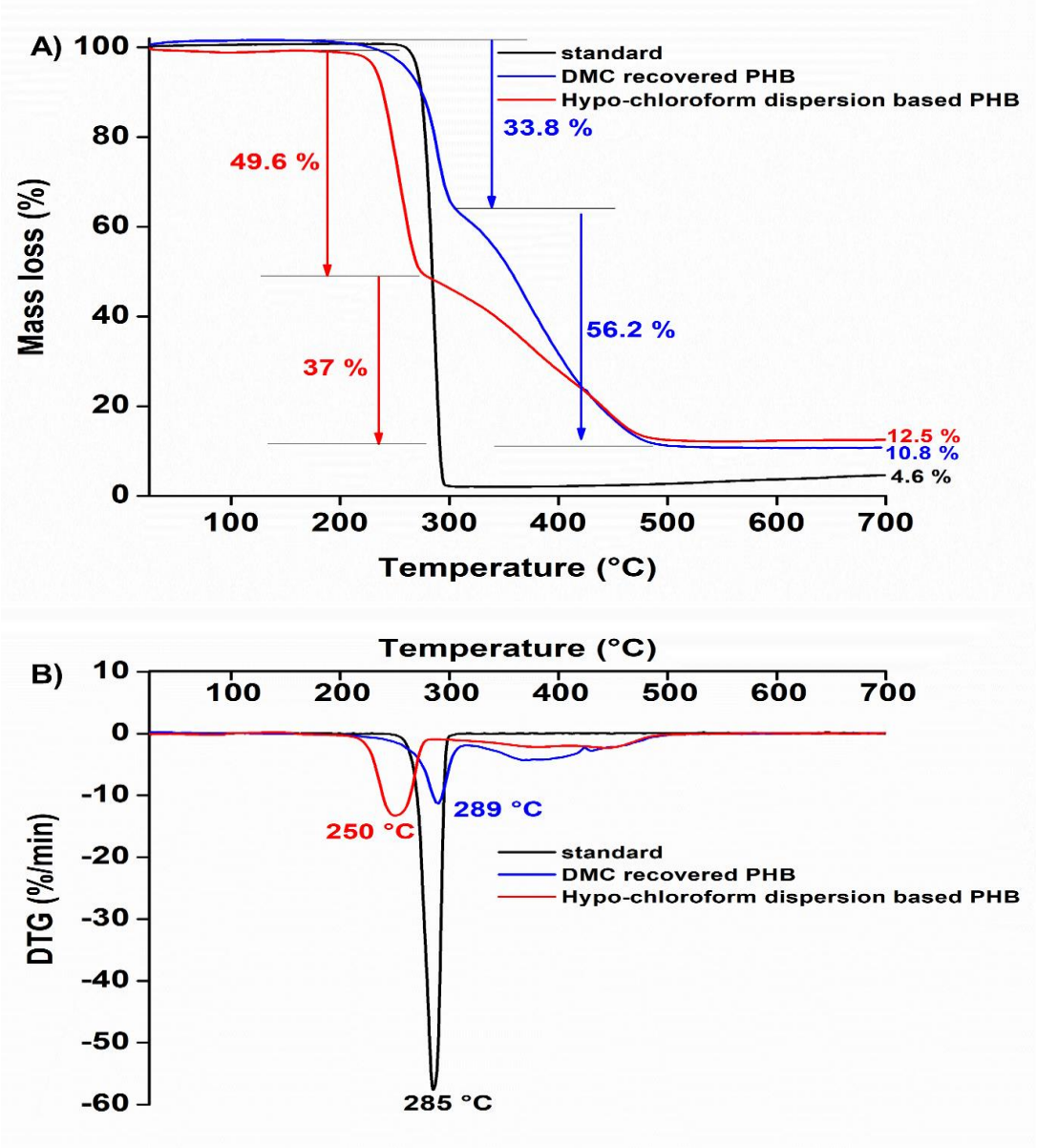

Fig. 7.4: Thermograms of PHB recovered from *C. fritschii* under inert atmosphere. **A)** Comparison of TGA curve of hypochlorite-chloroform dispersion based PHB and DMC recovered PHB with standard PHB (Sigma-Aldrich). The TGA curve depicts the step wise degradation of PHB with temperature range of 25 – 700 °C. **B)** Comparison of DTG curve of hypochlorite-chloroform dispersion based PHB and DMC recovered PHB with standard PHB (Sigma-Aldrich). The DTG curve depicts the rate of degradation and maximum degradation temperature of the polymer.

Table 7.2: Comparison of degradation temperatures of PHB recovered from *C. fritschii* using hypochlorite-chloroform dispersion and DMC based recovery with standard (Sigma-Aldrich) using TGA and DTG analysis.

Sample	T_5 (°C)	T_{10} (°C)	T_{max} (°C)	Residual mass (%)
Standard PHB (Sigma-Aldrich)	270	274	285	4.6
PHB (Dimethyl Carbonate)	261.6	274.2	289	10.8
PHB (hypochlorite-chloroform dispersion)	232.7	238	250	12.5

7.6.5.3. Differential scanning calorimetry

The thermal and calorimetric properties of PHB recovered from the hypochlorite-chloroform dispersion method and DMC method were studied using Differential scanning calorimetry (DSC). The thermograms were used to determine glass transition temperature (T_g), melting temperature (T_m), crystallization temperature (T_c), and degree of crystallinity (X_c). The first heating scan (-30 °C to 200 °C) was used to eliminate the prior thermal history of the polymer. The T_c was calculated using the cooling cycle from 200 °C to -30 °C.

The point of inflection during the second heating cycle is referred to as glass transition temperature (T_g). The T_g for standard, DMC recovered PHB and PHB recovered from the dispersion method are 4, 4.3, and 4.6 °C respectively (Fig. 7.5A and Table 7.3). Previously, PHB recovered from *Nostoc muscorum* had a T_m of 171 °C (Ansari & Fatma, 2016) which is close to the T_m of PHB recovered from *C. fritschii* using dispersion and DMC in the present study. Previous study showed that PHB from *C. fritschii* TISTR 8527 had a T_g of 3.2 °C (Monshupanee et al.,

2016). The melting points (T_m) for dispersion-based PHB and DMC-recovered PHB were 169 and 174 °C respectively, which were close to the T_m of standard (174 °C) (Fig. 7.5A and Table 7.3). Chemical synthesis of PHB by ring open polymerization of racemic diolide (rac-DL) resulted in complete isotactic PHB with T_m of 170.7 ºC (Tang & Chen, 2018). The crystallization temperature (T_c) of PHB recovered from both methods was determined from the cooling curve and were found to be 48.4 °C (DMC recovered PHB) and 48.2 °C (dispersion) respectively which were less than T_c of standard (84 °C) (Fig. 7.5B and Table 7.3). This was due to the lower degree of crystallinity (X_c) of 38.4 % and 35.9 %, respectively. The crystallinity (X_c) of the standard from Sigma-Aldrich is 60.3 % (Table 7.3). It was found that PHB recovered with chloroform from the same strain had a reported crystallinity of 45 % in previous findings (Monshupanee et al., 2016).

DSC data of PHB from *C. fritschii* was also compared with fossil-based polymers such as polypropylene (PP) and polyethylene terephthalate (PET) (Table 7.3). Among the fossil-based polymers, PET was highly amorphous with a high melting temperature of 260 ºC (McAdam et al., 2020). PLA had a higher T_g of 60.4 °C whereas it was highly amorphous in nature with X_c of 5.1 %. Irrespective of crystallinity the solubility parameter (δ) of PLA (19.5-20.5 $MPa^{1/2}$) was close to that of PHB (18.5 - 20.1 $MPa^{1/2}$), which aided the blending of both materials in the manufacturing of food packaging material while enhancing the crystallinity of packing material (Arrieta et al., 2014). Apart from these high concentrations of amorphous PHB has been blended with PAZO to form a photonic material while enhancing the miscibility of materials with different solubility parameters (Sharma et al., 2005). Hence DSC helps in manufacturing materials of interest with enhanced solubility along with improved crystallinity.

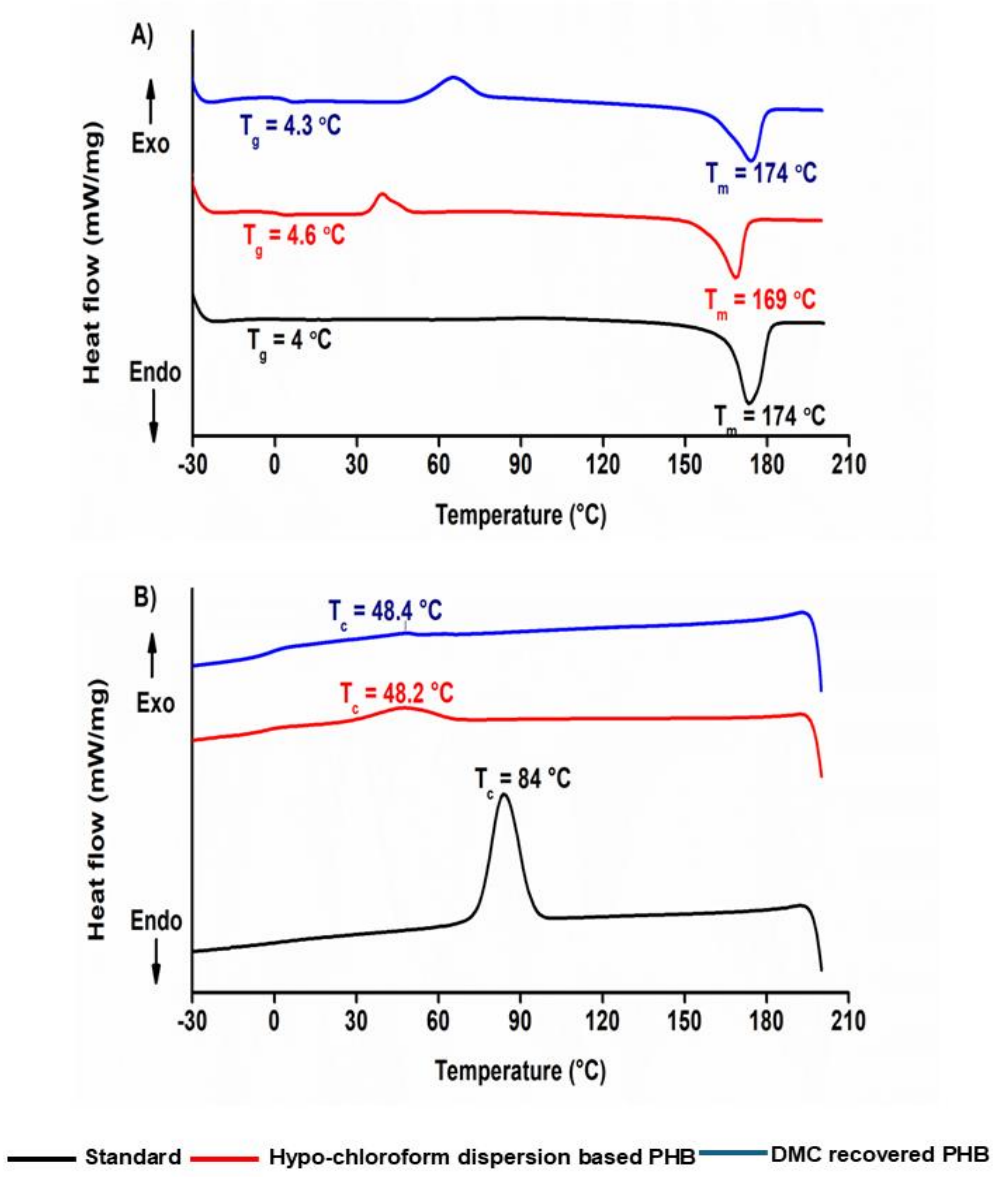

Fig. 7.5: Differential scanning calorimetric (DSC) curve of PHB recovered from *C. fritschii* by hypochlorite-chloroform dispersion and DMC based recovery with comparison to standard PHB (Sigma-Aldrich) for analysis of thermal properties such as glass transition temperature (T_g), melting temperature (T_m), and crystallization temperature (T_c). **A)** Heating curve and **B)** Cooling curve.

7.6.5.4. Powder X-ray diffraction

X-ray diffractograms of standard, PHB recovered from the hypochlorite-chloroform dispersion method and DMC method were obtained using Cu-α X-ray (λ = 1.54 A^{o}) in the range of 2θ = 10-80 ^{o}. Six prominent peaks were observed at 2θ: 13.6, 17, 21.6, 22.7, 25.69, and 27.3°. These peaks correspond to different planes (020, 110, 101, 111, 121, and 040) of orthorhombic unit cells of PHB crystal. Peaks at 2θ = 21.6 and 2θ = 22.7° represented that the tested polymer is α-PHB crystal (Sun et al., 2011). The peaks at 2θ = 25.69° and 2θ = 27.3° indicated that the PHB from *C. fritschii* is of partial crystalline nature (Fig 7.6). XRD data of PHB from *C. fritschii* was similar to the PHB obtained from *Cupriavidus necator*, *Bacillus megaterium,* and *Bacillus cereus* (Devi et al., 2015; Pradhan et al., 2018). The % crystallinity (X_c) was calculated from analysis of XRD peaks. The X_c of PHB recovered using hypochlorite-chloroform dispersion method and DMC from *C. fritschii* were found to be 56.45 ± 1.81 and 56.84 ± 1.56 % respectively (Table 7.3). The X_c of standard PHB is 63.33 ± 4.80 % and is in agreement with a previous study (Anbukarasu et al., 2015). From the above analysis, it can be concluded that PHB from *C. fritschii* is semi-crystalline in nature.

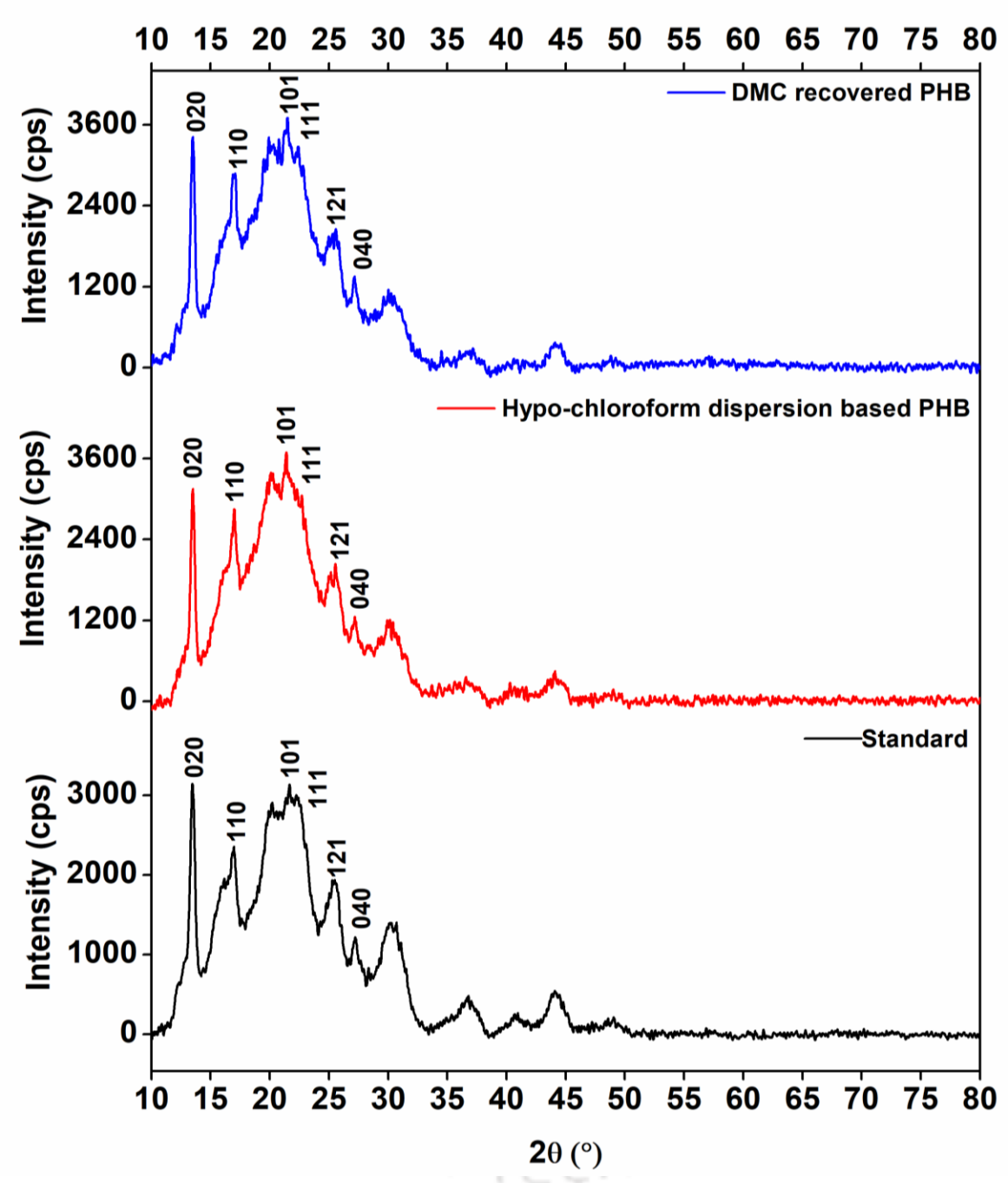

Fig. 7.6: X-ray diffraction (XRD) characterization of PHB recovered from *C. fritschii* by hypochlorite-chloroform dispersion and DMC based recovery with comparison to standard PHB (Sigma-Aldrich)**.**

7.6.5.5. Determination of molecular weight by Gel permeation chromatography

The molecular weight of PHB recovered from *C. fritschii* via both methods were determined using gel permeation chromatography (GPC). The weight average molecular weight (M_w) and number average molecular weight (M_n) have been determined using GPC. The hypochlorite-chloroform dispersion based PHB had a M_w of 319784 Da and M_n of 150268. Whereas DMC recovered PHB had M_w of 440067 and M_n of 155963. The M_w and M_n of standard PHB (Sigma-Aldrich) were 570885 and 216638 Da respectively. The polydispersity index (PDI) of PHB recovered using both methods agreed with that of standard (Table 7.3). Monshupanee et al. reported M_w of 545000 Da of PHB recovered with methanol for pigment removal and chloroform as an extraction solvent from *C. fritschii* in previous studies (Monshupanee et al., 2016). As the extraction reported by Monshupanee et al. and current PHB extraction conditions are different the M_w can be affected. In a study of PHB recovery from *Alcaligenes eutrophus* by the hypochlorite-chloroform dispersion method, M_w has reduced drastically due to severe degradation of PHB molecules (Hahn et al., 1994). In the current study, similar phenomena have been observed with PHB recovered by dispersion. But M_w of PHB with DMC solvent has not decreased that much. Hence, with the same species molecular weight of PHB can be different (M_w and M_n) based on recovery conditions. PHB which was isotactic in nature and synthesized by ring opening polymerization of rac-DL had a PDI of 1.01 with M_n of 154000 (Tang & Chen, 2018). Even though the chemical synthesis of PHB resulted in an isotactic PHB but had a lower molecular weight than PHB from biological origin (Table 7.3). In conclusion, the molecular weight of the polymer depends on the selected species and upstream and downstream conditions that affect material properties. In the present study, the M_w is slightly lower in the case of dispersion method due to chain reduction by hypochlorite. Whereas the green solvent DMC could recover PHB with M_w close to that of standard. In

conclusion, the molecular weight of the polymer depends on the selected species, upstream and downstream conditions.

7.6.5.6. Mechanical properties of PHB

Mechanical properties were studied to characterize the biopolymer. Solvent casted PHB films (0.1 mm thickness) were cut into rectangular films of dimensions (5 cm x 2 cm) and subjected to tensile strength studies at a rate of 1 mm/min (Fig. 7.7A - D). The tensile strength and elongation at break were determined using stress-strain curve. The tensile strength (σ) and elongation at break (ε) of PHB recovered using hypochlorite-chloroform dispersion were found to be 11.11 ± 2.92 MPa and 5.13 ± 2.66 %. Similarly, PHB recovered using DMC resulted in tensile strength and elongation at break of 11.57 ± 0.35 MPa and 6.42 ± 1.04 %, respectively. The standard PHB has a tensile strength of 20.47 ± 1.70 MPa and elongation at break value of 6.39 ± 1.34 % (Table 7.3 and Fig 7.7E). The mechanical properties of PHB recovered from *C. fritschii* depend on its molecular weight. In a study of PHB production with *Zobellela tiwanensis* using banana peel as a feed source, tensile strength of 10.344 MPa was reported with hypochlorite digestion followed by solvent extraction (Maity et al. 2020). The tensile strength of PHB from *C. fritschii* was well agreed with the polymer of *Z. tiwanensis*. Even though higher crystallinity was present, the low strength of recovered polymer films may be caused by the loose bonding of polymer chains and eased mobility at lower molecular weights due to weak interactions.

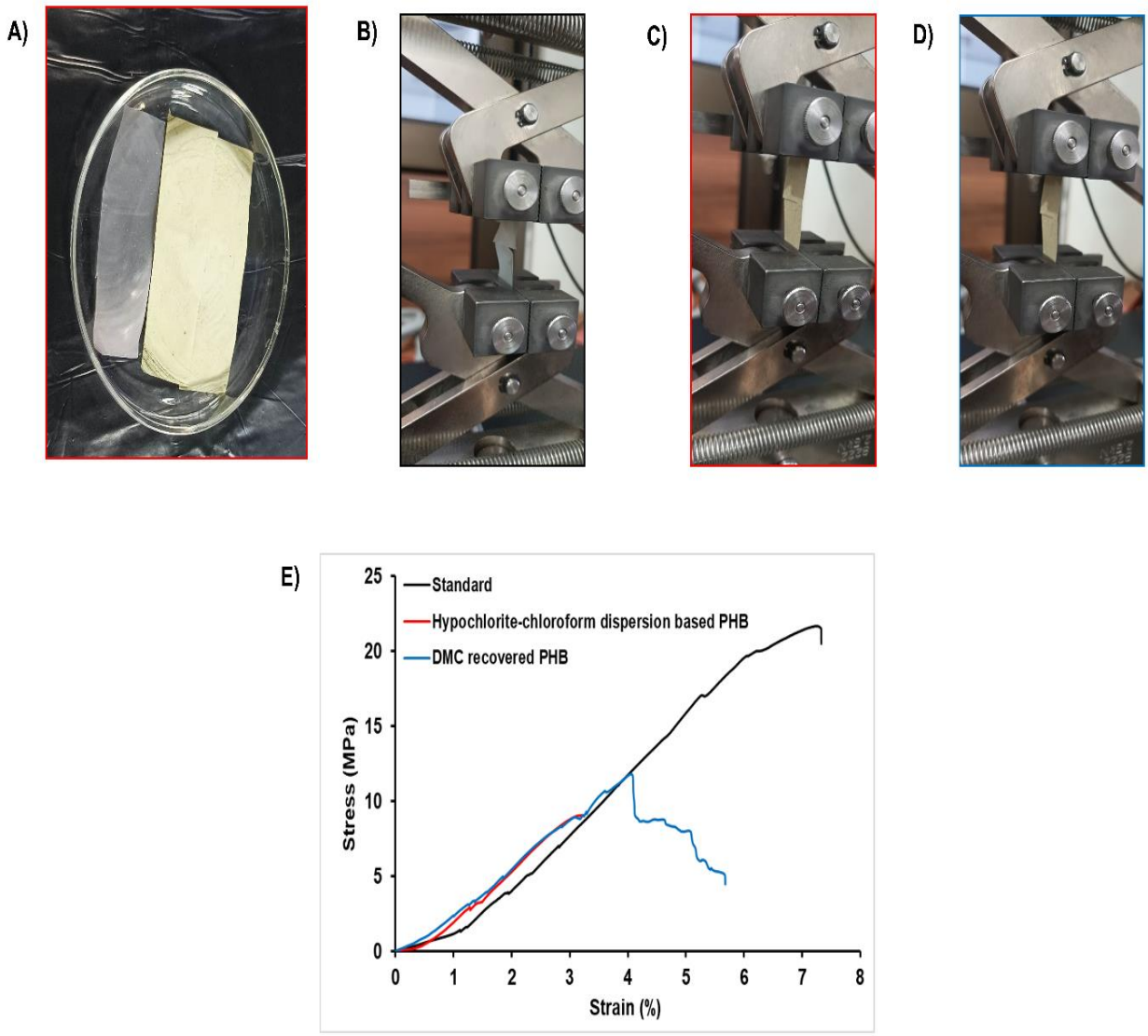

Fig. 7.7: Study of mechanical properties of PHB. **A)** Solvent casted PHB films (0.1 mm thickness) were cut into rectangular film of dimensions (5 cm x 2 cm) and subjected to tensile strength studies at a rate of 1 mm/min, **B)** break of standard PHB film, **C)** break of hypochlorite-chloroform dispersion based PHB film, **D)** break of DMC recovered PHB film observed under 5kN UTM with 2.5kN load, and **E)** Stress-strain behavior of PHB films: standard (black), hypochlorite-chloroform dispersion based PHB (red), and DMC recovered PHB (blue) studied under 5kN Universal testing machine at a rate of 1 mm/min.

Table 7.3: Comparison of material properties of PHB recovered from *C. fritschii* with various sources.

Sources of PHB	Thermal Properties (DSC)					Crystallinity from XRD	Mechanical properties		Molecular Weight			References
	T_m (°C)	T_g (°C)	T_c (°C)	ΔH_f (J g^{-1})	X_c (%)	X_c (%)	Tensile strength (MPa)	Elongation at break (%)	M_w (Da)	M_n (Da)	*PDI* (M_w/ M_n)	
Standard (Sigma-Aldrich)	174	4	84	88.42	60.3	63.3 ± 4.8	20.47 ± 1.70	6.39 ± 1.34	570885	216638	2.63	current study
C. fritschii (Dispersion method)	169	4.6	48.2	52.58	35.9	56.4 ± 1.8	11.11 ± 2.92	5.13 ± 2.66	319784	150268	2.12	current study
C. fritschii (DMC)	174	4.3	48.4	56.34	38.4	56.8 ± 1.5	11.57 ± 0.35	6.42 ± 1.04	440067	155963	2.82	current study
C. fritschii (Chloroform)	171.6	3.2	54	65	45	-	23 ± 6	5.5 ± 1.8	545000	256000	2.1	(Monshupanee et al., 2016)
Nostoc muscorum (chloroform)	171	6	78.8	83.25	56.78	-	31.1	8.6	-	-	-	(Ansari & Fatma, 2016)
PHB (Chemically synthesized)	170.7	-	82.2	78.6	53	-	-	-	155540	154000	1.01	(Tang & Chen, 2018)
PET (Fossil based)	260	67-81	-	-	7.9	-	62	230	-	-	-	(McAdam et al., 2020)
PP (Fossil based)	160-169	-20-(-5)	-	-	42-58	-	31-45	50-145	-	-	-	(McAdam et al., 2020)

T_m, melting temperature; T_g, glass-transition temperature; T_c, cold-crystallization temperature; ΔH_f, enthalpy of fusion; X_c, crystallinity; M_w, weight-average molecular weight; M_n, number-average molecular weight; *PDI*, polydispersity index. The values are represented as mean ± SD of the three independent experiments.

7.6.5.7. Visualization of PHB films under Scanning electron microscope

PHB films recovered from *C. fritschii* by hypochlorite-chloroform dispersion and DMC were opaque whereas standard PHB was transparent (Fig. 7.7A). Scanning electron microscopy (SEM) revealed no aggregation or void gaps, indicating uniform surface morphology in PHB recovered by both methods when compared to standard PHB (Fig.7.8). PHB recovered from *Nostoc muscorum* NCCU-442 was also found to be homogenous with uniform surface topography under SEM (Ansari & Fatma, 2016).

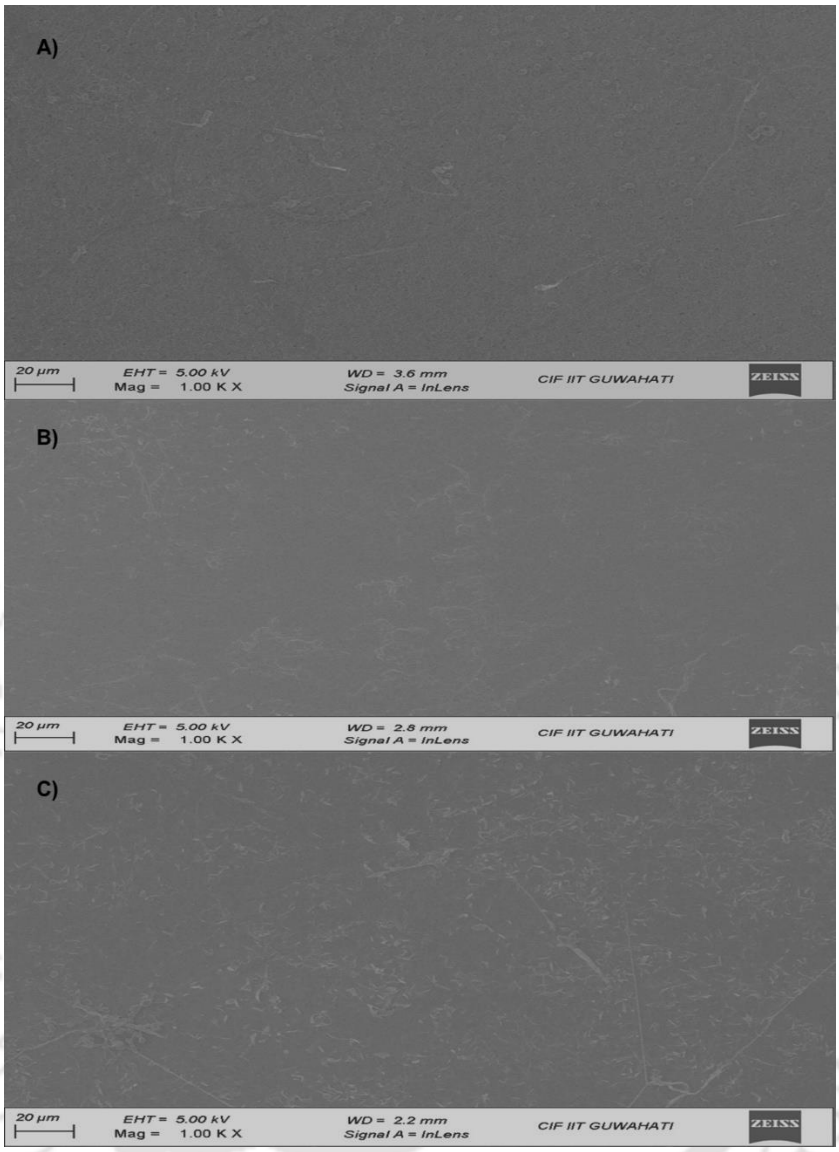

Fig. 7.8: Surface characterization of PHB films recovered from *C. fritschii* by hypochlorite-chloroform dispersion and DMC based recovery with comparison to standard PHB (Sigma-Aldrich) by scanning electron microscopy under 1.00KX magnification**. A)** Standard PHB, **B)** hypochlorite- chloroform dispersion based PHB and **C)** DMC recovered PHB.

7.7. Conclusions

In the current work, PHB recovery from the cyanobacterium *C. fritschii* was performed with different methods. The dispersion method and solvent extraction were the main focus. The dispersion method achieved 95.51 % PHB recovery along with pigment removal. Various solvents showed lower recovery of PHB due to unsuitable operating conditions for PHB recovery. Among such solvents, the selection of a green solvent was critical. Optimization of the recovery process using DMC resulted in a recovery yield of 83.31 % with pigment removal using methanol. DSC and XRD analysis showed that PHB from *C. fritschii* was partially crystalline. Characterization of recovered PHB suggested that *C. fritschii* can accumulate biopolymer similar to commercial PHB. Overall, biopolymer recovery using DMC is an eco-friendly process and can be employed for bioplastic recovery from other cyanobacteria.

CHAPTER 8

Overall Conclusions

Chlorogloea fritschii TISTR 8527 is capable of accumulating PHB under stress conditions with the utilization of diurnal light. *C. fritschii* can replace the heterotrophic bacteria in PHB production without supplementation of sugars, with CO_2 fixation and with supplementation of low-cost substrates such as acetate. For cyanobacterial cultivation growth medium, light intensity, CO_2 levels, pH, mixing and mass transfer, and temperature play important roles. Current research is performed without temperature control either for growth or for PHB induction. Effects of light, nutrients and CO_2 was studied. In earlier studies two stage cultivation of *C. fritschii* may resulted in a higher PHB production but the replacement of growth medium with nutrient limiting medium may add costs in large scale PHB production. Hence our study mainly focuses on the development of cost-effective single stage cultivation with utilization of diurnal light and CO_2 with minimal supply of acetate as PHB inducer without media replacement. PHB production in *C. fritschii* is a multi-objective problem where growth of the same required nutrient sufficient conditions whereas PHB production and sedimentation of *C. fritschii* require stress or nutrient deprivation conditions. PHB is stored as an intracellular product by cyanobacteria under nutrient limitations. Recovering PHB from cytoplasm increases production cost by up to 50 % of the cost of the polymer since PHB must be purified in multiple steps. The molecular weight of the recovered polymer may decrease because of NPCM digestion with hypochlorite. Hypochlorite and chloroform dispersion can decrease the loss in molecular weight of recovered PHB while raising the yield and purity along with pigment removal. Solvent recovery is the most used method due to its high recovery efficiency resulting in polymer of high molecular weight along with the removal of endotoxins. Among such solvents, the selection of a green solvent was critical.

An increase in light intensity enhanced the growth of *C. fritschii* with peak light intensity of 1890 µmol/m^2/s resulting in biomass concentration of 1.84 g/L on 16 d in modified BG-11 medium. *C. fritschii* can be cultivated under simulated diurnal light mimic to sunlight resulting in dry cell weight of 2.1 g/L in flask setup equipped with silicone tubing sparger. Nitrate concentration of 1.5 g/L and acetate level of 0.2 % (w/v) as inducer were shown as optimal levels for PHB production under diurnal light. Single stage cultivation is economical since the intermediate biomass harvesting step can be avoided before PHB production. Single stage PHB accumulation of *C. fritschii* resulted in a maximum PHB content of 16.4 % on the 4^{th} day of induction with 0.2 % (w/v) acetate. Cultivation of *C. fritschii* in medium scale flat panel PBR under diurnal light resulted in DCW of 2.06 g/L with 11.2 % polymer content. A phosphate and nitrate feeding-batch strategy in flat panel PBR enhanced the PHB content to 46.9 % with a 4.2-fold increment when compared to control.

C. fritschii has an unique nature of auto-sedimentation which reduces the cost of biomass harvesting by centrifugation and eases downstream. In the current study with *C. fritschii*, it has been seen that the auto-sedimentation rate of biomass and percentage of PHB in biomass are conflicting with each other and both are dependent on the nutrient composition in media. Also, biomass concentration and percentage of PHB in biomass conflict with each other since there is a requirement of nutrient rich media for biomass growth and nutrient-depleted media for PHB accumulation. Desirability based multi-objective optimization approach has been used to develop media for single-stage cultivation of *C. fritschii* to increase PHB, biomass concentration and auto-sedimentation of biomass under diurnal light mimic to sunlight. The model used for multi-objective optimization has been developed using Response surface methodology. A set of Pareto points has been generated in multi-objective optimization which presents flexibility to choose

suitable media composition for profitability. An optimized medium selected from the pareto set enhances the bioplastic PHB content and sedimentation concentration factor by 2.72 and 1.64-fold respectively with a loss of biomass concentration compared to non-optimal media under autotrophic conditions. But ultimately the amount of PHB (g/L) was enhanced by 69 % using optimized media. This multi-objective approach developed here with *C. fritschii* TISTR 8527 can be used for other cyanobacteria to optimize value added products.

C. fritschii was cultivated in flat panel PBR using optimized BG-11 medium under diurnal simulated sunlight with various levels of CO_2 starting from air to 5 %. A higher specific growth rate of 1.538 d^{-1} had resulted with 1 % CO_2 with PHB accumulation of 31.78 % in single stage cultivation. The maximum PHB productivity of 33.15 mg/L/d with polymer production of 28 % was observed with 3 % CO_2. Air resulted in higher SCF values of 148 and PHB content of 19.85 %. Lower levels of CO_2 resulted in higher polymer content and SCF values. The supplementation of 1 and 3 % CO_2 resulted in higher PHB production which in turn affect SCF values. Intracellular phosphate plays a significant role in cellular growth and carbon flow towards PHB accumulation. At the initial stage of cultivation, an average intracellular phosphate concentration (P_{intra}) of approximately 105.6 mg/g was observed which was utilized during cultivation process for cellular growth and later for carbon trafficking of supplemented acetate for PHB synthesis. PHB productivity of 30.3 mg/L/d and 33.15 mg/L/d had resulted due to P_{intra} of 4.024 ± 0.03 mg/g (0.042 mmol/g) and 6.96 ± 0.2 mg/g (0.073 mmol/g) with 1 and 3 % CO_2 respectively. Multiple addition of acetate during induction didn't enhance the PHB productivity after second feeding.

The hypochlorite-chloroform dispersion method achieved 95.51 % PHB recovery along with pigment removal. Apart from this, solvent recovery method was used due to its high polymer recovery efficiency after hypochlorite pretreatment for pigment removal. Various solvents showed

lower recovery of PHB due to unsuitable operating conditions for PHB recovery at 100 °C after hypochlorite pretreatment. Among such solvents, the selection of a green solvent dimethyl carbonate was critical. Optimization of the recovery process using DMC resulted in a recovery yield of 83.31 % with pigment removal using methanol. DSC and XRD analysis showed that PHB from *C. fritschii* was partially crystalline. TGA and GPC characterization of the recovered PHB demonstrated that *C. fritschii* can accumulate biopolymer that is comparable to that of commercial PHB. Considering all factors biopolymer recovery with DMC is a sustainable method that may be used to extract bioplastics from different cyanobacteria.

The major outcomes of the study were single stage cultivation of *C. fritschii* under diurnal light with utilization of CO_2 for growth and acetate for PHB induction of high-density biomass without media replacement. The cost-effective auto-sedimentation of *C. fritschii* added an extra significance in avoiding cell harvesting by centrifugation. The multi-objective medium optimization with single stage cultivation seeks its attention in optimization of PHB accumulation in various cyanobacteria. Recovery of intracellular polymer using eco-friendly green solvents reduce the usage of toxic halogenated solvents and PHB recovered from *C. fritschii* using DMC is of commercial standard. Utilizing CO_2 to produce PHB from *C. fritschii* can be exploited effectively by competing with heterotrophic bacteria to reduce the demand of food sources for continuous supply of sugar while making the process cost-effective.

FUTURE PROSPECTS

- ✓ Implementation of single-stage cultivation without intermediate biomass harvesting appears to be economically favorable for PHB production. Further research could focus on refining this process to improve efficiency and reduce costs for various cyanobacteria under diurnal simulated sunlight.
- ✓ Outdoors cultivation of *C. fritschii* or other cyanobacteria for utilizing the natural sunlight and CO_2 for PHB production with implementation of autosedimentation strategy for biomass harvesting can reduce the cost of cyanobacterial PHB production.
- ✓ Extend the developed multi-objective optimization approach to optimize PHB production in other cyanobacterial strains, considering their unique metabolic characteristics.
- ✓ Investigate and optimize the recovery process of PHB from *C. fritschii* biomass, focusing on improving efficiency and sustainability, especially in large-scale operations.
- ✓ Conduct scale-up studies to assess the feasibility and productivity of PHB production from *C. fritschii* in larger bioreactor systems, moving towards commercialization.
- ✓ Implementing genetic engineering techniques to enhance PHB production in *C. fritschii* by manipulating key metabolic pathways or introducing genetic modifications aimed at improving carbon flux towards PHB synthesis.
- ✓ Investigating the mechanisms more thoroughly that explain the function of intracellular phosphate in cell growth and accumulation of PHB. This can include looking at the processes through which phosphate is utilized and how those processes affect the dynamics of carbon transport inside the cells.
- ✓ Exploration of other green solvents such as dioxolane with optimization of PHB recovery.

- ✓ Life cycle assessment of the *C. fritschii* cultivation in large scale cultivation along with biomass harvesting and product recovery. Evaluate the environmental sustainability and impact of PHB production from *C. fritschii*, considering factors such as carbon footprint, energy consumption, and waste generation.
- ✓ Understanding the properties of the PHB produced by *C. fritschii* is crucial for determining its potential applications. Future research could focus on characterizing bioplastics and exploring its suitability for various industrial applications.
- ✓ Exploring the concept of a biorefinery approach where various valuable products, such as biofuels are co-produced alongside PHB from *C. fritschii* cultivation, enhancing the overall economic viability and sustainability of the process.
- ✓ Complete cost analysis of upstream and downstream processes of PHB production in *C. fritschii*.

REFERENCES

Abdo, S.M., Ali, G.H. 2019. Analysis of polyhydroxybutrate and bioplastic production from microalgae. *Bulletin of the National Research Centre*, **43**(1), 1-4.

Ahmad, A.L., Yasin, N.H.M., Derek, C.J.C., Lim, J.K. 2012. Crossflow microfiltration of microalgae biomass for biofuel production. *Desalination*, **302**, 65-70.

Ahn, W.S., Park, S.J., Lee, S.Y. 2000. Production of poly (3-hydroxybutyrate) by fed-batch culture of recombinant Escherichia coli with a highly concentrated whey solution. *Applied and environmental microbiology*, **66**(8), 3624-3627.

Ali, W., Ali, H., Souissi, S., Zinck, P. 2023. Are bioplastics an ecofriendly alternative to fossil fuel plastics? *Environmental Chemistry Letters*, 1-12.

Allen, M.M., Smith, A.J. 1969. Nitrogen chlorosis in blue-green algae. *Archives of Microbiology*, **69**(2), 114-120.

Alvarez, X., Alves, A., Ribeiro, M.P., Lazzari, M., Coutinho, P., Otero, A. 2021. Biochemical characterization of Nostoc sp. exopolysaccharides and evaluation of potential use in wound healing. *Carbohydrate polymers*, **254**, 117303.

Anbukarasu, P., Sauvageau, D., Elias, A. 2015. Tuning the properties of polyhydroxybutyrate films using acetic acid via solvent casting. *Scientific reports*, **5**(1), 17884.

Ansari, S., Fatma, T. 2016. Cyanobacterial polyhydroxybutyrate (PHB): screening, optimization and characterization. *PLoS One*, **11**(6), e0158168.

Aramvash, A., Moazzeni Zavareh, F., Gholami Banadkuki, N. 2018. Comparison of different solvents for extraction of polyhydroxybutyrate from Cupriavidus necator. *Engineering in Life Sciences*, **18**(1), 20-28.

Ariffin, H., Nishida, H., Shirai, Y., Hassan, M.A. 2008. Determination of multiple thermal degradation mechanisms of poly (3-hydroxybutyrate). *Polymer Degradation and Stability*, **93**(8), 1433-1439.

Arrieta, M.P., Samper, M.D., López, J., Jiménez, A. 2014. Combined effect of poly (hydroxybutyrate) and plasticizers on polylactic acid properties for film intended for food packaging. *Journal of Polymers and the Environment*, **22**, 460-470.

Bade, D.L., Cole, J.J. 2006. Impact of chemically enhanced diffusion on dissolved inorganic carbon stable isotopes in a fertilized lake. *Journal of Geophysical Research: Oceans*, **111**(C1), 1-10.

Balmer, M.B., Downing, J.A. 2011. Carbon dioxide concentrations in eutrophic lakes: undersaturation implies atmospheric uptake. *Inland Waters*, **1**(2), 125-132.

Bansal, S., Kushwah, S.S., Garg, A., Sharma, K. 2023. Utilization of plastic waste in construction industry in India–A review. *Materials Today: Proceedings*.

Barros, A.I., Gonçalves, A.L., Simões, M., Pires, J.C. 2015. Harvesting techniques applied to microalgae: a review. *Renewable and sustainable energy reviews*, **41**, 1489-1500.

Bhange, K., Nath, A., Singh, N., Chaturvedi, V., Bhatt, R. 2023. Statistical optimization and prediction of significant nutritional factors for keratinase production by Stenotrophomonas maltophilia Kb2 and its application as dehairing agent. *Bioresource Technology Reports*, 101541.

Bhati, R., Mallick, N. 2016. Carbon dioxide and poultry waste utilization for production of polyhydroxyalkanoate biopolymers by Nostoc muscorum Agardh: a sustainable approach. *Journal of applied phycology*, **28**, 161-168.

Bhati, R., Samantaray, S., Sharma, L., Mallick, N. 2010. Poly-β-hydroxybutyrate accumulation in cyanobacteria under photoautotrophy. *Biotechnology journal*, **5**(11), 1181-1185.

Bhatnagar, A., Bhatnagar, M., Chinnasamy, S., Das, K. 2010. Chlorella minutissima—a promising fuel alga for cultivation in municipal wastewaters. *Applied biochemistry and biotechnology*, **161**(1-8), 523-536.

Bhave, R., Kuritz, T., Powell, L., Adcock, D. 2012. Membrane-Based Energy Efficient Dewatering of Microalgae in Biofuels Production and Recovery of Value Added Co-Products. *Environmental Science & Technology*, **46**(10), 5599-5606.

Bilad, M.R., Vandamme, D., Foubert, I., Muylaert, K., Vankelecom, I.F.J. 2012. Harvesting microalgal biomass using submerged microfiltration membranes. *Bioresource Technology*, **111**, 343-352.

Borrelle, S.B., Ringma, J., Law, K.L., Monnahan, C.C., Lebreton, L., McGivern, A., Murphy, E., Jambeck, J., Leonard, G.H., Hilleary, M.A. 2020. Predicted growth in plastic waste exceeds efforts to mitigate plastic pollution. *Science*, **369**(6510), 1515-1518.

Bottomley, P., Stewart, W. 1976. ATP pools and transients in the blue-green alga, Anabaena cylindrica. *Archives of microbiology*, **108**(3), 249-258.

Bustos, R., Castrillo, G., Linhares, F., Puga, M.I., Rubio, V., Pérez-Pérez, J., Solano, R., Leyva, A., Paz-Ares, J. 2010. A central regulatory system largely controls transcriptional activation and repression responses to phosphate starvation in Arabidopsis. *PLoS genetics*, **6**(9), e1001102.

Campbell, J., Stevens, S., Balkwill, D. 1982. Accumulation of poly-beta-hydroxybutyrate in Spirulina platensis. *Journal of Bacteriology*, **149**(1), 361-363.

Carpine, R., Olivieri, G., Hellingwerf, K., Pollio, A., Marzocchella, A. 2015. The cyanobacterial route to produce poly-β-hydroxybutyrate. *Chem. Eng. Trans*, **43**, 289-294.

Carr, N. 1966. The occurrence of poly-β-hydroxybutyrate in the blue-green alga, Chlorogloea fritschii. *Biochimica et Biophysica Acta -Biophysics including Photosynthesis*, **120**(2), 308-310.

Castellano, D., Sanchis, A., Blanes, M., Pérez del Caz, M.D., Ruiz-Saurí, A., Piquer-Gil, M., Pelacho, B., Marco, B., Garcia, N., Ontoria-Oviedo, I. 2018. Electrospun poly (hydroxybutyrate) scaffolds promote engraftment of human skin equivalents via macrophage M2 polarization and angiogenesis. *Journal of Tissue Engineering and Regenerative Medicine*, **12**(2), e983-e994.

Castro-Castellon, A.T., Horton, A.A., Hughes, J.M., Rampley, C., Jeffers, E.S., Bussi, G., Whitehead, P. 2022. Ecotoxicity of microplastics to freshwater biota: Considering exposure and hazard across trophic levels. *Science of the Total Environment*, **816**, 151638.

Cataldo, D., Maroon, M., Schrader, L.E., Youngs, V.L. 1975. Rapid colorimetric determination of nitrate in plant tissue by nitration of salicylic acid. *Communications in soil science and plant analysis*, **6**(1), 71-80.

Chavez, B.A., Raghavan, V., Tartakovsky, B. 2022. A comparative analysis of biopolymer production by microbial and bioelectrochemical technologies. *RSC advances*, **12**(25), 16105-16118.

Chen, G.-Q., Wu, Q. 2005. The application of polyhydroxyalkanoates as tissue engineering materials. *Biomaterials*, **26**(33), 6565-6578.

Chen, M., Li, J., Zhang, L., Chang, S., Liu, C., Wang, J., Li, S. 2014. Auto-flotation of heterocyst enables the efficient production of renewable energy in cyanobacteria. *Scientific reports*, **4**(1), 1-9.

Choi, J.-i., Lee, S.Y. 1997. Process analysis and economic evaluation for poly (3-hydroxybutyrate) production by fermentation. *Bioprocess engineering*, **17**, 335-342.

Costa, J.A.V., Moreira, J.B., Lucas, B.F., Braga, V.d.S., Cassuriaga, A.P.A., Morais, M.G.d. 2018. Recent advances and future perspectives of PHB production by cyanobacteria. *Industrial Biotechnology*, **14**(5), 249-256.

Das, M., Maiti, S.K. 2022. Current knowledge on cyanobacterial biobutanol production: advances, challenges, and prospects. *Reviews in Environmental Science and Bio/Technology*, **21**(2), 483-516.

Dasgupta, S., Sarraf, M., Wheeler, D. 2022. Plastic waste cleanup priorities to reduce marine pollution: A spatiotemporal analysis for Accra and Lagos with satellite data. *Science of the Total Environment*, **839**, 156319.

Deb, K. 2003. Multi-objective evolutionary algorithms: Introducing bias among Pareto-optimal solutions. in: *Advances in evolutionary computing: theory and applications*, Springer, pp. 263-292.

Deb, K., Gupta, H. 2005. Searching for robust Pareto-optimal solutions in multi-objective optimization. *Evolutionary Multi-Criterion Optimization: Third International Conference, EMO 2005, Guanajuato, Mexico, March 9-11, 2005. Proceedings 3*. Springer. pp. 150-164.

Debnath, M., Bhadury, P. 2016. Adaptive responses and arsenic transformation potential of diazotrophic Cyanobacteria isolated from rice fields of arsenic affected Bengal Delta Plain. *Journal of Applied Phycology*, **28**, 2777-2792.

Defoirdt, T., Halet, D., Vervaeren, H., Boon, N., Van de Wiele, T., Sorgeloos, P., Bossier, P., Verstraete, W. 2007. The bacterial storage compound poly-β-hydroxybutyrate protects Artemia franciscana from pathogenic Vibrio campbellii. *Environmental microbiology*, **9**(2), 445-452.

Delledonne, D., Rivetti, F., Romano, U. 2001. Developments in the production and application of dimethylcarbonate. *Applied Catalysis A: General*, **221**(1-2), 241-251.

Derringer, G., Suich, R. 1980. Simultaneous optimization of several response variables. *Journal of quality technology*, **12**(4), 214-219.

Devi, A.B., Nachiyar, C.V., Kaviyarasi, T., Samrot, A.V. 2015. Characterization of polyhydroxybutyrate synthesized by Bacillus cereus. *International Journal of Pharmacy and Pharmaceutical Sciences*, **7**(3), 140-144.

Drexler, I.L.C., Yeh, D.H. 2014. Membrane applications for microalgae cultivation and harvesting: a review. *Reviews in Environmental Science and Bio-Technology*, **13**(4), 487-504.

Drosg, B., Fritz, I., Gattermayr, F., Silvestrini, L. 2015. Photo-autotrophic production of poly (hydroxyalkanoates) in cyanobacteria. *Chemical and Biochemical Engineering Quarterly*, **29**(2), 145-156.

Eberly, J.O., Ely, R.L. 2012. Photosynthetic accumulation of carbon storage compounds under CO2 enrichment by the thermophilic cyanobacterium Thermosynechococcus elongatus. *Journal of Industrial Microbiology and Biotechnology*, **39**(6), 843-850.

Eixler, S., Selig, U., Karsten, U. 2005. Extraction and detection methods for polyphosphate storage in autotrophic planktonic organisms. *Hydrobiologia*, **533**(1), 135-143.

Elcik, H., Cakmakci, M. 2017. Harvesting microalgal biomass using crossflow membrane filtration: critical flux, filtration performance, and fouling characterization. *Environmental Technology*, **38**(12), 1585-1596.

Elhami, V., van de Beek, N., Wang, L., Picken, S.J., Tamis, J., Sousa, J.A., Hempenius, M.A., Schuur, B. 2022. Extraction of low molecular weight polyhydroxyalkanoates from mixed microbial cultures using bio-based solvents. *Separation and purification technology*, **299**, 121773.

Fang, Z., Chen, P., Ji, Q., Yan, C., Gong, A. 2023. Stimuli-responsive hydrogel for disease therapy. *Polymer Bulletin*, 1-20.

Farinacci, J., Laurent, J. 2023. Critical assessment of the sulfo-phospho-vanillin method to quantify lipids in freeze-dried microalgae. *Journal of Applied Phycology*, 1-12.

Fasaei, F., Bitter, J.H., Slegers, P.M., Van Boxtel, A.J. 2018. Techno-economic evaluation of microalgae harvesting and dewatering systems. *Algal research*, **31**, 347-362.

Fedeson, D.T., Ducat, D.C. 2017. Cyanobacterial surface display system mediates engineered interspecies and abiotic binding. *ACS synthetic biology*, **6**(2), 367-374.

Fiorese, M.L., Freitas, F., Pais, J., Ramos, A.M., de Aragão, G.M., Reis, M.A. 2009. Recovery of polyhydroxybutyrate (PHB) from Cupriavidus necator biomass by solvent extraction with 1, 2-propylene carbonate. *Engineering in Life Sciences*, **9**(6), 454-461.

Fogg, G.E., Thake, B. 1987. *Algal cultures and phytoplankton ecology*. Univ of Wisconsin Press.

Garcia-Gonzalez, L., De Wever, H. 2017. Valorisation of CO2-rich off-gases to biopolymers through biotechnological process. *FEMS Microbiology Letters*, **364**(20), 196.

Geyer, R., Jambeck, J.R., Law, K.L. 2017. Production, use, and fate of all plastics ever made. *Science advances*, **3**(7), e1700782.

Gopi, K., Balaji, S., Muthuvelan, B. 2014. Isolation purification and screening of biodegradable polymer PHB producing cyanobacteria from marine and fresh water resources. *Iranica Journal of Energy and Environment*, **5**(1).

Grima, E.M., Belarbi, E.-H., Fernández, F.A., Medina, A.R., Chisti, Y. 2003. Recovery of microalgal biomass and metabolites: process options and economics. *Biotechnology advances*, **20**(7-8), 491-515.

Hahn, S.K., Chang, Y.K., Kim, B.S., Chang, H.N. 1994. Optimization of microbial poly (3-hydroxybutyrate) recover using dispersions of sodium hypochlorite solution and chloroform. *Biotechnology and Bioengineering*, **44**(2), 256-261.

Hahn, S.K., Chang, Y.K., Lee, S.Y. 1995. Recovery and characterization of poly (3-hydroxybutyric acid) synthesized in Alcaligenes eutrophus and recombinant Escherichia coli. *Applied and environmental microbiology*, **61**(1), 34-39.

Halami, P.M. 2008. Production of polyhydroxyalkanoate from starch by the native isolate Bacillus cereus CFR06. *World Journal of Microbiology and Biotechnology*, **24**(6), 805-812.

Hauf, W., Schlebusch, M., Huege, J., Kopka, J., Hagemann, M., Forchhammer, K. 2013. Metabolic changes in Synechocystis PCC6803 upon nitrogen-starvation: excess NADPH sustains polyhydroxybutyrate accumulation. *Metabolites*, **3**(1), 101-118.

Ho, S.-h., Lai, Y.-Y., Chiang, C.-Y., Chen, C.-N.N., Chang, J.-S. 2013. Selection of elite microalgae for biodiesel production in tropical conditions using a standardized platform. *Bioresource technology*, **147**, 135-142.

Hondo, S., Takahashi, M., Osanai, T., Matsuda, M., Hasunuma, T., Tazuke, A., Nakahira, Y., Chohnan, S., Hasegawa, M., Asayama, M. 2015. Genetic engineering and metabolite profiling for overproduction of polyhydroxybutyrate in cyanobacteria. *Journal of bioscience and bioengineering*, **120**(5), 510-517.

Hosseinizand, H., Sokhansanj, S., Lim, C.J. 2018. Studying the drying mechanism of microalgae Chlorella vulgaris and the optimum drying temperature to preserve quality characteristics. *Drying Technology*, **36**(9), 1049-1060.

Hürlimann, H.C., Stadler-Waibel, M., Werner, T.P., Freimoser, F.M. 2007. Pho91 is a vacuolar phosphate transporter that regulates phosphate and polyphosphate metabolism in Saccharomyces cerevisiae. *Molecular biology of the cell*, **18**(11), 4438-4445.

Iasimone, F., Seira, J., Desmond-Le Quéméner, E., Panico, A., De Felice, V., Pirozzi, F., Steyer, J.-P. 2020. Bioflocculation and settling studies of native wastewater filamentous cyanobacteria using different cultivation systems for a low-cost and easy to control harvesting process. *Journal of Environmental Management*, **256**, 109957.

Imamura, M., Tsuzuki, M., Shiraiwa, Y., Miyachi, S. 1983. Form of inorganic carbon utilized for photosynthesis in Chlamydomonas reinhardtii. *Plant and Cell Physiology*, **24**(3), 533-540.

Issac, M.N., Kandasubramanian, B. 2021. Effect of microplastics in water and aquatic systems. *Environmental Science and Pollution Research*, **28**, 19544-19562.

Jendrossek, D. 2009. Polyhydroxyalkanoate granules are complex subcellular organelles (carbonosomes). *Journal of bacteriology*, **191**(10), 3195-3202.

John, M.K. 1970. Colorimetric determination of phosphorus in soil and plant materials with ascorbic acid. *Soil Science*, **109**(4), 214-220.

Jordan, A., Chandler, J., MacCready, J.S., Huang, J., Osteryoung, K.W., Ducat, D.C. 2017. Engineering cyanobacterial cell morphology for enhanced recovery and processing of biomass. *Appl. Environ. Microbiol.*, **83**(9), e00053-17.

Juengert, J.R., Bresan, S., Jendrossek, D. 2018. Determination of polyhydroxybutyrate (PHB) content in Ralstonia eutropha using gas chromatography and Nile red staining. *Bio-protocol*, **8**(5).

Kaewbai-Ngam, A., Incharoensakdi, A., Monshupanee, T. 2016. Increased accumulation of polyhydroxybutyrate in divergent cyanobacteria under nutrient-deprived photoautotrophy: An efficient conversion of solar energy and carbon dioxide to polyhydroxybutyrate by Calothrix scytonemicola TISTR 8095. *Bioresource technology*, **212**, 342-347.

Kamravamanesh, D., Pflügl, S., Nischkauer, W., Limbeck, A., Lackner, M., Herwig, C. 2017. Photosynthetic poly-β-hydroxybutyrate accumulation in unicellular cyanobacterium Synechocystis sp. PCC 6714. *AMB express*, **7**(1), 1-12.

Kamravamanesh, D., Slouka, C., Limbeck, A., Lackner, M., Herwig, C. 2019. Increased carbohydrate production from carbon dioxide in randomly mutated cells of cyanobacterial strain Synechocystis sp. PCC 6714: Bioprocess understanding and evaluation of productivities. *Bioresource technology*, **273**, 277-287.

Kanzariya, R., Gautam, A., Parikh, S., Shah, M., Gautam, S. 2023. Structure analysis and thermal stability of PHB recovered from sugar industry waste. *Biotechnology and Genetic Engineering Reviews*, 1-23.

Khademi, M. 2014. Application of tubular crossflow microfiltration in harvesting microalgae. in: *Biological and Agricultural Engineering*, Louisiana State University. Louisiana

Khanna, S., Srivastava, A.K. 2005. Recent advances in microbial polyhydroxyalkanoates. *Process biochemistry*, **40**(2), 607-619.

Khetkorn, W., Incharoensakdi, A., Lindblad, P., Jantaro, S. 2016. Enhancement of poly-3-hydroxybutyrate production in Synechocystis sp. PCC 6803 by overexpression of its native biosynthetic genes. *Bioresource technology*, **214**, 761-768.

Kobayashi, D., Fujita, K., Nakamura, N., Ohno, H. 2015. A simple recovery process for biodegradable plastics accumulated in cyanobacteria treated with ionic liquids. *Applied Microbiology and Biotechnology*, **99**(4), 1647-1653.

Köbler, C., Schultz, S.J., Kopp, D., Voigt, K., Wilde, A. 2018. The role of the Synechocystis sp. PCC 6803 homolog of the circadian clock output regulator RpaA in day–night transitions. *Molecular Microbiology*, **110**(5), 847-861.

Koch, M., Doello, S., Gutekunst, K., Forchhammer, K. 2019. PHB is produced from glycogen turn-over during nitrogen starvation in Synechocystis sp. PCC 6803. *International journal of molecular sciences*, **20**(8), 1942.

Koller, M., Niebelschütz, H., Braunegg, G. 2013. Strategies for recovery and purification of poly [(R)-3-hydroxyalkanoates](PHA) biopolyesters from surrounding biomass. *Engineering in life sciences*, **13**(6), 549-562.

Konstantinidis, S., Welsh, J.P., Titchener-Hooker, N.J., Roush, D.J., Velayudhan, A. 2018. Data-driven multi-objective optimization via grid compatible simplex technique and desirability approach for challenging high throughput chromatography applications. *Biotechnology Progress*, **34**(6), 1393-1406.

Koutinas, A.A., Xu, Y., Wang, R., Webb, C.J.E., technology, M. 2007. Polyhydroxybutyrate production from a novel feedstock derived from a wheat-based biorefinery. *Enzyme and Microbial technology*, **40**(5), 1035-1044.

Krasaesueb, N., Incharoensakdi, A., Khetkorn, W. 2019. Utilization of shrimp wastewater for poly-β-hydroxybutyrate production by Synechocystis sp. PCC 6803 strain ΔSphU cultivated in photobioreactor. *Biotechnology Reports*, **23**, e00345.

Kumar, K., Dasgupta, C.N., Nayak, B., Lindblad, P., Das, D. 2011. Development of suitable photobioreactors for CO_2 sequestration addressing global warming using green algae and cyanobacteria. *Bioresource technology*.

Lackner, M., Kamravamanesh, D., Krampl, M., Itzinger, R., Paulik, C., Chodak, I., Herwig, C. 2019. Characterization of photosynthetically synthesized poly (3-hydroxybutyrate) using a randomly mutated strain of Synechocystis sp. PCC 6714. *International Journal of Biobased Plastics*, **1**(1), 48-59.

Lau, N.-S., Matsui, M., Abdullah, A.A.-A. 2015. Cyanobacteria: photoautotrophic microbial factories for the sustainable synthesis of industrial products. *BioMed research international*, **2015**.

Leal Filho, W., Saari, U., Fedoruk, M., Iital, A., Moora, H., Klöga, M., Voronova, V. 2019. An overview of the problems posed by plastic products and the role of extended producer responsibility in Europe. *Journal of cleaner production*, **214**, 550-558.

Lee, J.S., Sung, Y.J., Kim, D.H., Lee, J.Y., Sim, S.J. 2022. Development of a limitless scale-up photobioreactor for highly efficient photosynthesis-based polyhydroxybutyrate (PHB)-producing cyanobacteria. *Bioresource technology*, **364**, 128121.

Lee, S.Y., Choi, J.-i., Han, K., Song, J.Y. 1999. Removal of endotoxin during purification of poly (3-hydroxybutyrate) from gram-negative bacteria. *Applied and environmental microbiology*, **65**(6), 2762-2764.

Lemoigne, M. 1926. de l'acide 3-oxybutyrique. *Bull Soc Chim Biol*, **8**, 770.

Leong, Y.K., Show, P.L., Lan, J.C.-W., Loh, H.-S., Lam, H.L., Ling, T.C. 2017. Economic and environmental analysis of PHAs production process. *Clean Technologies and Environmental Policy*, **19**, 1941-1953.

Lim, H.G., Lee, J.H., Noh, M.H., Jung, G.Y. 2018. Rediscovering acetate metabolism: its potential sources and utilization for biobased transformation into value-added chemicals. *Journal of agricultural and food chemistry*, **66**(16), 3998-4006.

Liu, X., Miao, R., Lindberg, P., Lindblad, P. 2019. Modular engineering for efficient photosynthetic biosynthesis of 1-butanol from CO2 in cyanobacteria. *Energy and Environmental Science*, **12**(9), 2765-2777.

Lopez-Arenas, T., González-Contreras, M., Anaya-Reza, O., Sales-Cruz, M. 2017. Analysis of the fermentation strategy and its impact on the economics of the production process of PHB (polyhydroxybutyrate). *Computers and Chemical Engineering*, **107**, 140-150.

Ma, J., Tominac, P., Pfleger, B.F., Zavala, V.M. 2021. Infrastructures for phosphorus recovery from livestock waste using cyanobacteria: Transportation, techno-economic, and policy implications. *Sustainable Chemistry & Engineering*, **9**(34), 11416-11426.

Ma, J., Wang, P. 2021. Effects of rising atmospheric CO2 levels on physiological response of cyanobacteria and cyanobacterial bloom development: A review. *Science of the Total Environment*, **754**, 141889.

Mahesh, R., Yashavanth, P., Maiti, S.K. 2023. Modulation of macro and micronutrients to enhance lipid production by Scenedesmus abundans in a flat-panel photobioreactor under outdoor natural sunlight. *Biofuels*, 1-16.

Markl, E., Grünbichler, H., Lackner, M. 2018. PHB-bio based and biodegradable replacement for PP: a review. *Nov. Tech. Nutr. Food Sci*, **2**(5), 206-209.

Martino, L., Cruz, M.V., Scoma, A., Freitas, F., Bertin, L., Scandola, M., Reis, M.A.M. 2014. Recovery of amorphous polyhydroxybutyrate granules from Cupriavidus necator cells grown on used cooking oil. *International Journal of Biological Macromolecules*, **71**, 117-123.

Maruyama, H., Seki, H., Suzuki, A. 2009. Flotation of blue-green algae using methylated egg ovalbumin. *Chemical Engineering Journal*, **155**(1-2), 49-54.

McAdam, B., Brennan Fournet, M., McDonald, P., Mojicevic, M. 2020. Production of polyhydroxybutyrate (PHB) and factors impacting its chemical and mechanical characteristics. *Polymers*, **12**(12), 2908.

Meixner, K., Fritz, I., Daffert, C., Markl, K., Fuchs, W., Drosg, B. 2016. Processing recommendations for using low-solids digestate as nutrient solution for poly-ß-hydroxybutyrate production with Synechocystis salina. *Journal of Biotechnology*, **240**, 61-67.

Miyake, M., Erata, M., Asada, Y. 1996. A thermophilic cyanobacterium, Synechococcus sp. MA19, capable of accumulating poly-β-hydroxybutyrate. *Journal of Fermentation and Bioengineering*, **82**(5), 512-514.

Miyake, M., Schnackenberg, J., Kurane, R., Asada, Y. 2000. Phosphotransacetylase as a key factor in biological production of polyhydroxybutyrate. *Applied biochemistry and biotechnology*, **84**, 1039-1044.

Mohanrasu, K., Rao, R.G.R., Dinesh, G., Zhang, K., Prakash, G.S., Song, D.-P., Muniyasamy, S., Pugazhendhi, A., Jeyakanthan, J., Arun, A. 2020. Optimization of media components and culture conditions for polyhydroxyalkanoates production by Bacillus megaterium. *Fuel*, **271**, 117522.

Mongili, B., Abdel Azim, A., Fraterrigo Garofalo, S., Batuecas, E., Re, A., Bocchini, S., Fino, D. 2021. Novel insights in dimethyl carbonate-based extraction of polyhydroxybutyrate (PHB). *Biotechnology for Biofuels*, **14**, 1-16.

Monshupanee, T., Incharoensakdi, A. 2014. Enhanced accumulation of glycogen, lipids and polyhydroxybutyrate under optimal nutrients and light intensities in the cyanobacterium S ynechocystis sp. PCC 6803. *Journal of applied microbiology*, **116**(4), 830-838.

Monshupanee, T., Nimdach, P., Incharoensakdi, A. 2016. Two-stage (photoautotrophy and heterotrophy) cultivation enables efficient production of bioplastic poly-3-hydroxybutyrate in auto-sedimenting cyanobacterium. *Scientific reports*, **6**(1), 37121.

Moseley, J.L., Chang, C.-W., Grossman, A.R. 2006. Genome-based approaches to understanding phosphorus deprivation responses and PSR1 control in Chlamydomonas reinhardtii. *Eukaryotic cell*, **5**(1), 26-44.

Mourão, M.M., Gradíssimo, D.G., Santos, A.V., Schneider, M.P.C., Faustino, S.M.M., Vasconcelos, V., Xavier, L.P. 2020. Optimization of polyhydroxybutyrate production by amazonian microalga Stigeoclonium sp. B23. *Biomolecules*, **10**(12), 1628.

Murata, N., Takahashi, S., Nishiyama, Y., Allakhverdiev, S.I. 2007. Photoinhibition of photosystem II under environmental stress. *Biochimica et Biophysica Acta -Bioenergetics,* **1767**(6), 414-421.

Naira, V.R., Das, D., Maiti, S.K. 2019. Real time light intensity based carbon dioxide feeding for high cell-density microalgae cultivation and biodiesel production in a bubble column photobioreactor under outdoor natural sunlight. *Bioresource technology*, **284**, 43-55.

Nayak, B.K., Das, D. 2013. Improvement of carbon dioxide biofixation in a photobioreactor using Anabaena sp. PCC 7120. *Process Biochemistry*, **48**(8), 1126-1132.

Netrusov, A.I., Liyaskina, E.V., Kurgaeva, I.V., Liyaskina, A.U., Yang, G., Revin, V.V. 2023. Exopolysaccharides producing Bacteria: a review. *Microorganisms*, **11**(6), 1541.

Nie, M., Yin, X., Jia, J., Wang, Y., Liu, S., Shen, Q., Li, P., Wang, Z. 2011. Production of a novel bioflocculant MNXY1 by Klebsiella pneumoniae strain NY1 and application in precipitation of cyanobacteria and municipal wastewater treatment. *Journal of applied microbiology*, **111**(3), 547-558.

Nishida, H., Tokiwa, Y. 1993. Effects of higher-order structure of poly (3-hydroxybutyrate) on its biodegradation. II. Effects of crystal structure on microbial degradation. *Journal of environmental Polymer degradation*, **1**(1), 65-80.

Nishioka, M., Nakai, K., Miyake, M., Asada, Y., Taya, M. 2001. Production of poly-β-hydroxybutyrate by thermophilic cyanobacterium, Synechococcus sp. MA19, under phosphate-limited conditions. *Biotechnology letters*, **23**, 1095-1099.

Nonato, R.v., Mantelatto, P., Rossell, C. 2001. Integrated production of biodegradable plastic, sugar and ethanol. *Applied microbiology and biotechnology*, **57**, 1-5.

Oliveira, H.R., Bassin, I.D., Cammarota, M.C. 2019. Bioflocculation of cyanobacteria with pellets of Aspergillus niger: Effects of carbon supplementation, pellet diameter, and other factors in biomass densification. *Bioresource Technology*, **294**, 122167.

Padermshoke, A., Sato, H., Katsumoto, Y., Ekgasit, S., Noda, I., Ozaki, Y. 2004. Crystallization behavior of poly (3-hydroxybutyrate-co-3-hydroxyhexanoate) studied by 2D IR correlation spectroscopy. *Polymer*, **45**(21), 7159-7165.

Pahl, S.L., Lee, A.K., Kalaitzidis, T., Ashman, P.J., Sathe, S., Lewis, D.M. 2012. Harvesting, thickening and dewatering microalgae biomass. in: *Algae for biofuels and energy*, Springer, pp. 165-185.

Panda, B., Jain, P., Sharma, L., Mallick, N. 2006. Optimization of cultural and nutritional conditions for accumulation of poly-β-hydroxybutyrate in Synechocystis sp. PCC 6803. *Bioresource technology*, **97**(11), 1296-1301.

Paschalidis, L., Beer, B., Sutiono, S., Sieber, V., Burger, J. 2022. Design of enzymatic cascade reactors through multi-objective dynamic optimization. *Biochemical Engineering Journal*, **181**, 108384.

Patnaik, P.R. 2007. " Intelligent" descriptions of microbial kinetics in finitely dispersed bioreactors: neural and cybernetic models for PHB biosynthesis by Ralstonia eutropha. *Microbial Cell Factories*, **6**, 1-8.

Patyna, A., Płaczek, M., Witczak, S. 2018. Study of Chlorella vulgaris sedimentation process. *MATEC Web of Conferences*. EDP Sciences. pp. 05023.

Petrusevski, B., Bolier, G., Van Breemen, A., Alaerts, G. 1995. Tangential flow filtration: a method to concentrate freshwater algae. *Water Research*, **29**(5), 1419-1424.

Plackett, R.L., Burman, J.P. 1946. The design of optimum multifactorial experiments. *Biometrika*, **33**(4), 305-325.

Pradhan, S., Dikshit, P.K., Moholkar, V.S. 2018. Production, ultrasonic extraction, and characterization of poly (3-hydroxybutyrate)(PHB) using Bacillus megaterium and Cupriavidus necator. *Polymers for Advanced Technologies*, **29**(8), 2392-2400.

Prathyusha, A., Sheela, G.M., Bramhachari, P. 2018. Chemical characterization and antioxidant properties of exopolysaccharides from mangrove filamentous fungi Fusarium equiseti ANP2. *Biotechnology Reports*, **19**, e00277.

Price, S., Kuzhiumparambil, U., Pernice, M., Ralph, P. 2022. Techno-economic analysis of cyanobacterial PHB bioplastic production. *Journal of Environmental Chemical Engineering*, **10**(3), 107502.

Price, S., Kuzhiumparambil, U., Pernice, M., Ralph, P.J. 2020. Cyanobacterial polyhydroxybutyrate for sustainable bioplastic production: critical review and perspectives. *Journal of Environmental Chemical Engineering*, **8**(4), 104007.

Pringsheim, E.G. 2016. *Pure cultures of algae*. Cambridge University Press.

Ramos, A.F., Muñoz, M., Espinosa, A., Cabeza, I.O., Moreno-Sarmiento, N. 2020. Evaluation of poly (3-hydroxybutyrate) solubility in non-halogenated solvents to achieve an environmentally friendly recovery process from Burkholderia cepacia B27 cells. *Journal of Chemical Technology & Biotechnology*, **95**(6), 1657-1665.

Ren, Q., de Roo, G., Ruth, K., Witholt, B., Zinn, M., Thöny-Meyer, L. 2009. Simultaneous accumulation and degradation of polyhydroxyalkanoates: futile cycle or clever regulation? *Biomacromolecules*, **10**(4), 916-922.

Riis, V., Mai, W. 1988. Gas chromatographic determination of poly-β-hydroxybutyric acid in microbial biomass after hydrochloric acid propanolysis. *Journal of Chromatography A*, **445**, 285-289.

Rippka, R., Deruelles, J., Waterbury, J.B., Herdman, M., Stanier, R.Y. 1979. Generic assignments, strain histories and properties of pure cultures of cyanobacteria. *Microbiology*, **111**(1), 1-61.

Roh, H., Lee, J.S., Choi, H.I., Sung, Y.J., Choi, S.Y., Woo, H.M., Sim, S.J. 2021. Improved CO2-derived polyhydroxybutyrate (PHB) production by engineering fast-growing cyanobacterium Synechococcus elongatus UTEX 2973 for potential utilization of flue gas. *Bioresource technology*, **327**, 124789.

Romano, S., Schulz-Vogt, H.N., González, J.M., Bondarev, V. 2015. Phosphate limitation induces drastic physiological changes, virulence-related gene expression, and secondary metabolite production in Pseudovibrio sp. strain FO-BEG1. *Applied and environmental microbiology*, **81**(10), 3518-3528.

Rueda, E., Altamira-Algarra, B., García, J. 2022. Process optimization of the polyhydroxybutyrate production in the cyanobacteria Synechocystis sp. and Synechococcus sp. *Bioresource technology*, **356**, 127330.

Rueda, E., García-Galán, M.J., Ortiz, A., Uggetti, E., Carretero, J., García, J., Díez-Montero, R. 2020. Bioremediation of agricultural runoff and biopolymers production from cyanobacteria cultured in demonstrative full-scale photobioreactors. *Process Safety and Environmental Protection*, **139**, 241-250.

Rueda, E., García, J. 2021. Optimization of the phototrophic Cyanobacteria polyhydroxybutyrate (PHB) production by kinetic model simulation. *Science of the Total Environment*, **800**, 149561.

Samadhiya, K., Ghosh, A., Bhatnagar, A., Bala, K. 2023. Effect of acute vs chronic stress on Polyhydroxybutyrate production by indigenous cyanobacterium. *International Journal of Biological Macromolecules*, **227**, 416-423.

Samantaray, S., Mallick, N. 2012. Production and characterization of poly-β-hydroxybutyrate (PHB) polymer from Aulosira fertilissima. *Journal of Applied Phycology*, **24**, 803-814.

Samorì, C., Abbondanzi, F., Galletti, P., Giorgini, L., Mazzocchetti, L., Torri, C., Tagliavini, E. 2015a. Extraction of polyhydroxyalkanoates from mixed microbial cultures: impact on polymer quality and recovery. *Bioresource technology*, **189**, 195-202.

Samorì, C., Basaglia, M., Casella, S., Favaro, L., Galletti, P., Giorgini, L., Marchi, D., Mazzocchetti, L., Torri, C., Tagliavini, E. 2015b. Dimethyl carbonate and switchable anionic surfactants: two effective tools for the extraction of polyhydroxyalkanoates from microbial biomass. *Green chemistry*, **17**(2), 1047-1056.

Sangsanoh, P., Israsena, N., Suwantong, O., Supaphol, P. 2017. Effect of the surface topography and chemistry of poly (3-hydroxybutyrate) substrates on cellular behavior of the murine neuroblastoma Neuro2a cell line. *Polymer Bulletin*, **74**, 4101-4118.

Schembri, M.A., Bayly, R.C., Davies, J.K. 1995. Phosphate concentration regulates transcription of the Acinetobacter polyhydroxyalkanoic acid biosynthetic genes. *Journal of Bacteriology*, **177**(15), 4501-4507.

Scherholz, M.L., Curtis, W.R. 2013. Achieving pH control in microalgal cultures through fed-batch addition of stoichiometrically-balanced growth media. *J BMC biotechnology*, **13**(1), 1-17.

Schlebusch, M., Forchhammer, K. 2010. Requirement of the nitrogen starvation-induced protein Sll0783 for polyhydroxybutyrate accumulation in Synechocystis sp. strain PCC 6803. *Applied and Environmental Microbiology*, **76**(18), 6101-6107.

Scholz, B., Björke, J. Northern Icelandic Cyanobacteria Biorefinery as source of a versatile platform. *Energy (kJ g^{-1})*, **11**(11.5), 11-7.

Sekar, A., Varghese, G.K., Varma, R. 2023. Exposure to volatile organic compounds and associated health risk among workers in lignite mines. *International Journal of Environmental Science and Technology*, **20**(4), 4293-4306.

Senior, P., Dawes, E. 1971. Poly-β-hydroxybutyrate biosynthesis and the regulation of glucose metabolism in Azotobacter beijerinckii. *Biochemical Journal*, **125**(1), 55-66.

Senior, P.J., Dawes, E.A. 1973. The regulation of poly-β-hydroxybutyrate metabolism in Azotobacter beijerinckii. *Biochemical Journal*, **134**(1), 225-238.

Shang, L., Jiang, M., Chang, H.N. 2003. Poly (3-hydroxybutyrate) synthesis in fed-batch culture of Ralstonia eutropha with phosphate limitation under different glucose concentrations. *Biotechnology letters*, **25**, 1415-1419.

Sharma, L., Mallick, N. 2005. Accumulation of poly-β-hydroxybutyrate in Nostoc muscorum: regulation by pH, light–dark cycles, N and P status and carbon sources. *Bioresource technology*, **96**(11), 1304-1310.

Sharma, L., Nishida, K., Kanaya, T. 2005. The Effect of Solvent on the Miscibility of Blends of Poly 1-[4-(3-carboxy-4-hydroxy-phenylazo) benzene Sulphonamido-1, 2-ethanediyl,

sodium salt)](PAZO) and Polyhydroxybutyrate,(PHB. *Polymers and Polymer Composites*, **13**(5), 443-452.

Shrivastav, A., Mishra, S.K., Mishra, S. 2010. Polyhydroxyalkanoate (PHA) synthesis by Spirulina subsalsa from Gujarat coast of India. *International journal of biological macromolecules*, **46**(2), 255-260.

Singh, S.P., Montgomery, B.L. 2015. Regulation of BolA abundance mediates morphogenesis in Fremyella diplosiphon. *Frontiers in microbiology*, **6**, 1215.

Singh, V.R. 2015. Polyhydroxybutyrate (PHB): Biodegradable, Bioplastics Produced by Microorganisms. *International Journal of Pharmaceutical Research*, **7**(2), 17-23.

Sivashankari, R.M., Miyahara, Y., Tsuge, T. 2023. Poly (3-Hydroxybutyrate) Biosynthesis from [U-13C6] D-Glucose by Ralstonia eutropha NCIMB 11599 and Recombinant Escherichia coli. *Microbiology Research*, **14**(4), 1894-1906.

Stuart, K.R., Eversole, A.G., Brune, D.E. 2001. Filtration of green algae and cyanobacteria by freshwater mussels in the partitioned aquaculture system. *Journal of the World Aquaculture Society*, **32**(1), 105-111.

Sun, X., Guo, L., Sato, H., Ozaki, Y., Yan, S., Takahashi, I. 2011. A study on the crystallization behavior of poly (β-hydroxybutyrate) thin films on Si wafers. *Polymer* **52**(17), 3865-3870.

Taki, K., Seki, T., Mononobe, S., Kato, K. 2008. Zeta potential measurement on the surface of blue-green algae particles for micro-bubble process. *Water Science and Technology*, **57**(1), 19-25.

Tang, X., Chen, E.Y.-X. 2018. Chemical synthesis of perfectly isotactic and high melting bacterial poly (3-hydroxybutyrate) from bio-sourced racemic cyclic diolide. *Nature communications*, **9**(1), 2345.

Terada, M., Marchessault, R. 1999. Determination of solubility parameters for poly (3-hydroxyalkanoates). *International Journal of Biological Macromolecules*, **25**(1-3), 207-215.

tLAM, G., Vermuë, M., Olivieri, G., van den Broek, L., Barbosa, M., Eppink, M., Wijffels, R., Kleinegris, D. 2014. Cationic polymers for successful flocculation of marine microalgae. *Bioresource technology*, **169**, 804-807.

Tokiwa, Y., Calabia, B.P., Ugwu, C.U., Aiba, S. 2009. Biodegradability of plastics. *International journal of molecular sciences*, **10**(9), 3722-3742.

Troschl, C., Meixner, K., Drosg, B. 2017. Cyanobacterial PHA production—Review of recent advances and a summary of three years' working experience running a pilot plant. *Bioengineering*, **4**(2), 26.

Vandamme, D., Foubert, I., Muylaert, K. 2013. Flocculation as a low-cost method for harvesting microalgae for bulk biomass production. *Trends in biotechnology*, **31**(4), 233-239.

Verlinden, R.A., Hill, D.J., Kenward, M., Williams, C.D., Radecka, I. 2007. Bacterial synthesis of biodegradable polyhydroxyalkanoates. *Journal of applied microbiology*, **102**(6), 1437-1449.

Verspagen, J.M., Van de Waal, D.B., Finke, J.F., Visser, P.M., Huisman, J. 2014. Contrasting effects of rising CO 2 on primary production and ecological stoichiometry at different nutrient levels. *Ecology letters*, **17**(8), 951-960.

Wang, C., Yang, Y., Hou, J., Wang, P., Miao, L., Wang, X., Guo, L. 2020. Optimization of cyanobacterial harvesting and extracellular organic matter removal utilizing magnetic nanoparticles and response surface methodology: A comparative study. *Algal Research*, **45**, 101756.

Weber, A., Schwiebs, A., Solhaug, H., Stenvik, J., Nilsen, A.M., Wagner, M., Relja, B., Radeke, H.H. 2022. Nanoplastics affect the inflammatory cytokine release by primary human monocytes and dendritic cells. *Environment International*, **163**, 107173.

Wei, Y.-H., Chen, W.-C., Huang, C.-K., Wu, H.-S., Sun, Y.-M., Lo, C.-W., Janarthanan, O.-M. 2011. Screening and evaluation of polyhydroxybutyrate-producing strains from indigenous isolate Cupriavidus taiwanensis strains. *International journal of molecular sciences*, **12**(1), 252-265.

Woitzik, D., Weckesser, J., Jurgens, U.J. 1988. Isolation and characterization of cell wall components of the unicellular cyanobacterium Synechococcus sp. PCC 6307. *Microbiology*, **134**(3), 619-627.

Wölfle, H., Kopacka, H., Wurst, K., Preishuber-Pflügl, P., Bildstein, B. 2009. On the way to biodegradable poly (hydroxy butyrate) from propylene oxide and carbon monoxide via β-butyrolactone: Multisite catalysis with newly designed chiral indole-imino chromium (III) complexes. *Journal of Organometallic Chemistry*, **694**(16), 2493-2512.

Wu, G., Bao, T., Shen, Z., Wu, Q. 2002. Sodium acetate stimulates PHB biosynthesis in Synechocystis sp. PCC 6803. *Tsinghua Science Technology*, **7**(4), 435-438.

Wu, G., Wu, Q., Shen, Z. 2001. Accumulation of poly-β-hydroxybutyrate in cyanobacterium Synechocystis sp. PCC6803. *Bioresource technology*, **76**(2), 85-90.

Yabueng, N., Napathorn, S.C. 2018. Toward non-toxic and simple recovery process of poly (3-hydroxybutyrate) using the green solvent 1, 3-dioxolane. *Process Biochemistry*, **69**, 197-207.

Yang, Y.-H., Brigham, C.J., Budde, C.F., Boccazzi, P., Willis, L.B., Hassan, M.A., Yusof, Z.A.M., Rha, C., Sinskey, A.J. 2010. Optimization of growth media components for

polyhydroxyalkanoate (PHA) production from organic acids by Ralstonia eutropha. *Applied microbiology and biotechnology*, **87**, 2037-2045.

Yashavanth, P.R., Das, M., Maiti, S.K. 2021. Recent progress and challenges in cyanobacterial autotrophic production of polyhydroxybutyrate (PHB), a bioplastic. *Journal of Environmental Chemical Engineering*, **9**(4), 105379.

Yashavanth, P.R., Maiti, S.K. 2024. A multi-objective optimization approach for the production of polyhydroxybutyrate via Chlorogloea fritschii under diurnal light with single-stage cultivation. *International Journal of Biological Macromolecules*, **255**, 128067.

Yuheng, W., Shengguang, Z., Na, L., Yixin, Y. 2016. Influences of various aluminum coagulants on algae floc structure, strength and fotation effect. *Procedia Environmental Sciences*, **8**, 75-80.

Zavřel, T., Sinetova, M.A., Červený, J. 2015. Measurement of chlorophyll a and carotenoids concentration in cyanobacteria. *Bio-protocol*, **5**(9), e1467-e1467.

LIST OF PUBLICATIONS

Manuscripts

1. **Yashavanth PR**, Maiti SK. Recovery and characterization of polyhydroxybutyrate from *Chlorogloea fritschii* TISTR 8527 using halogenated and green solvents. Journal of Applied Phycology. 2024, 36(5), 2593-606.

2. **Yashavanth PR**, Maiti SK. A multi-objective optimization approach for the production of polyhydroxybutyrate via *Chlorogloea fritschii* under diurnal light with single-stage cultivation. International Journal of Biological Macromolecules. 2024, 255, 128067-128078.

3. Mahesh R, **Yashavanth PR**, Maiti SK. Modulation of macro and micronutrients to enhance lipid production by *Scenedesmus abundans* in a flat-panel photobioreactor under outdoor natural sunlight. Biofuels. 2023, 14(7), 1-6.

4. **Yashavanth PR**, Das M, Maiti SK. Recent progress and challenges in cyanobacterial autotrophic production of polyhydroxybutyrate (PHB), a bioplastic. Journal of Environmental Chemical Engineering. 2021, 9(4),105379-105390.

5. **Yashavanth PR**, Maiti SK. Improvement of polyhydroxybutyrate using single stage cultivation of *Chlorogloea fritschii* with phosphate and nitrate feeding under diurnal light. (Under review)

Book chapter

1. Mahesh R, Panda SK, Das M, **Yashavanth PR**, Dhull S, Negi BB, Jakhwal P, Maiti SK. Advances in biotechnological tools for bioremediation of wastewater using bacterial–algal symbiotic system. In Wastewater Treatment. 2021, 385-411, Elsevier.

CONFERENCES/WORKSHOPS

Conferences attended

1. **Yashavanth PR** and Maiti SK. Effect of light intensity on the growth of *Chlorogloea fritschii* and Polyhydroxybutyrate production. Algae, Fungi and Plants: Systematics to Applications-2020 (AFPSA 2020). Jan 24-25, 2020, Department of Botany, Calcutta University in association with Botanical Survey of India. *[Poster presentation]*

2. **Yashavanth PR** and Maiti SK. Multi-objective media screening for Polyhydroxybutyrate production from auto-sedimenting cyanobacteria *C. fritschii*. 3rd International Conference for Bioresource Technology for Bioenergy, Bioproducts & Environmental Sustainability-2021 (BIORESTEC 2021). May 17-19, 2021, Elsevier. *[Poster presentation]*

3. **Yashavanth PR** and Maiti SK. Flat-panel photobioreactor based cultivation of *Chlorogloea fritschii* under simulated sunlight for Polyhydroxybutyrate production. International Conference on Algal Biomass, Biofuels & Bioproducts-2021 (ALGALBBB 2021). June 14-16, 2021, Elsevier. *[Poster presentation]*

4. **Yashavanth PR** and Maiti SK. Effect of Sodium Nitrate on the growth of *Chlorogloea fritschii* TISTR 8527 under diurnal light and Polyhydroxybutyrate production. North East Research Conclave-2022 (NERC 2022). May 20-22, 2022, Indian Institute of Technology Guwahati (IITG). *[Poster presentation]*

Workshops attended

1. “Theory and demonstration on thermal analysis (DSC-TGA) of materials”. May 24, 2019. Organized by the Department of Chemical Engineering, IIT Guwahati in association with Central Instruments facility, IIT Guwahati.

2. “Flow Cytometry Techniques and Applications”. Dec 21-22, 2020. Jointly organized by North East Centre for Biological Sciences and Healthcare Engineering (NECBH), Indian Institute of Technology Guwahati, Assam with Becton, Dickinson and Company – BD.